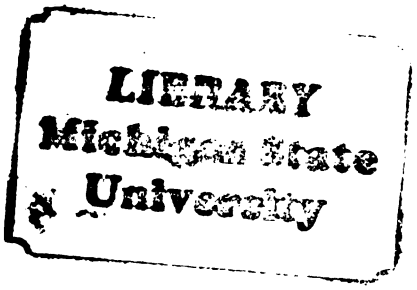

This is to certify that the

thesis entitled

BEHAVIOR OF SELECTED TRACE METALS IN SEDIMENTS FROM THE CONTINENTAL SHELF OF THE AMAZON RIVER

presented by

Sandra M. Pelowski

has been accepted towards fulfillment
of the requirements for

M.S. degree in Geology

DAVID T. LONG

Major professor

David T. Long

Date August 8, 1983

BEHAVIOR OF SELECTED TRACE METALS IN SEDIMENTS FROM THE CONTINENTAL SHELF OF THE AMAZON RIVER

By

Sandra M. Pelowski

A THESIS

Submitted to
Michigan State University
in partial fulfillment of the requirements
for the degree of

MASTER OF SCIENCE

Department of Geology

1983

ABSTRACT

BEHAVIOR OF SELECTED TRACE METALS IN SEDIMENTS FROM THE CONTINENTAL SHELF OF THE AMAZON RIVER

By

Sandra M. Pelowski

This research was to determine the chemical partitioning of Fe, Mn, Zn, Cu, Pb, Ni, Cr, Co, Ba and Al in sediments of the Amazon River Continental Shelf. Partitioning of metals was determined by a method of selective chemical attacks. The chemical data were studied in raw form and after reduction by R and Q-mode factor analysis. These data and previous studies on shelf hydrodynamics were used to conclude that: (1) the Amazon River is dominate over all other sources of trace metals to shelf sediments; (2) repartitioning of metals in sediments occurs between river and shelf environments; (3) the river sediment can be a potential source of metals to seawater, during passage to seawater. Importance as a source decreases as Ni>Co>Fe>Cr; (4) metal concentrations in the shelf sediments are dependent on grain-type; (5) Amazon Shelf Sediments remain oxic to a depth of 450 cm; (6) little repartitioning occurs with sediment depth.

Dedicated to my parents for all their loving support and encouragement.

ACKNOWLEDGEMENTS

I would like to express my sincere thanks to the members of my committee Dr. David T. Long, Chairman, Dr. Grahame Larson, and Dr. Duncan Sibley for their criticism, support and encouragement in completing this project. I would like to thank North Carolina State University, particularly Dr. David DeMaster for supplying the cores for analysis. I would also like to thank my friends and colleagues with whose help and support have made this project endurable.

This thesis was partially funded by a grant from Sigma Xi, the Research Society and a Research Scholarship from Marathon Oil Corporation.

TABLE OF CONTENTS

LIST OF TABLES

LIST OF FIGURES

INTRODUCTION

The geochemical cycle of any trace metal is defined in terms of sources, pathways, and sinks. In continental shelf environments continental fresh water and marine waters mix. Upon mixing more than 95% of the terrigenous sediment contained in the freshwater settles out prior to 3 0/00 salinity (Milliman et al., 1975), thereby making continental shelf sediments a possible major sink for trace metals in exogenic systems.

Two major sources of trace metal influx into oceanic sediments exist; a river source and a hydrothermal source (Schutz and Turekian, 1965). Traditionally, continental runoff has been considered the major source of metals to seawater and marine sediments (Gibbs, 1965; Sholkovitz and Price, 1980). Recently, however, it has been suggested, and in part demonstrated, that hydrothermal activity associated with oceanic ridge systems could also be a significant source of metals to marine environments (Gordon and Corliss, 1979; Edmond et al., 1979; Windom et al., 1971; Brumsack, 1980; Dymond, 1981; Marchig et al., 1982; Bischoff and Dickson, 1975). The significance of this source, though, has as yet not been assessed.

The purpose of this research is to determine the controls on trace metal concentrations in continental shelf sediments as well as their source. The area for this study is the Amazon Continental Shelf which is a relatively contaminate free environment (Drever, 1982). The

working hypothesis for this study is that patterns of trace metal chemical partitioning among various chemical phases in shelf sediments should reflect the controls on their chemical behavior and sources of metals to the sediment (Loring, 1976; Loring, 1982; Luoma and Bryan, 1981).

SIGNIFICANCE AND RESEARCH GOALS

The Amazon River Continental Shelf was selected as a study area because it is an unpolluted system whose river source drains through diverse environments. Hence, it offers an excellent opportunity to study trace metal geochemical behaviors. It is also one of the major rivers of the world, supplying 18% of all river water to the ocean. Consequently, the study of the nature of trace metals in the associated shelf sediments should be particularly important in helping to understand the chemical processes occurring in shelf sediments.

The goals of this research are to:

(1) Determine the partitioning fate of selected trace metals upon interaction with shelf sediments,

(2) Determine the fate of selected trace metals during shelf sediment diagenesis,

(3) Define trace metal sources to shelf sediments.

NATURE OF METALS IN MARINE AND CONTINENTAL SHELF ENVIRONMENTS

This section discusses previous work on the geochemical cycle of elements in marine environments. The geochemical cycles are defined in terms of sources, pathways, and sinks of the elements. Discussion is focused on those aspects of the marine environment that can be related to the geochemical behavior of metals in continental shelf environments. Trace metal diagenesis in marine sediments will also be discussed.

Sources of Metals to Shelf:

Sources of trace metals to marine and therefore continental shelf environments have been summarized by Schutz and Turekian (1965) as:

(1) stream and river,

(2) submarine volcanism,

(3) submarine alteration or solution of non-volcanic material,

(4) eolian,

(5) glacial discharge, and

(6) anthropogenic.

Eolian and glacial discharge are considered minor sources of trace metal input into the continental shelf (Schultz and Turekian, 1965). Submarine alteration and submarine volcanism on the other hand are difficult to distinguish as unique sources to shelf sediments and are therefore classified together as a ridge source. In the case of the Amazon River system, the anthropogenic input is considered negligible

(Drever, 1982). Ridge systems and river runoff can therefore be considered the two major sources of trace metal input into the shelf sediments.

Several marine environments have been studied (estuaries, deep ocean sediments, ridge systems, continental shelf and fjords) with regard to the delineation of separate trace metal sources. Factor analysis was used to define the relative importance of each source input (Imbrie and Van Andel, 1964). In this research two basic types of multivariant factor analysis were utilized, Q-mode and R-mode. Q-mode correlates two samples on the basis of the variables, whereas R-mode compares the relationships between the variables on the basis of the samples (Kerlinger, 1973; Nelson, 1981; Parks, 1970; Imbrie and Van Andel, 1964).

Mathematically, Q and R-mode factor analysis treat each sample or variable as a vector and resolves it into a small number of component vectors (Imbrie and Van Andel, 1964). Frequently, the original or raw data matrix must be transformed, but this transformation should in no way affect the accuracy of the program because relative proportions of variables are preserved (Bopp, 1981; Loring, 1982). This transformation of raw data allows every variable to have equal weight in the statistical program despite the ranges observed in variable's concentration.

The results of Q-mode factor analysis are written in two matrixes, the F_S-matrix and the B-matrix. The F_S-matrix is a table listing combinations of the variables that define the compositional end-members for each of the factors. The B-matrix is a matrix of the influence exerted by each end-member (i.e., matrix relates the intensity of

correlation between the factors) on each sample (Bopp, 1981; Bopp and Briggs, 1981). In the scaled varimax factor listing (F_S-matrix), if all variables were equally represented their varimax factor value would be 1.000. A strong positive value represents a positive correlation. A zero value represents no correlation and a strong negative value represents an inverse correlation with the matrix for that factor. A contour map of the matrix for each factor is generated and illustrates the distribution of factors in the study area (Bopp, 1981; Bopp and Biggs, 1981).

Most marine environments that have been studied have shown several source inputs. For example, Bopp and Biggs (1981) have identified three sources of metals to Delaware Bay sediments (representative of (1) a terrigenous natural background level source; (2) an oceanic source; and (3) a river source). Holmes and Martin (1978) on the other hand have determined two sources of trace metal origin to the continental shelf in the Gulf of Mexico (a natural background source and an anthropogenic source). In addition, Loring (1976, 1976b, 1979, 1982) has delineated two sources of trace metal input to the Saguenary Fjord; an industrial source and a natural source. Harding and Brown (1975) also investigated trace metal sources in the sediments of the Pamlico River Estuary, North Carolina. They found that the sources include a background (natural weathering) input source, and an industrial (anthropogenic) input source. Bender et al., (1971) studied sediments in the East Pacific Rise and found a seawater source and a ridge volcanism source. Edmond et al., (1982) dealt with sediments in the East Pacific Rise and concluded that the hydrothermal input in the oceans are substantial compared with fluvial transport. Heath and

Dymond (1981) identified 5 sources of input to Nazca plate sediments (a biogenic, detrital, hydrothermal, authigenic and solution residue). The detrital, hydrothermal and biogenic sources are the three dominate sources of trace metal input to the Plate sediments. The detrital component is the major input source for trace metals to the Plate sediments near the continental coast of South America, whereas the hydrothermal component is the major source of input to ocean sediments near the East Pacific Rise. The hydrothermal source is undetectable at 2500 km east of the East Pacific Rise (Heath and Dymond, 1981; Dymond, 1981).

The previous research cited above has shown that (1) when an anthropogenic source is present it is dominate; (2) when a study area is located near a ridge system, the hydrothermal source is dominate; (3) when a study area is located near a continental coast, the detrital input is dominate and (4) if 2500 km from a ridge source, ridge input is undetectable. Therefore, the concentrations and distributions of trace metals in a continental shelf environment should be able to be interpretated in terms of a single source.

Pathways and Sinks in Marine Systems:

The pathways of metals in exogenic systems can be defined in terms of five mechanisms of transport (Kharkar et al., 1968). They are:

(1) in solution (free and complexed),
(2) in the lattice of minerals of the suspended load,
(3) associated with oxides of the suspended load,
(4) adsorbed on the minerals of the suspended load, and
(5) associated with solid organic material.

Trace metals can be removed from active transport in the marine environment by:

(1) mechanical deposition of larger particles,

(2) coagulation of the colloidal fraction,
(3) humus colloids uptake
(4) plankton microorganism extraction,
(5) precipitation as oxide coatings,
(6) adsorption in cation exchange sites, and
(7) (in anaerobic conditions) forming insoluble sulfides (Krauskopf, 1956; Morozov, 1979; Harding and Brown 1975).

These seven removal mechanisms would be the major sinks of trace metals in marine and therefore continental shelf systems.

The chemical nature of the pathways and sinks of metals are very similar as shown above and reflect whether or not the metal is in an active state of transport. The chemical nature of a metal in exogenic systems (independent of its state of transport) is defined then by the chemical state it is in:

(1) dissolved (free and complexed),
(2) adsorbed on or in exchange position in clays,
(3) precipitated as hydroxides,
(4) adsorbed on or co-precipitated with Fe and Mn oxides,
(5) associated with organic matter,
(6) precipitated as sulfides,
(7) in lattice sites of minerals.

States of 2-6 are the states of the metal associated with the sediment. States 2-5 are collectively called the hydromorphic fraction or phase and state 6 is called the detrital or residual fraction. Metals in these fractions are normally differentiated by a series of selective chemical attacks on the sediment as discussed in the methods section. After the sediment has been chemically characterized, the metals are said to be partitioned among the different fractions of the sediment.

The following is a summary of work that has been done in defining these fractions for metals in marine sediments. Loring (1975, 1976, 1976b, 1979, 1982) studied trace metals in the sediments of the Saguenary Fjord. He found that the highest concentrations are found in mud (fine-grained) sediments and that the lowest concentrations occur

in the sandy (coarse) sediments (i.e. Co, Ni, Cr, Zn, Cu, and Pb concentrations increase with decreasing grain size). The detrital phase of Co, Ni, Cr, Zn, Cu, and Pb concentrations account for 71-98% of the total elemental concentrations in Fjord sediments. Holmes and Martin (1978) trace Cr, Cu, Fe, Mn, Ni, Zn, Ba and Pb migration in a continental shelf environment in the northwest Gulf of Mexico. They concluded that the most important factor affecting physical and chemical process within the sedimentary environment are variation in sediment accumulation rates. Brannon et al., (1979) researched Cu, Fe, Mn, and Zn in sediments from Mobil Bay, Alabama. They defined selective extraction phases investigated as adsorbed (ion exchangeable) on sediment material, reducible (solubility and migration controlled by oxidation-reduction reactions), bound in organic matter and residual. Iron in the reducible phase has a value of 68-79%. Of secondary importance to Fe is the organic phase (12-19%). Combined, the reducible and organic phases represent 90% of the total Fe concentration in the sediments. Manganese has 15-35% of total metal concentration in the reducible phase, 35-44% in the organically bound phase and 8-12% in the residual phase. Together, the organically bound, residual and reducible phases account for 78-80% of total Mn concentrations in the sediments. Copper has 51-61% of total metal retained in the residual phase. The organically bound phase is of secondary importance with 32-41% of total metal concentration. Combining the residual and organic phases, they represent 92% of total Cu in the sediments. Zinc has 52-59% of total metal concentration held in the organic phase and 38-44% in the residual phase. United, they equal 95% of total Zn concentration to the Bay sediments (Brannon et al., 1974). Harding and Brown (1975) studied Co,

Cr, Cu, Ni, Pb and Zn in the Pamlico River Estuary. They found that factors affecting trace metal uptake in sediments included an enrichment of trace metal concentrations in clays and organic matter. They stated that the surficial distribution of fine sediments appear to be due to the patterns of water circulation. Trace metal incorporation with clay sediments and organic matter in the estuary were dependent on temperature, pH, Eh and clay mineral type (the relative importance of each was undefined). Harding and Brown (1975) explain trace metal dispersal in the estuary based on the relative mobility of the elements. Cr is the most immobile element studied. It quickly drops out of the water column upon entering the estuary and is not dispersed throughout the Bay sediments. The moderately immobile trace elements, Co, Cu, Ni and Pb (relatively compared to the other elements studied) remain in solution, are circulated from their industrial source and are dispersed in clays and organic matter throughout the estuary sediments. Cosma et al. (1979) studied trace metals (Cr, Cu, Ni, Mn) in surface sediments in the continental shelf area between Arenzano and Capo Noli in the Liqurian Sea. Cr was controlled by pollution inputs. Nickel concentrations were accounted for by stream input of eroded basic rock outcrops. Copper concentrations are associated with the organic fraction. Manganese concentrations are related to sediment textures. Turekian and Imbrie (1966) researched deep sea sediments from the Atlantic Ocean. They found that the trace elements Ba, Co, Cu, Ni, Pb, Cr and Mn showed no correlation with clay mineralogy or depth of water. There was a strong correlation of metals Mn, Ni, Co with areas of low clay accumulation rates possibly due to a fine grained pelagic component. Morozov (1979) studied migration of Fe, Mn, Zn, Cu, Ni, Co, Cr,

and Pb around the mouths of several rivers. The general conclusions of this investigations were: Trace metal concentration in the suspended and dissolved forms decreased in the sequence river-estuary-sea-ocean; The portion of suspended Fe and Mn forms decrease from the river (97%) to ocean (7%); the mechanical deposition of the larger particles occurs near the mouth of a river; coagulation of the colloidal fraction and the humus colloids take up a large fraction of trace metals at the mouth of a river; and sea/fresh water zones show extensive plankton microorganism development which extract metals from the water column.

Summarizing past research these conclusions can be drawn: (1) trace metal concentrations increase with decreasing grain size; (2) there is no correlation with clay mineralogy or depth of water from the Atlantic deep-sea sediment core samples; (3) an important factor affecting processes in a basin is the variation in sediment accumulation rates; and (4) the relatively immobile elements will drop out of the water column upon entering an estuary from a river source.

Diagenesis of Metals in Marine Sediments:

Chemical conditions of sediments can change with depth as a result of compaction and age (Bonatti et al., 1971). Factors affecting the chemical conditions are: changes in Eh, sediment compositon, temperature, bioturbation, and pH (Yen and Tang, 1977). Eh values normally decrease with depth in sediments (Addy et al., 1976). The relatively mobile elements should be enriched in the oxidized sediment zone (Ni, Fe, Mn, Co) (Addy et al., 1976; Holmes and Martin, 1978; Heath and Dymond, 1981); while less mobile elements like zinc and copper show little migration in the sediment column (Addy et al., 1976). Brooks et al., (1968), Bonatti et al., (1971) concluded that Fe and Cu are not

mobile elements and show no overall trend to increase with sediment depth, and Fe seems to show inconsistent behavior during diagenesis. Ba and Pb are also relatively immobile elements and according to Holmes and Martin (1978) show no overall trend with depth. Brannon et al., (1979) stated that no patterns of migration for the elements Fe, Mn, Cu and Zn could be conclusively drawn. Generally, if an environment is reducing, the elements with higher redox potentials should go into solution and if an environment is oxidizing they should precipitate. In this way the higher redox potential elements migrate up the sediment column, creating an enriched metal concentration on the top centimeters of the ocean floor (Addy et al., 1976).

In summary, these investigations show that: (1) Ni, Co, Mn should be enriched in the upper centimeters of the sediment column; (2) Ba, Pb, Zn, Cu should not be enriched nor depleted in the upper centimeters of the sediment column; and (3) Conflicting Fe behavior exists.

This summary shows that much research still needs to be done. No research involving source delineation in unpolluted continental shelf sediments has been reported. In this investigation, the chemical partitioning data on the Amazon Continental Shelf coupled with factor analysis can aid in the resolution of trace metal sources to shelf sediments. Chemical partitioning data with depth in Amazon Shelf sediments will help to eliminate conflicting diagenetic trace metal behavioral observations. Exploring trace metal behaviors encountered when fresh and oceanic waters merge will aid in the investigation of the controls or aid in determining the controls of geochemical cycling of trace metals.

STUDY AREA

The study area is located on the Continental Shelf at the mouth of the Amazon River (Figure 1) and extends from a latitude of 52°W to 46°E and a longitude of 2°S to 6°N. The Amazon River Basin lies entirely in the central equatorial area, extending from 5°N to 20°S longitude and from 50°W to 77°W latitude (Gibbs, 1967; Stallard, 1980). The Amazon River drains a diverse climatic area ranging from the artic Andean Mountains to the tropical rain forests. Temperatures vary from less than 15°C in the Andeas to 28°C in the tropical forests (Gibbs, 1967).

The Amazon River Drainage Basin is the largest in the world, draining an area 6.3×10^6 km^2 (Keller, 1962). The river drains diverse geological environments (Figure 2) comprising active orogenic zones, epiorogenic uplift zones, stable cratonic zones and active sedimentary basin zones (Gibbs, 1967; Stallard, 1980). The Amazon River has an average discharge of 1.7×10^5 m^3/sec, supplying 18% of all water from rivers into the ocean (Oltman, 1968; Drever, 1982). Sediment influx ranges from 8-9 $\times 10^8$ tonnes/year; influx was measured at Óbidos a site marking 80% river flowage (Figure 4) (Holeman, 1968). The dissolved load is 2.9×10^8 tonnes/year (Meade et al., 1979). The clay content at the mouth of the river consists of 33% illite, 31% kaolinite, 27% montmorillite, and 2% chlorite (Milliman et al., 1975).

Precipitation in the Amazon River Basin ranges from less than 2000 mm/year to over 3500 mm/year (Stallard, 1980; Hoffman, 1968). The

Figure 1. Study area and location of sampling stations.

Figure 2. Morphostructural Map of Amazon Drainage Basin (Stallard, 1980).

1. Amazon Trough
2. Subandean Trough
3. Shields
4. Western Cordillera (Cordillera Occidental)
5. Intercordilleran Zone (includes the altiplano regions)
6. Eastern Cordillera (Cordillera Oriental)
7. Subandean Uplifts

Symbol key:

CONSTRUCTIVE STRUCTURAL RELIEF ELEMENTS


Trend of folded young mountain ranges of the Andean system.


Crest of horst mountains and monoclimes.


Fault flexure.


Lithological. Step, escarpment.

DESTRUCTIVE NON-STRUCTURAL RELIEF ELEMENTS


Old erosion. Surfaces of Mesozoic Tertiary age.


Occurrence of inselbergs.


Crest of residual relief.

ACCUMULATIVE RELIEF ELEMENTS


Quaternary fluvial. Alluvial or eolian deposits (in the Andes including glacio-fluvial and volcanic tectonic mudflow deposits).


Occurrence of Late-Tertiary and Quaternary lacustrine or marine deposits.


Pleistocene loess with ash-admixtures.


Sand dunes.


Pleistocene glacial deposits.


Occurrence of volcanoes.


Salt flat.


Lake.

Figure 3. Typical Surface-water salinities (0/00) during wet season conditions (April-May, 1968) and dry season conditions (November, 1967) of the surface waters off the Amazon. Profiles in the upper right hand corners show vertical salinity gradients in profiles taken directly seaward of the Amazon mouth. (Milliman et al., 1975).

Figure 4. Map of Amazon river, showing locations on mainstream tributaries where sediment loads were measured in 1977 for the study by Meade et al., 1979.

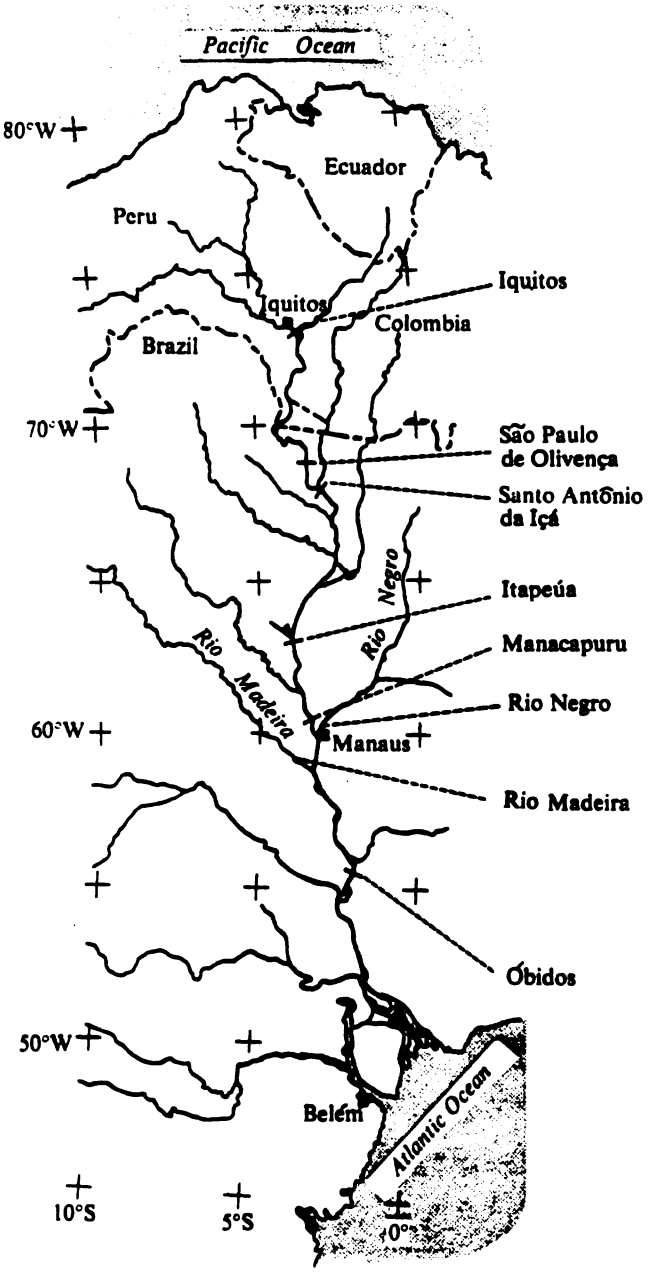
Pacific Ocean
80°W
Ecuador
Peru
Iquitos
Iquitos
Colombia
Brazil
70°W
São Paulo
de Olivença
Santo Antônio
da Içá
Rio Negro
Itapeúa
Rio Madeira
Manacapuru
Rio Negro
60°W
Manaus
Rio Madeira
Óbidos
50°W
Belém
Atlantic Ocean
10°S
5°S
0°

river has a low buffering capacity and pH values range from 6.5-7.5 throughout the year (Schmidt, 1972). The waters of the Amazon also appear thoroughly mixed vertically (Gibbs, 1967).

The Amazon River flows onto the shelf and into the Guiana Current. The Guiana Current is an extension of the South Equatorial Current which flows in a northwesterly direction along the east coast of South America (Ryther et al., 1967; Eisma et al., 1971). At the mouth of the river, 95% of the terrigenous sediment from surface waters settle out prior to 3 0/00 salinity (Milliman et al., 1975). Figure 3 shows surface water salinities for two seasons--the dry season, November, and the wet season, April-May.

The width of the Shelf ranges from 100 to 300 km. The bathymetric chart (Figure 1) of the Continental Shelf reveals a relatively flat inner shelf to the 40 meter isobath. There is an abrupt change at this point and a steepening in slope appears until the 60 meter isobath. The change of slope represents the foreset of a subaqueous prograding delta (Kuehl et al., 1982; Nittrouer et al., 1983). Surface grain size type distribution are shown in Figure 5. The upper two centimeters of shelf sediments are composed of (1) a mud (silt and clay) zone occupying the inner shelf seaward and northwestward of the Amazon River mouth and (2) a sand zone dominating the rest of the outer shelf region. Three detrital sedimentary deposits are observed from the surface sediment on the Amazon Continental Shelf (1) an outer shelf sand deposit; (2) an inner shelf mud deposit; and (3) mud interbedded with sand deposit (Kuehl et al., 1982; Nittrouer et al., 1983). The areal distribution of sediment grain size is in Figure 6. Outer shelf sands (median grain size 1.5-3.0 Ø) show moderate to good sorting. Inner

Figure 5. Distribution of grain types at Ø-2 cm depth on the Amazon Continental Shelf (Nittrouer *et al.*, 1983).

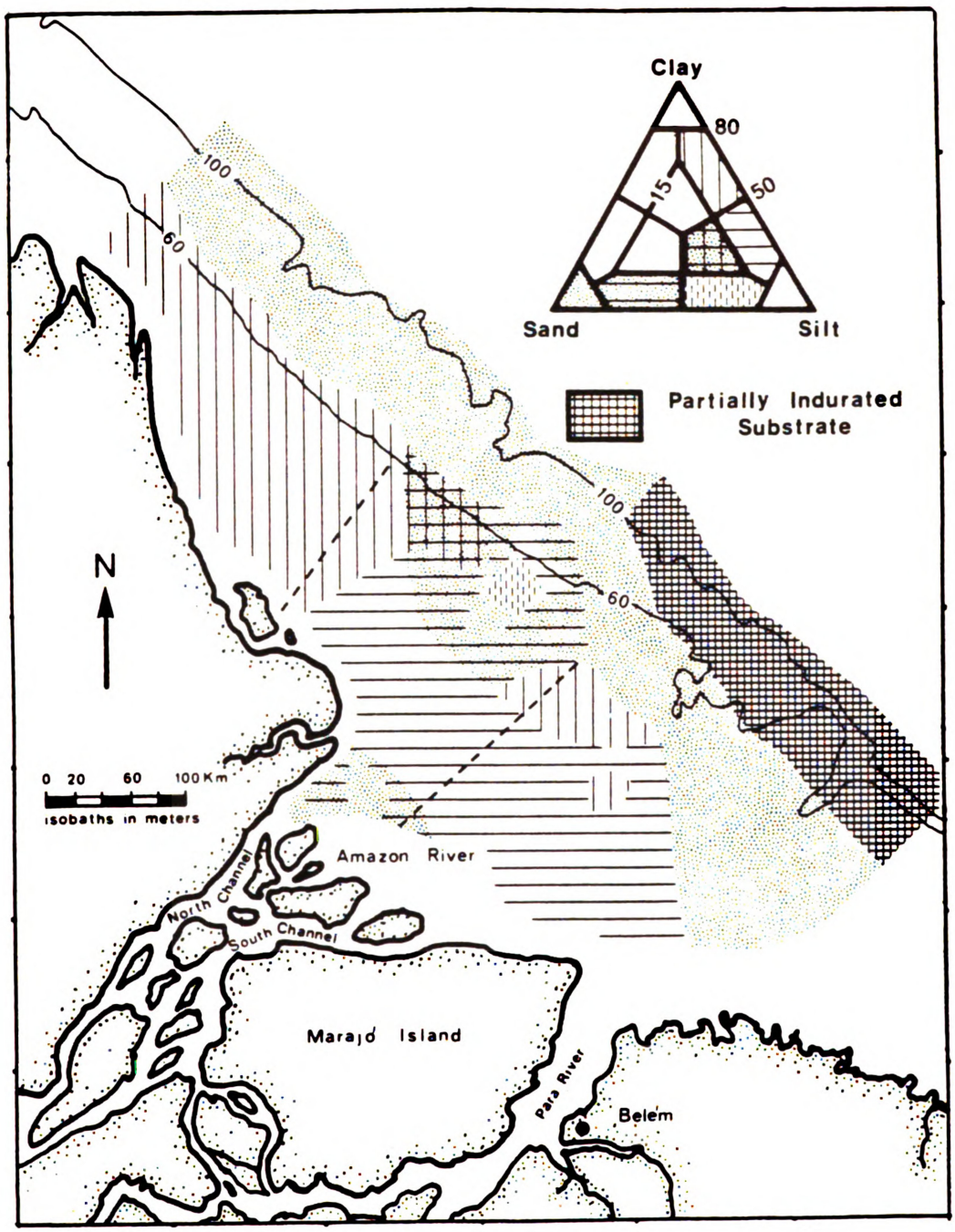
Clay
80
15
50
Sand
Silt
Partially Indurated Substrate
100
60
100
60
N
0 20 60 100 Km
isobaths in meters
Amazon River
North Channel
South Channel
Marajó Island
Pará River
Belem

Figure 6. Areal distribution of mean grain size on the Amazon Continental Shelf (Nittrouer et al., 1983).

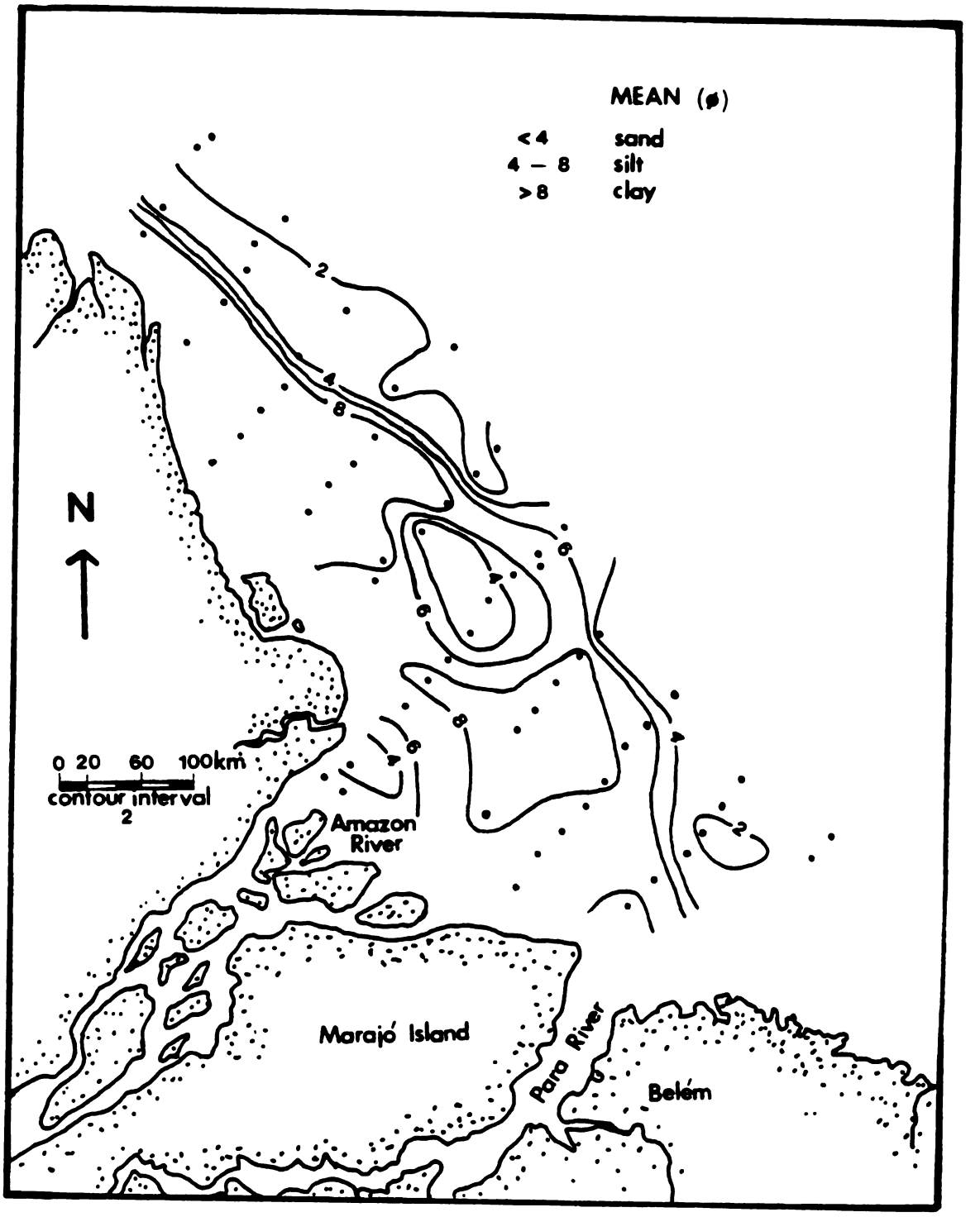
MEAN (ø)
< 4 sand
4 – 8 silt
> 8 clay
2
4
8
6
N
0 20 60 100km
contour interval
2
Amazon
River
Marajó Island
Para River
Belém

shelf muds (median grain size 6-9 Ø) are poorly sorted (Nittrouer et al., 1983).

Several models have been proposed to explain the sedimentary structures and grain size distribution on the Amazon Continental Shelf (Milliman et al., 1975; Gibbs, 1976; Nittrouer et al., 1983). Milliman et al., (1975) hypothesizes that no modern muds are being deposited on the Amazon Shelf, except on a small nearshore zonal area. However, Milliman et al., (1975) states that two distinct periods of sedimentation have occurred in Quaternary time. One occurring at high sea level and the other at low sea level (60-80 meters below present sea level). During high sea level periods, inner shelf sediment accumulation occurs only in a narrow nearshore belt of mud. The majority of muds, however, are deposited at low sea levels. In direct opposition to Milliman et al., (1975) theory are Pb-210 data on shelf sediments. The Pb-210 dates indicate that modern mud accumulation is presently occurring (Figure 7) (Kuehl et al., 1982; Gibbs, 1976).

A second theory to explain the physical processes on the Amazon Continental Shelf was proposed by Gibbs (1976). Gibbs (1976) states that the Amazon River waters move offshore as a plume and is carried northwestward. Upon entry into the shelf, river particles settle out and are transported landward by bottom currents. A landward fining of particle size should result. Recent data, however, reveal an absence of reverse grading, contradicting the sedimentation model of Gibbs (1976) (Figure 8) (Nittrouer et al., 1983; DeMaster, personal communication 1982).

A recent model proposed by Nittrouer et al. (1983) suggests that modern sediment accumulation occurs as a result of a subaqueous delta

Figure 7. Distribution of sediment accumulation rates on the Amazon Continental Shelf based on ^{210}Pb geochronology. (Kuehl *et al.*, 1982).

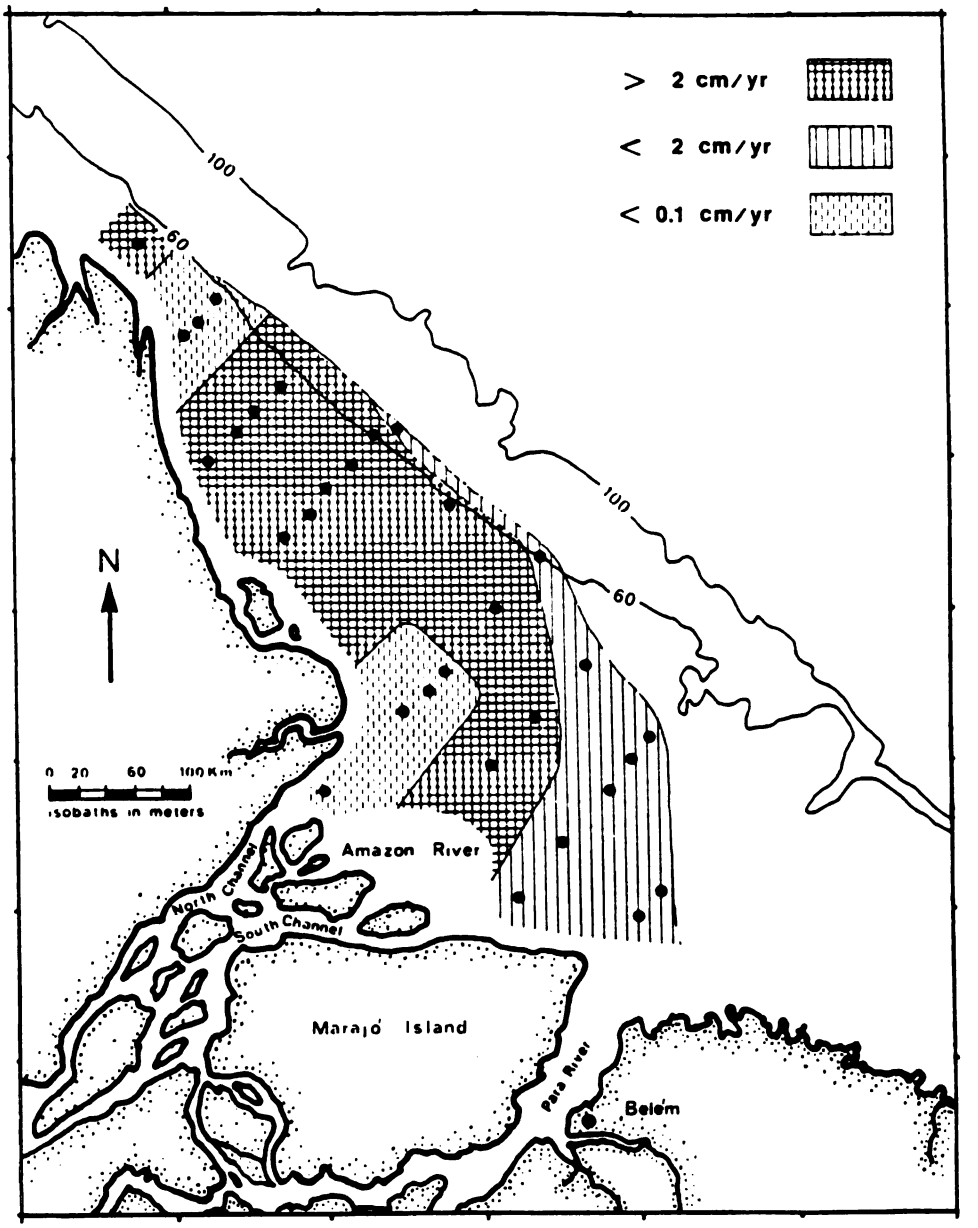
> 2 cm/yr
< 2 cm/yr
< 0.1 cm/yr
100
60
100
60
N
0 20 60 100 Km
isobaths in meters
Amazon River
North Channel
South Channel
Marajó Island
Pará River
Belém

Figure 8. Clay mineral distribution along the Amazon Shelf from Nittrouer et al. (1983) and Gibbs (1977).

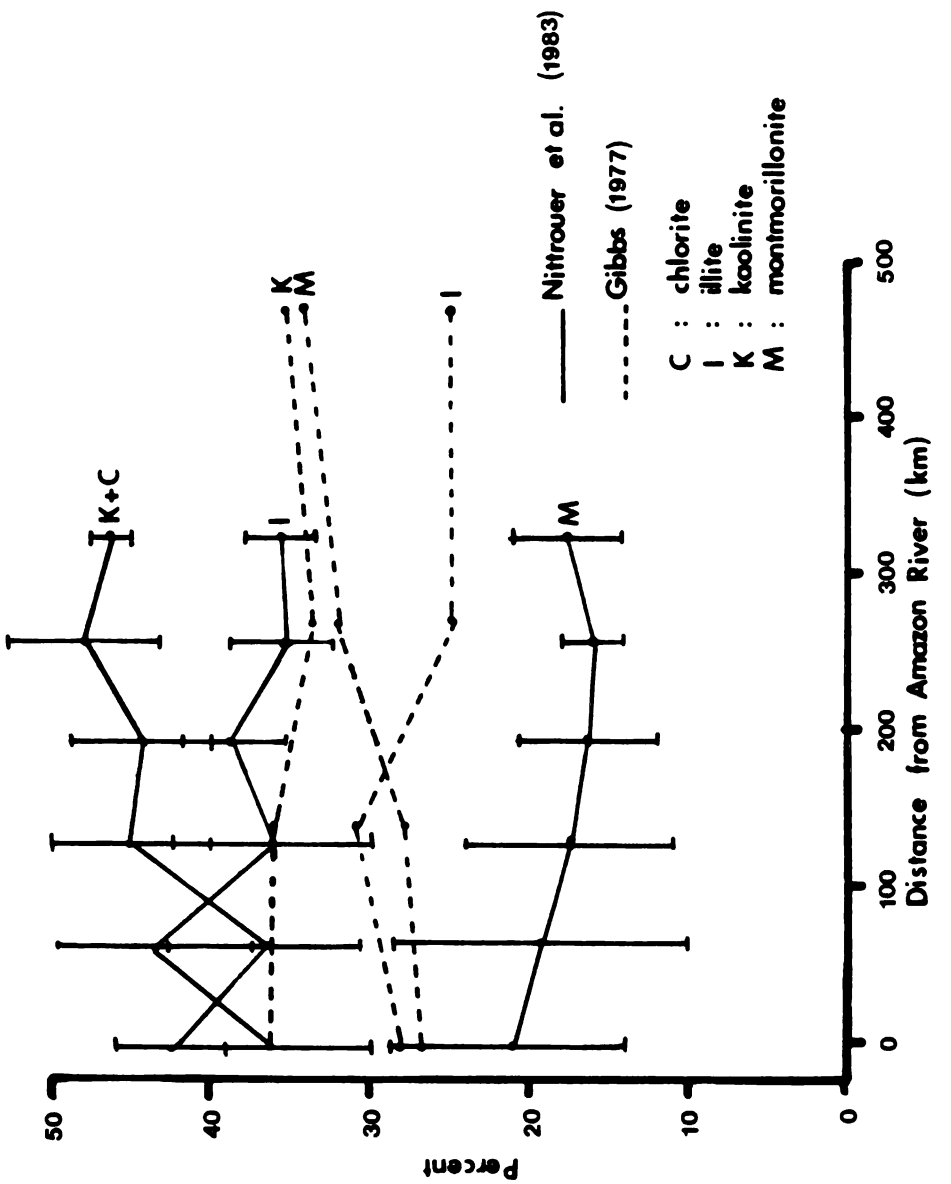
Nittrouer et al. (1983)
Gibbs (1977)
C : chlorite
I : illite
K : kaolinite
M : montmorillonite
K+C
I
K
M
I
M
Percent
0
10
20
30
40
50
0
100
200
300
400
500
Distance from Amazon River (km)

prograding over relict basal sands. Nittrouer et al., (1983) hypothesizes that a turbulent jet emanates from the river mouth and flows across the inner shelf. Their hypothesis is consistant with sediment accumulation rates based on Pb-210 data (Figure 7), sedimentary deposit data (Figure 5) and sediment grain distribution data (Figure 5).

At low sediment accumulation rates, the effects of bioturbation on the disruption of sedimentary structures increases (i.e., original stratification is preserved in areas of highest sediment accumulation rates with minimal bioturbation). A strong correlation therefore exists between accumulation rate and sedimentary structure (Kuehl et al., 1982). The model of Nittrouer et al., (1983) is the most consistant with present data and is therefore the accepted theory for use in this research.

METHODOLOGY

A research cruise to the Amazon Continental Shelf took place in October 1979. Shelf sediments (Figure 1) were sampled using an N.E.L.-Reineck type box corer (20 cm x 30 cm cross-sectional area), in order to maintain core stratigraphic integrity. These cores and soil samples from Belèm (Figure 1) were immediately subsampled and shipped to North Carolina State University Laboratories. At North Carolina State University a series of analysis including grain-size analysis and Pb-210 analysis for sediment accumulation rate data were performed (Nittrouer et al., 1983).

The cores were again subsampled for trace metal analysis in the Michigan State University Geochemistry Laboratory. The vials containing the Amazon sediments were placed in a 40°C oven for 96 hours, to completely dry the wet core samples. Each sample was dry sieved with a brass U.S. standard .212 mm sieve opening (65 mesh) sieve. After each sample, the sieve was placed in a sonic cleaner filled with distilled water for washing. After 10 minutes in the sonic cleaner, the sieve was rinsed with double distilled water and placed on its side to dry to prevent atmospheric or dust contamination (Bopp, 1981). To insure no contamination of the brass sieve on sediment samples, two identical samples were processed; one passing through the sieve, the second unsieved. Differences in the two samples were not statistically

different, therefore the sieve offered no significant source of contamination to the sample.

Each sample (5.000 grams dry weight of the less than .212 mm fraction) was weighed on a Mettler HL 52 scale and placed directly into pre-treated polyethylene centrifuge bottles. (Pre-treatment of the polyethylene centrifuge bottles included the following: (1) washing with soap and water, (2) rinsing with distilled water, (3) soaking in a 1:3 HCL solution overnight, (4) rinsing in double distilled water three times and (5) thoroughly drying).

A series of sequential chemical extractions were performed on each 5.000 gram sample (Figure 9). Extractions were performed in order to determine the partitioning of trace metals from four hypothesized fractions:

Hypothesized sediment fraction		Chemical response of sediment to attack
(1) Clay		Exchangeable
(2) Fe, Mn oxide	Hydromorphic	Easily and moderately reduced
(3) Organic		Oxidized
(4) Residual	Detrital	Resisent

(Gephart, 1982).

The procedure utilized is a combination of attacks performed by Tessier et al., (1979); Gibbs (1977); Gephart (1982); and Gupta and Chen (1975) and is summarized below:

(1) Exchangeable: 40 ml of 1 M $MgCl_2$, pH=7 were added to the 5.000 gram less than .212 mm dry sediment sample. The mixture was continuously agitated at room temperature for one hour (Tessier et al., 1979; Gibbs, 1977).

Figure 9. Flow chart of selective chemical attacks.

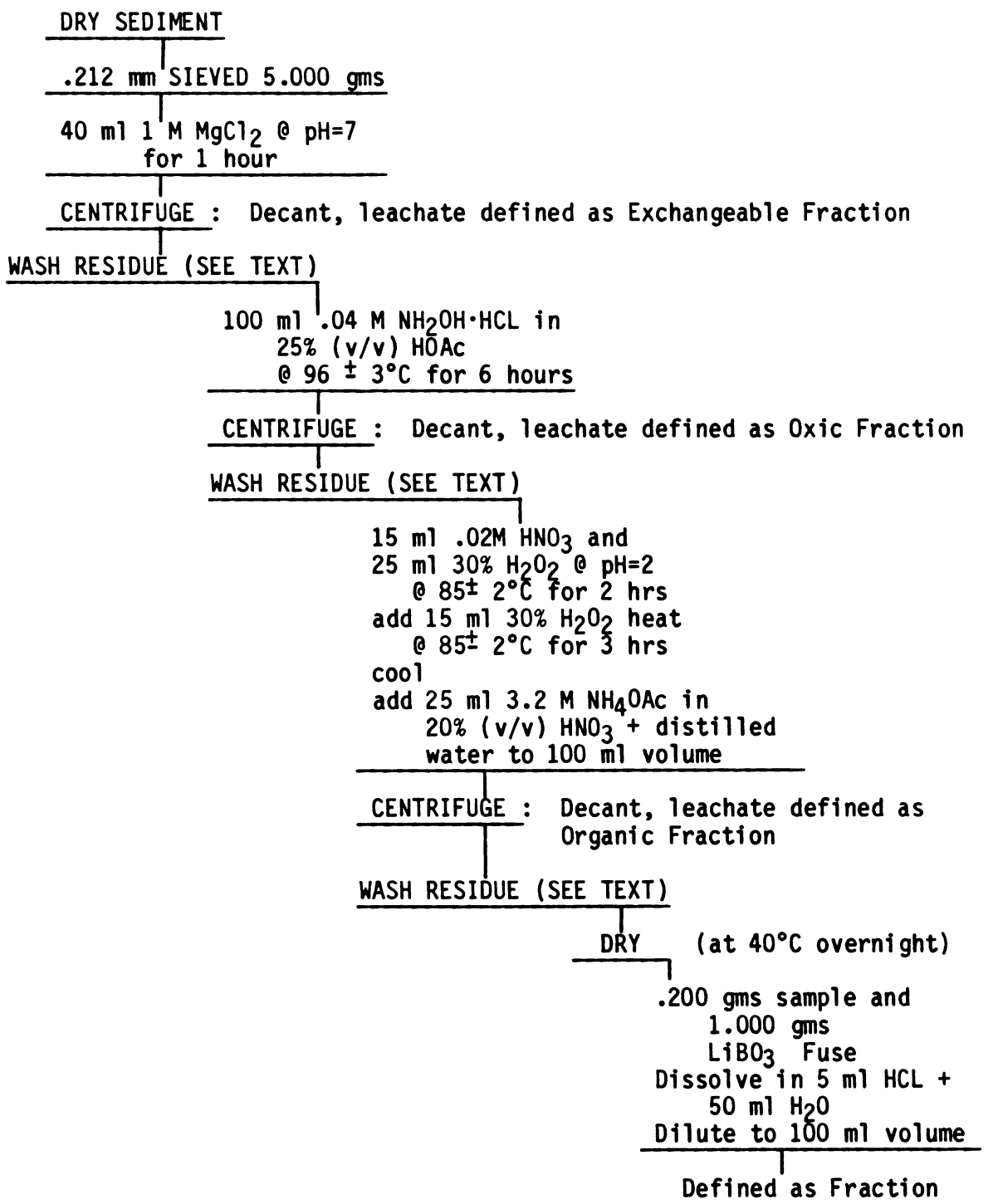

(2) Fe-Mn Oxide: The residue from (1) was leached with 100 ml of 0.04 M $NH_2OH \cdot HCL$ in 25% (v/v) HOAc. This extraction was performed at 96 ± 3°C for six hours (Tessier et al., 1979; Gephart, 1982).

(3) Organic: The residue from (2) was extracted with 15 ml of 0.02 M HNO_3 and 25 ml of 30% H_2O_2 pH=2 (adjusted with HNO_3) heated to 85±2°C for two hours with occasional agitation (every 15-20 minute agitation). At the conclusion of two hours a second aliquot of 15 ml 30% H_2O_2 was added. The sample was then returned to the water bath of 85±2°C for three additional hours, occasionally agitating. After three hours, the sample was cooled to room temperature, at which time 25 ml of 3.2 M NH_4OAc in 20% (v/v) HNO_3 and double distilled water (diluting sample to 100 ml) were added. This mixture was stirred continuously at room temperature for 30 minutes (Gephart, 1982; Gupta and Chen, 1975).

(4) Residual: 0.200 grams of dry residue from (3) were fused with 1.000 gram of $LiBO_3$ at 1000°C in graphit crucibles for 15 minutes. The fused sample was removed from the furnace and immediately placed in a pre-prepared solution of 5 ml HCL and 50 ml double distilled water. Once dissolved, the sample was diluted to 100 ml with double distilled water. Duplicate fusions were run on each sample (Perkin Elmer Atomic Adsorption Instruction Manual, 1973; Gephart, 1982).

Upon completion of each attack, except the residual fraction, the sample was centrifuged for 12 minutes at 15,000 RPM. The supernate was drawn off and stored in pre-treated 250 ml polyethylene storage bottles. The residue sample was then rinsed with double distilled water and centrifuged at 15,000 RPM for 12 minutes, prior to subsequent extraction phases.

The supernate from each selective chemical extraction phase and the residual $LiBO_3$ fraction were analyzed by either a flame atomic adsorption 560 spectrophotometer or by a graphite furnace atomic adsorption HGA-2200 spectrophotometer. Atomic adsorption control settings for the elements analyzed by flame attachment in all matrixes were modified from conditions stated in the Perkin Elmer Atomic Adsorption Instruction Manual (1978). The Instruction Manual does not, however, offer optimized control settings for different matrixes when analyzing by graphite furnace. Optimization for each element analyzed by the graphite furnace for each of the four matrixes had to be performed. Optimization for each element in each matrix analyzed was in accordance with guidelines set forth in the Perkin Elmer Atomic Adsorption Instruction Manual for furnace (1978). Optimized control settings for the graphite furnace found in this study are summarized in Appendix II.

All sample sediments were also analyzed for total organic carbon content by a modified Walkley-Black titration method (Gaudette et al., 1974). A .200 gram dried, less than .212 mm sieved sediment sample was placed in a 500 ml Erlenmeyer flask. Precisely 10 ml of 1 N $K_2Cr_2O_7$ solution was added to each sample. The flask is then gently swirled to mix sediment and solution. Next, 20 ml of concentrated H_2SO_4 were added to the flask and again gently swirled for one minute. The mixture in the flask was allowed to stand at room temperature for 30 minutes. A standardization blank was run with each batch of samples. After standing 30 minutes, the solution was diluted to 200 ml volume with double distilled water and 10 ml 85% H_3PO_4, .20 grams NaF and 15 drops of diphenylamine indicator were added to the flask.

The solution in the flask was then back titrated with 0.5 N ferrous ammonium sulfate solution. The color progressed from an opaque green-brown to green upon the addition of the ferrous ammonium sulfate solution. The color continuously shifted upon further titration to a bluish-black-grey; at this point the addition of a few drops of ferrous solution shifted the color to a brilliant green end point (a one-drop end point) (Gaudette et al., 1974). The results of the analysis were calculated by the following equation:

Organic Carbon = $10(1-T/S)((.34)(.003)(100/.20))$

T= sample titrated; S = standardization blank titration;
.003 = meq weight of carbon; .34 = normality of $K_2Cr_4O_7$;
W = weight of sediment sample; 10 = volume of $K_2Cr_4O_7$

(Gaudette et al., 1974).

The total organic carbon (TOC) content is presented in Appendix I.

The data from the chemical partitioning attacks were reduced by factor analysis, both R and Q-mode. Factor analysis can aid in revealing simple patterns from complex data sets. Data from the chemical partitioning attacks fulfills the three requirements of factor analysis utilization:

(1) conveniently coded -- values in ppm,
(2) large number of sample volume -- 84 samples, chemically fractionated into four phases, analyzed for 10 elements, and
(3) prior knowledge of relationships is inadequate

(Kerlinger, 1973;
Imbrie and Van Andel, 1964).

The data were factored by factor analysis in original (raw) form and after transformation of the data by natural log. The transformation of the data was done in order to see if any improvements on correlation could be made since geochemical data frequently does not have a normal distribution.

RESULTS AND DISCUSSION

Results of the chemical partitioning studies for the metals are presented in Appendix I. These results will be discussed in three parts; general nature of partitioning of metals in the sediments, diagenesis of metals in the sediments in terms of metal partitioning, and source of trace metals to the sediments as interpreted from R and Q-mode factor analysis of the partitioning data.

Chemical Partitioning of Metals in Amazon Shelf Sediments

Two aspects of the chemical partitioning of the metals in the sediments are discussed: (1) a general summary of the nature of the partitioning in the sediments and (2) the nature of the partitioning over the shelf. In Table 1 the partitioning results from Appendix I are summarized as a function of sediment type. The sediments in the study area were classified by Nittrouer et al., (1983) as to type using the classification scheme of Folk (1974). Sediment types are defined as a function of where the sediment plots on a ternary diagram with respect to the three end-member compositions of clay-sand-slit. Numerical representation of sediment types found by Nittrouer et al., (1983) is shown below in Figure 10:

Figure 10. Numerical representation of sediment type from Folk (1974).

Type 1 = sand
Type 2 = sand-silt
Type 3 = silt-sand

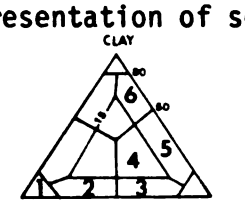

Type 4 = sand-silt-clay
Type 5 = clayey-silt
Type 6 = silty-clay

Four chemically defined sediment fractions are shown on Table 1 (exchangeable, Fe-Mn oxide, organic matter, and detrital). The values are the average of the percent of the metal in a particular fraction. Since these values are averages of percents, the totals of a metal in a sediment type are not necessarily 100%.

Table 1 also present a summary of the work of Gibbs (1977) on the partitioning of selected metals in the suspended load of the Amazon River. Gibbs samples were taken off Macapa' Brazil and therefore would not be influenced by marine water (Gibbs, 1977). Although Gibbs samples were taken approximately five years before the present study samples were taken, little has happened climatically or environmentally that would change the nature of the partitioning of metals in the suspended load. It is suggested then that the results of Gibbs (1977) in general reflect the nature of metal partitioning in the suspended sediment today. Gibbs data can therefore be used to study gross differences in metal partitioning in the sediments between the freshwater environment of the Amazon River and the marine continental shelf environment. Table 2 is a summary of partitioning of metals in the soils. Soil samples were taken at Belèm.

A summary of the behavior of each metal follows. Suspended load sediments refers to Gibbs (1977), shelf sediments refer to surficial (Ø-5cm) Continental Shelf sediments.

Chromium: Most of the Cr (usually greater than 90%) is associated in the residual fractions of the suspended load, shelf sediments, and soils and suggests that most of the Cr addition to the oceans is in the detrital phase of sediments. Of the hydromorphic phases in the shelf sediment, Fe-Mn oxides are the most important in sequestering Cr;

TABLE 1

Trace metal partitioning of Cr, Mn, Co, Cu, Fe, Ni, Zn in Amazon River suspended load and surfacial shelf sediment as a function of sediment type

	Gibbs[1] Solid	Mean Shelf Surface	Shelf Surface		Shelf Surface		Shelf Surface		Shelf Surface		Shelf Surface	
Cr												
S Type[2] #	----[8]	4.29	1		2		3		4		5		6	
Smpl[3] #	----	41	7		3		1		2		16		12	
	% [9]	%	%	SDev[10]	%	SDev	%	%	SDev	%	SDev	%	SDev
EX[4]	3.96	.74	.27	.27	.12	.02	.01	.095	.15	.096	.15	.077	.06
OXD[5]	3.44	4.05	12.75	10.4	3.66	1.02	5.22	5.32	.33	4.37	3.57	3.39	.73
ORG[6]	8.43	1.53	1.31	1.11	.98	.47	1.95	1.15	.44	1.83	1.32	1.47	.56
RES[7]	84.16	94.35	85.67	11.7	95.35	1.43	92.83	93.44	.15	93.71	4.09	95.06	1.21
Mn												
S Type #	----	4.29	1		2		3		4		5		6	
Smpl #	----	41	7		3		1		2		16		12	
	%	%	%	SDev	%	SDev	%	%	SDev	%	SDev	%	SDev
EX	.95	15.47	6.44	6.41	23.29	21.3	11.17	6.07	1.37	14.52	15.5	13.14	12.0
OXD	59.15	47.12	35.76	19.7	25.39	8.44	45.90	50.21	6.71	50.95	12.7	55.68	9.89
ORG	5.92	5.08	1.84	1.13	1.88	.30	34.26	3.71	.74	5.02	1.67	6.72	1.58
RES	33.98	33.00	55.96	21.2	56.68	17.80	38.67	40.01	8.83	29.51	6.17	24.51	4.46
Co												
S Type #	----	4.29	1		2		3		4		5		6	
Smpl #	----	41	7		3		1		2		16		12	
	%	%	%	SDev	%	SDev	%	%	SDev	%	SDev	%	SDev
EX	8.21	.06	.12	.304	.025	.043	0.0	0.0	0.0	.079	.186	.24	.43
OXD	28.02	4.20	2.54	2.18	8.47	2.07	6.66	4.92	2.43	3.84	1.84	4.06	2.66
ORG	19.32	1.99	.48	.471	1.27	.45	1.85	1.19	.10	2.31	.682	2.62	.62
RES	44.44	94.31	96.80	2.82	90.23	2.49	91.52	93.88	2.53	93.77	1.88	93.41	2.56
Cu												
S Type #	----	4.29	1		2		3		4		5		6	
Smpl #	----	41	7		3		1		2		16		12	
	%	%	%	SDev	%	SDev	%	%	SDev	%	SDev	%	SDev
EX	5.26	1.79	2.2	2.70	1.34	1.17	.554	.428	.605	.45	.555	.34	.34
OXD	8.65	13.14	12.38	11.0	12.71	5.38	6.04	29.68	31.2	17.44	9.96	18.26	5.44
ORG	6.39	6.15	6.82	12.4	10.08	6.69	3.91	3.74	3.51	7.32	4.23	8.54	5.85
RES	79.70	79.61	78.57	20.4	75.86	10.1	54.33	66.15	28.3	74.80	14.2	72.87	10.80

Table 1 (cont'd.)

	Gibbs[1] Solid	Mean Shelf Surface	Shelf Surface		Shelf Surface		Shelf Surface	Shelf Surface		Shelf Surface		Shelf Surface	
Fe													
S Type[2] #	----[8]	4.29	1		2		3	4		5		6	
Smpl[3] #	----	41	7		3		1	2		16		12	
	%[9]	%	%	SDev[10]	%	SDev	%	%	SDev	%	SDev	%	SDev
EX[4]	0.0	.05	.101	.1	.132	.171	.005	.03	.004	.049	.025	.05	.048
OXD[5]	46.83	17.46	26.18	14.10	15.66	2.97	20.13	17.32	1.41	17.52	4.21	17.55	3.04
ORG[6]	6.7	.22	.17	.182	.34	.34	.13	.09	.04	.15	.034	.27	.367
RES[7]	46.47	82.82	73.56	14.3	83.98	3.32	79.73	82.56	1.45	82.29	4.21	82.13	3.22
Ni													
S Type #	----	4.29	1		2		3	4		5		6	
Smpl #	----	41	7		3		1	2		16		12	
	%	%	%	SDev	%	SDev	%	%	SDev	%	SDev	%	SDev
EX	3.19	1.60	.33	.223	.72	.993	.021	.195	.017	.319	.288	.43	.303
OXD	45.09	7.44	4.38	1.95	10.75	2.77	13.74	10.84	2.07	6.87	1.85	7.63	2.41
ORG	13.23	5.11	1.28	1.06	8.21	6.24	4.72	3.25	1.71	6.24	4.01	4.81	1.21
RES	38.44	87.10	94.00	2.90	80.32	7.88	81.53	85.72	.344	86.57	3.27	87.13	2.55
Zn													
S Type #	----	4.29	1		2		3	4		5		6	
Smpl #	----	41	7		3		1	2		16		12	
	----	%	%	SDev	%	SDev	%	%	SDev	%	SDev	%	SDev
EX	----	1.28	1.65	2.69	1.87	3.07	.095	.138	.120	.408	.633	.106	.194
OXD	----	21.15	27.02	9.84	26.78	2.92	29.41	31.93	6.24	22.97	3.59	17.90	3.18
ORG	----	5.49	6.57	2.28	7.47	.60	8.27	8.40	.273	5.64	.879	4.82	.429
RES	----	73.34	64.78	10.9	72.88	9.26	62.23	59.53	6.63	71.00	3.98	77.16	3.24

[1] Gibbs (1977) Study of Suspended load Sedments
[2] Sediment type based on Folk classification (1974)
[3] Number of samples
[4] Exchangable/loosely adsorded fraction
[5] Fe-Mn oxide fraction
[6] Organic fraction
[7] Residual fraction
[8] Missing or unknown datas
[9] Average of N samples of percent metal in fraction (values in percent)
[10] Standard deviation

TABLE 2

Trace metal partitioning of Cr, Mn, Co, Cu, Fe, Ni, Zn in selected soils of the Amazon River Drainage Basin

		Soil Core[7]							Soil Horizons[8]				
		0-[6] 2.	2- 4.4	4.4 7.5	7.5 11.1	11.1- 15.	15- 23.	23- 31.	A[9] •	B •	C •	D •	
		% [5]	%	%	%	%	%	%	%	%	%	%	
Cr	EX[1]	.17	.67	.61	.99	.69	.58	.35	.27	.21	.17	.64	
	OXD[2]	.26	.34	.40	.67	.58	.94	.78	.93	2.46	2.79	4.38	Cr
	ORG[3]	5.44	6.95	5.78	6.68	6.31	4.60	6.88	9.33	7.42	4.94	4.81	
	RES[4]	94.13	92.04	93.20	91.65	92.40	93.88	91.98	89.46	89.90	92.08	90.17	
Mn	EX	9.71	4.44	8.00	0	0	0	0	10.02	2.98	4.19	3.82	
	OXD	0	0	0	0	0	0	0	.03	.03	.038	.10	Mn
	ORG	2.04	.14	.35	2.17	1.37	1.69	2.41	.30	.71	.99	1.43	
	RES	88.26	95.42	91.65	95.91	97.67	89.45	92.91	89.64	96.29	94.78	94.65	
Co	EX	0	0	.79	.02	0	0	0	0	0	0	0	
	OXD	0	0	0	0	0	0	0	0	.07	.11	.20	Co
	ORG	0	0	0	0	0	0	0	0	.098	.03	0	
	RES	100	100	99.21	99.98	100	100	100	100	99.84	99.86	99.8	
Cu	EX	2.71	5.54	4.06	10.96	5.65	9.86	10.37	1.99	2.40	0	1.73	
	OXD	5.95	9.73	9.35	3.83	25.74	20.64	24.16	1.89	3.87	4.12	7.05	
	ORG	36.96	65.21	63.11	69.71	36.81	13.93	16.41	20.02	11.45	6.72	8.46	Cu
	RES	54.38	19.52	23.47	15.51	31.81	55.56	49.06	76.08	82.28	89.17	82.76	
Fe	EX	3.13	2.13	2.26	4.7	1.91	6.98	.66	.567	.246	.233	.091	
	OXD	16.19	14.84	20.53	40.16	26.17	28.67	3.42	11.35	12.94	13.589	13.47	Fe
	ORG	.44	.30	.57	.42	.38	.26	0	.33	.14	.109	.062	
	RES	80.23	82.72	76.65	54.71	71.54	64.09	95.92	87.75	86.67	86.07	86.37	
Ni	EX	.23	.35	1.83	.086	.42	.58	.46	.738	.34	1.17	.36	
	OXD	0	0	0	0	0	0	0	0	0	0	0	Ni
	ORG	.25	.19	.47	0	0	.02	.06	.587	.13	3.79	.241	
	RES	99.51	99.45	97.69	99.91	99.57	99.39	99.48	98.67	99.50	95.02	99.39	

Table 2. (cont'd.)

		Soil Core[7]							Soil Horizons[8]				
		0-[6] 2.	2- 4.4	4.4 7.5	7.5 11.1	11.1- 15.	15- 23.	23- 31.	A[9] •	B •	C •	D •	
		% [5]											
Zn	EX[1]	34.61	19.87	44.67	38.13	13.23	36.42	29.97	12.37	4.83	4.20	6.58	
	OXD[2]	26.70	11.09	18.52	44.69	21.69	46.83	27.88	6.63	6.22	8.87	13.62	Zn
	ORG[3]	5.41	4.22	5.00	5.66	2.32	8.42	5.25	2.22	1.55	2.49	3.54	
	RES[4]	33.27	64.81	31.80	11.51	62.75	8.32	36.90	78.76	87.40	84.40	76.20	

[1]Exchangeable/loosely adsorded fraction
[2]Fe-Mn oxide fraction
[3]Organic fraction
[4]Residual fraction
[5]Average of percent metal in fraction
[6]Depth of core in cm
[7]Soil core depth in cm
[8]Soil horizon
[9]Soil horizon in core

organic matter is second with the exchangeable fraction playing a relatively minor role. This nature of Cr partitioning in sediments is consistent with past work (Gephart, 1982).

The relative partitioning of Cr amount in the sediment fraction does not appear to be strongly dependent on grain-type in the shelf sediments. There is, however, significantly more Cr in the hydromorphic fraction of the sediments composed of sand (Type 1) than the other sediment types, with the Fe-Mn oxide fraction becoming very dominate in the sequestering of Cr. The nature of Cr partitioning in the sand sediment is consistant with the higher amount of hydromorphic Fe in this sediment type with respect to the other sediments (Table 1).

In general, there is slightly less metal in the hydromorphic fraction of the shelf sediments compared to the suspended load sediments. Organic matter is more important in sequestering Cr than Fe-Mn oxides in the suspended load. The hydromorphic fraction of the soil better reflects the partitioning in the suspended load rather than the shelf sediments, in that the organic fraction is dominate. The exchangeable and Fe-Mn oxide fractions have very minor roles in the sequestering of Cr in the soil samples.

The nature of Cr partitioning in the Amazon River environment suggests that Cr undergoes a repartitioning from river to shelf (e.g., organic fraction to Fe-Mn oxide fraction) and that the suspended sediment could be a source for dissolved Cr to seawater (e.g., less Cr in hydromorphic fraction of shelf sediments). The direction of repartitioning (organic matter to Fe-Mn oxide) suggests that organic matter could be a source of the dissolved Cr within the sediment.

Manganese: The Fe-Mn oxide fraction and residual fraction, combined account for the majority of Mn concentration in both suspended load and shelf sediments (approximately 80-95%). The amount of Mn in the Fe-Mn oxide fraction, the dominate fraction, decreases from suspended load to marine environment, whereas Mn in the detrital fraction in both suspended load and shelf remains similar (33%). The Mn organic fraction concentrations are of minor importance (5%) and are similar for shelf and suspended load sediments. The exchangeable fraction accounts for less than 1% total Mn in the suspended load sediments but increases in the shelf sediments to 15%. In general Mn can be quite mobile in this system since most of the Mn occurs in the hydromorphic phase.

Mn partitioning in the oxide, organic and detrital fractions of shelf sediments, appear to be influenced by grain-type. There is more Mn hydromorphics in clay sediments (Type 6) than in the other sediments. Within the hydromorphic fraction, the oxide fraction is dominate and increases from sand (Type 1) to clay (Type 6) sediments, 35% to 55% respectively. The organic fraction behaves similar to the oxide fraction (e.g., Type 1 at 1.8% increases to Type 6 at 55%). This Mn behavior is contrary to Cr hydromorphic behavior which decreases from sands (Type 1) to clays (Type 6) and Cr detrital fraction behavior which increases from sand (Type 1) to clay (Type 6) sediments.

The Mn in soils have a different distribution pattern among the four fractions than either the suspended load or shelf sediments. Of major importance in Mn sequestering in soils is the detrital fraction (at greater than 89%). The hydromorphic fraction is of minor importance with the oxide fraction being the most insignificant. This is a drastic change from shelf and suspended load sediments which had the

oxide fraction being of primary importance. In general, the data from Table 1 indicates that Mn undergoes repartitioning within the hydromorphic fraction from a river to a marine environment (e.g., oxide fraction to exchangeable fraction).

Cobalt: The detrital fraction is the fraction accounting for most of Co in shelf sediments and soils (90% and 99%, respectively). The dominance of the detrital fraction over the hydromorphic fractions has been found previously (Loring, 1979). The detrital fraction is also dominate (44%) versus the exchangeable, organic or oxide fractions. In the suspended load sediments, the hydromorphic fraction is the dominate fraction for Co concentration. Within the hydromorphic fraction for the suspended load sediments, the Fe-Mn oxide fraction dominates (28%), of secondary importance is the organic fraction (19%), and of least importance is the exchangeable fraction (8%).

The partitioning of Co in shelf sediments and soils are similar and differ from suspended load sediments. Shelf sediments and soils have 90-99% of Co sequestered in the detrital fraction with the hydromorphic fraction playing a minor role. However, in the suspended load (River) sediments the hydromorphic fraction dominates (e.g., 56%).

There are slight grain-type variations observed in Co. The hydromorphic fraction increases from sand (Type 1) to clay (Type 6) sediment. Co partitioning among various grain-types in shelf sediments is similar to Mn partitioning (e.g., the hydromorphic fraction increases from Type 1 to Type 6).

Generally, the nature of Co partitioning in this system suggests that Co goes through repartitioning from river to shelf (e.g., hydromorphic fraction to detrital fraction) and that the change in relative

importance of the hydromorphic fraction (56% to 6%) could be a source for dissolved cobalt to seawater.

Copper: Approximately 79% of the Cu is associated in the detrital fraction (suspended, shelf, and soil horizons). Therefore, most of the Cu in sediments brought into the ocean is in the detrital phase. The hydromorphic fraction (suspended and shelf) comprise the remaining 21% of Cu sequestered in sediments. Within the hydromorphic fraction, the oxide fraction is dominate (8-13%), followed by the organic fraction (6%) and the exchangeable fraction (2-5%). Comparing the organic and detrital fractions for suspended loads and shelf sediments, similar percent concentration values exist (6% organic fraction and 79% detrital fraction). However, the exchangeable fraction drops from 5% to 2% and the oxide fraction increases from 8% to 13% in suspended versus shelf sediments.

There is little significant change among the different grain-types (Types 1-6) in the detrital or hydromorphic fractions, although, there is a slight influence of grain-type on the exchangeable fraction. The exchangeable fraction decreases from Type 1 (2%) to Type 6 (.3%).

The nature of Cu partitioning between a soil core (sample from Belèm) and soil horizons (A-D) are different. Soil horizons have a similar partitioning trend for Cu in shelf and suspended load sediments. The soil core has a residual fraction of Cu relative percent value of 23-55%. The hydromorphic fraction has a relative Cu concentration value of 21% for suspended load sediments, shelf sediments and soil horizons and increases to 45-77% for soil core.

In general, there is little repartitioning between the hydromorphic and detrital fractions from river to shelf environments. But,

within the hydromorphic fraction repartitioning occurs. Repartitioning of Cu from river to shelf environments is via the exchangeable fraction to the oxide fraction. This suggests that the oxide fraction is playing a greater role in sequestering Cu and that the exchangeable fraction may release Cu to seawater (i.e., be a source of Cu to seawater).

Iron: The major phases of Fe in the suspended sediments are the detrital fraction (46%) and oxide fraction (46%). There is a dramatic increase (46%-82%) in Fe detrital fraction and subsequent decrease in hydromorphic fraction from suspended load to shelf sediments. The dominate Fe fraction within the hydromorphic phase of the shelf sediments is the oxide fraction (17%). The organic and exchangeable phase are of minor significance.

Shelf sediments are slightly grain-type dependent. The detrital fraction in Type 1 is at a lower relative percent value than Type 6 (73% to 82%, respectively). There is a corresponding decrease in hydromorphic fraction from Type 1 to Type 6.

Soils (core and horizon) and shelf sediments have similar partitioning data. The detrital fraction dominates Fe partitioning with the oxide fraction of secondary importance. The organic fraction and exchangeable fraction are of minor importance.

Repartitioning does occur in Fe sediment concentrations between river and shelf sediments. The hydromorphic fraction decreases Fe concentration values while the residual fraction increases from river to shelf environments. This suggests that the suspended load can be a source of Fe to seawater.

Nickel. In the suspended load sediments the relative partitioning of Ni is dominated by the oxide fraction (45%) and the detrital fraction

(38%). Of minor importance are the organic fraction (13%) and the exchangeable fraction at 3%. The shelf sediments have different partitioning of Ni. Most of the Ni in the shelf sediments are in the detrital fraction (87%). Partitioning of Ni in the hydromorphic fraction of the shelf sediments is oxide fraction (7%), organic fraction (5%), exchangeable fraction 1%.

Shelf sediments appear slightly dependent on grain-type. The residual fraction has a slightly higher concentration percentage value in Type 1 grain-type (94%) as opposed to Type 6 (87%). Corresponding to this change, the hydromorphic fraction increases from Type 1 (6%) to Type 6 (13%).

Soils, both horizons and core samples, behave in a similar partitioning pattern as shelf sediments but not as suspended load sediments behave. Soils appear to have one dominate fraction (detrital 95-99%) for Ni. The hydromorphic fraction is minor and within this fraction, the oxide fraction is at undetectable levels.

The nature of Ni partitioning from suspended load to shelf environment suggests Ni repartitioning. The oxide fraction in the suspended load sediment repartitions to the detrital fraction in shelf sediments. This repartitioning of hydromorphic fraction (especially the oxide fraction) can be a potential source for Ni to seawater from suspended load sediments.

Zinc: Gibbs (1977) did not analyze for Zinc in suspended load sediments and therefore there will be no comparison between suspended load and shelf sediments for zinc. However, partitioning data for zinc is available for soil samples, shelf sediment and shelf sediment changes with grain-type (Table 1). The residual fraction (73% for shelf

sediments) is the dominate fraction of Zn in shelf sediments. The oxide fraction is of secondary importance at 21% with both organic (5%) and exchangeable (1%) fractions being of minor importance.

Grain-type dependency is observed in the residual as well as hydromorphic fractions. There is an increase in detrital Zn for Type 1 (64%) to Type 6 (77%). Corresponding to this increase, is a relative decrease in the hydromorphic fraction (Type 1 at 36% to Type 6 at 23%). All three individual phases (exchangeable, oxide, organic) within the hydromorphic fraction decrease from Type 1 (sand) to Type 6 (clay).

The soil horizons display a similar behavior as shelf sediments. The detrital phase is dominate (76-78%) and the hydromorphic is of lesser importance. However, soil core samples differ. They display two dominate fractions, the detrital and the oxide.

In summary:

(1) Only Cr and Cu have the majority of their concentration in the residual fraction for all three environments (suspended load, shelf, soil).

(2) Two fractions dominate the partitioning of Mn, Co, Ni, Fe in suspended load sediments (almost equal fractions): oxide and detrital.

(3) In general, most metals (90%) are in a combination of residual and oxide fractions.

(4) The hydromorphic fraction is dominate in controlling the behavior of Mn in both suspended and shelf environments.

(5) All metals except for Mn and Cu show a decrease in the organic fraction from river to shelf environments.

(6) All metals except for Mn and Cu show a decrease in the percentage of the metals in the hydromorphic fraction from river to shelf environments.

(7) In general, the relative partitioning trends as a function of grain-type are preserved for all metals.

(8) The hydromorphic fraction for Mn, Co, Cu, Ni all have grain-type trends which increase element concentrations from Type 1 and Type 6, Cr and Zn have a reverse trend.

(9) The relative partitioning within the hydromorphic fraction is highly variable between soil and shelf environment, except for Cr, the relative partitioning of the metals between the soils and suspended material are not similar.

(10) Cr, Co, Cu, Fe, Zn, Ni are partitioned similarly in shelf sediments (detrital 73-94%; oxide 4-27%; organic .2-6%; exchangeable 0-2%).

(11) Relative partitioning of Mn, Cr, Cu in the sediment percent is the same in river and shelf environments.

(12) Differences were observed in the relative partitioning of Fe, Co, and Ni between the sediments at the river and those of the shelf. The hydromorphic fraction (especially the oxide fraction) is much smaller in the shelf sediments.

The data can be interpretated to suggest that:

(1) Significant repartitioning occurs between water and shelf environments.

(2) Upon mixing with seawater the sediment could be a source of metals to seawater, the order of importance of this source decreases in the order Ni>Co>Fe>Cr.

(3) Decay (oxidation) of organic matter could be the source of metal to seawater within the sediment.

Distribution of Metals on the Shelf:

The behavior of selected trace metals in this system were studied by the construction of contour maps of elemental concentrations in the surface sediment (Figures 11-13). Distribution maps were created for Zn and Ba. Zinc behavior was studied as a representative of a metal with both significant hydromorphic as well as residual partitioning.

Figure 11. Contour map of zinc in the detrital fraction of the surface (Ø-5 cm) sediment of the Amazon Continental Shelf.

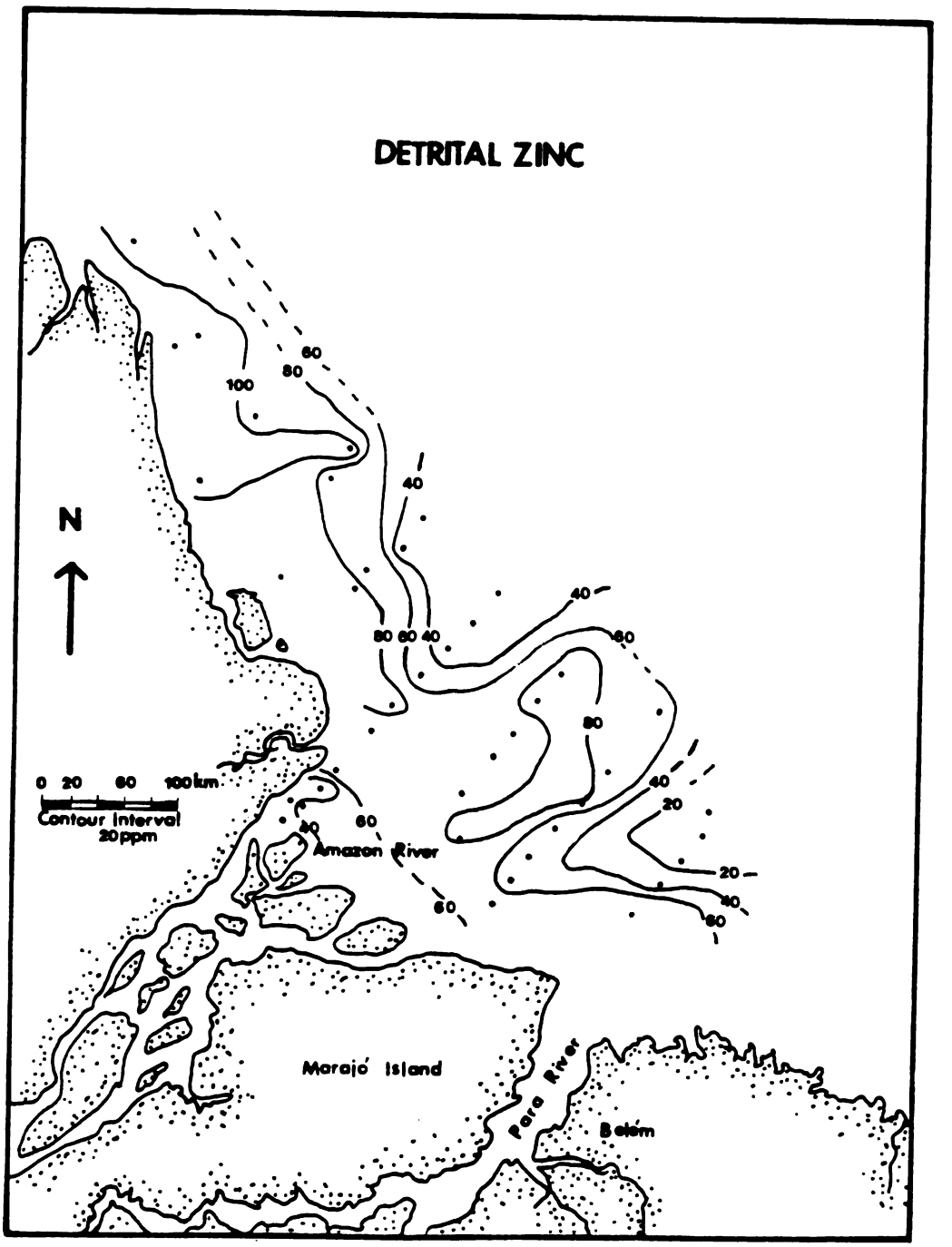
DETRITAL ZINC
N
0 20 60 100km
Contour Interval
20ppm
100
80
60
40
20
Amazon River
Marajó Island
Pará River
Belém

Figure 12. Contour map of zinc in the hydromorphic fraction of the surface (Ø-5 cm) sediment of the Amazon Continental Shelf.

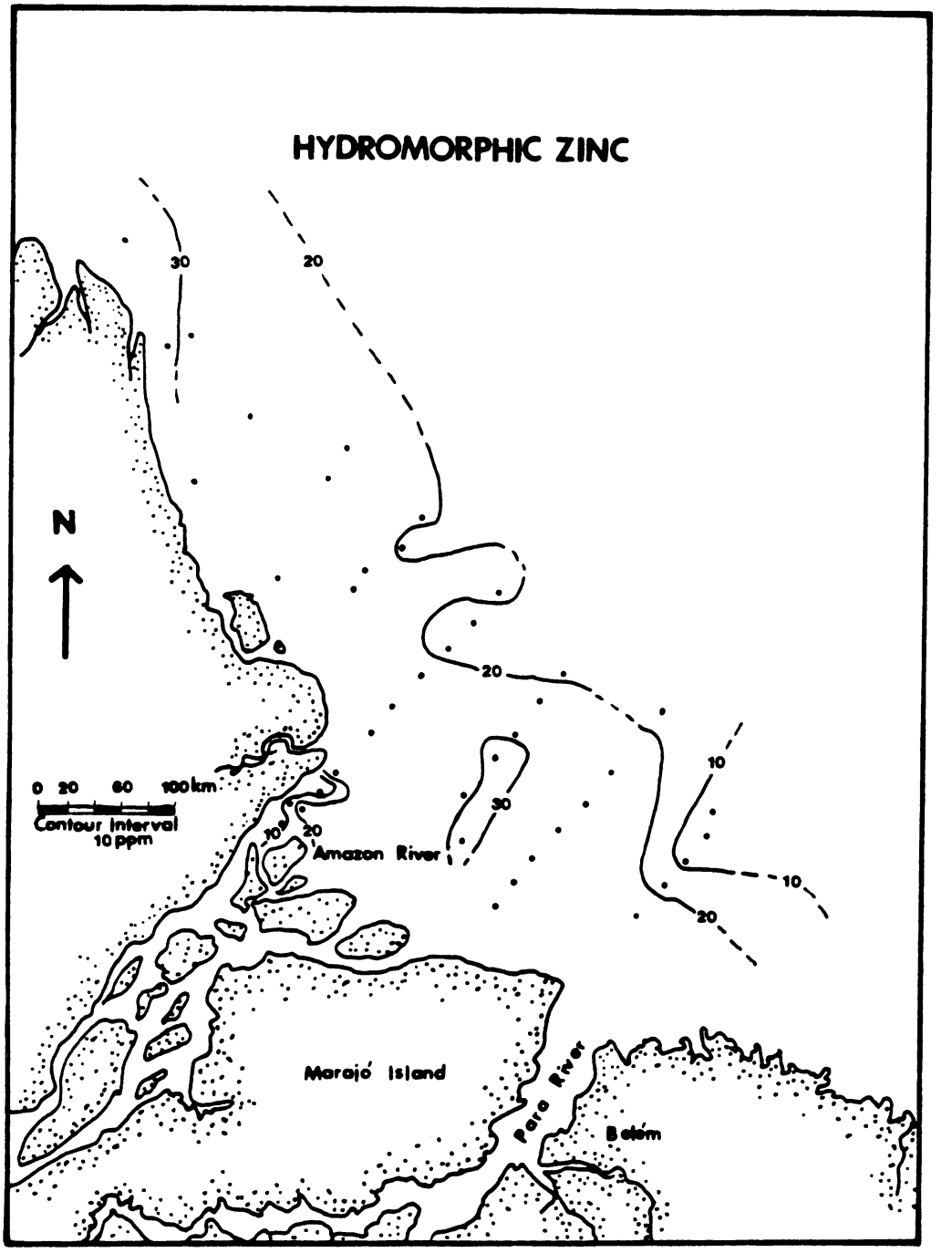
HYDROMORPHIC ZINC
30
20
N
20
10
0 20 60 100 km
Contour Interval
10 ppm
10
20
Amazon River
30
10
20
Marajó Island
Para River
Belém

Figure 13. Contour map of total zinc in the surface (Ø-5 cm) sediment of the Amazon Continental Shelf.

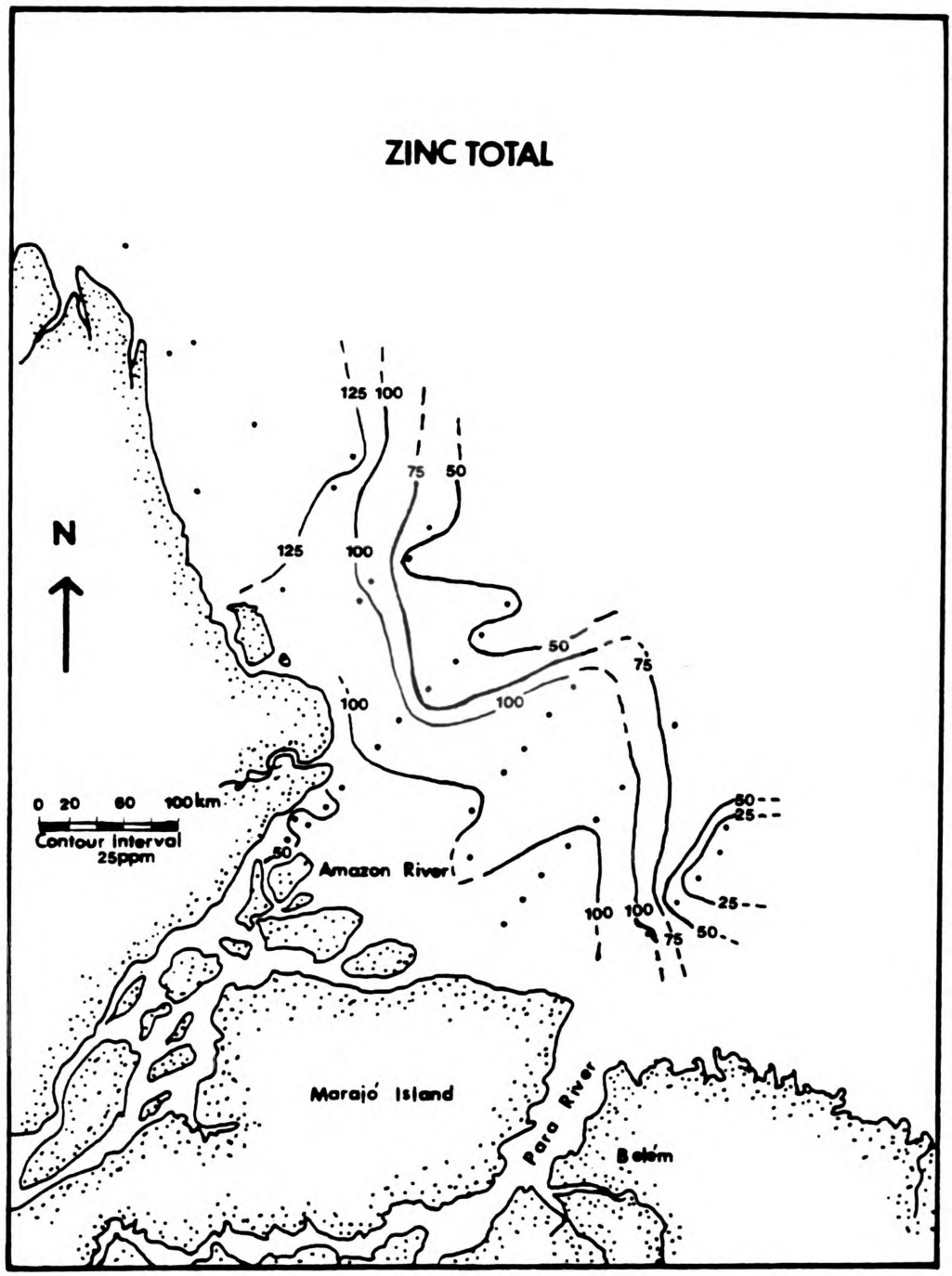
ZINC TOTAL
N
0 20 60 100km
Contour interval
25ppm
125
100
75
50
25
Amazon River
Marajó Island
Para River
Belém

Ba was chosen for study because it is an alkaline element and should behave differently than the transition metals studied.

Concentrations of zinc in the continental shelf sediments are shown in Figures 11, 12, and 13 representing absolute values of Zn in the detrital fraction, hydromorphic fraction and total sediment, respectively. The concentration patterns are similar in each figure and appear to reflect the distribution of sediment types on the shelf (Figure 5).

The concentration of Zn decreases from core location 2 (Type 6) to core locations 3,4,5,6 (Type 1). Core locations 30 and 33 (Type 1) have corresponding lower concentrations than core locations 31 and 32 (both of Type 5). Core locations 35, 29 and 28 all of similar type (Type 6) display similar concentrations. Cores 47-57, again reflect grain-type composition; they display similar grain-type compositions (Type 5) and therefore similar concentration values.

The dependency on grain-type for metal concentrations in the shelf sediments can be further demonstrated by plotting elemental concentration in the sediment versus grain-type. Figures 14, 15, and 16 are such plots for Zn-total, Zn-residual and Zn-hydromorphic, respectively. These Figures show distinct clusters of Zn concentrations depending on grain-type, with the biggest difference between Type 1 and Types 5 and 6 (sand and silt-clay, respectively). If the concentrations are plotted as ranked data, rather than as absolute data, the differences are made even clearer. For example, Figure 17 is a plot of sediment type versus Zn hydromorphic using ranked concentrations. One can clearly see that the concentration distribution of the Zn in the shelf sediment can be explained by the distribution of the various sediment

Figure 14. Plot of sediment type versus concentration of zinc total. Numbers refer to overlapped points.

Figure 15. Plot of sediment type versus concentration of zinc in the detrital fraction. Numbers refer to overlapped points.

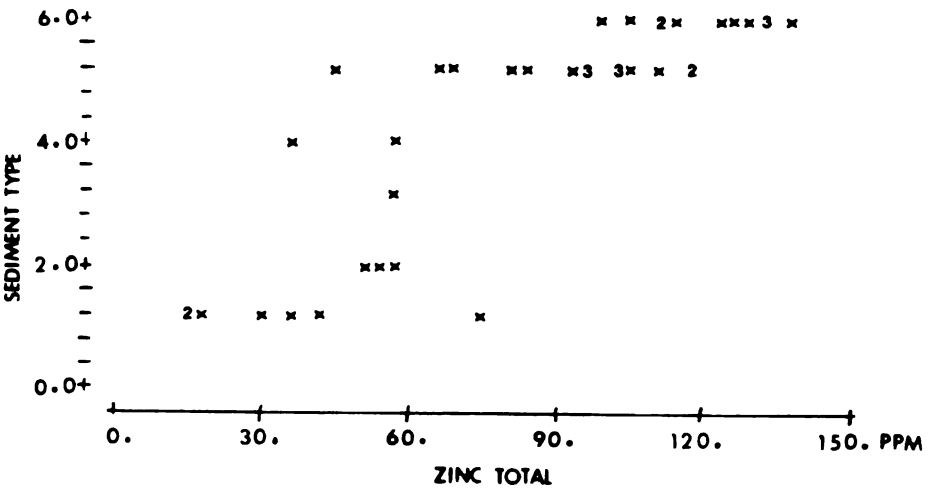
6.0+
4.0+
2.0+
0.0+
SEDIMENT TYPE
0.
30.
60.
90.
120.
150. PPM
ZINC TOTAL

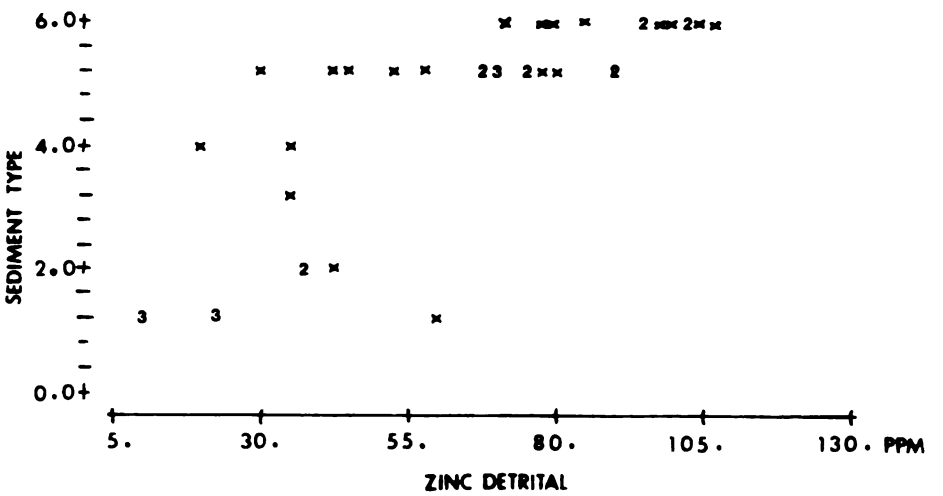
6.0+
4.0+
2.0+
0.0+
SEDIMENT TYPE
5.
30.
55.
80.
105.
130. PPM
ZINC DETRITAL

Figure 16. Plot of sediment type versus concentration of zinc in the hydromorphic fraction. Numbers refer to overlapped points.

Figure 17. Plot of sediment type versus concentration of zinc in the hydromorphic fraction plotted as ranked data.

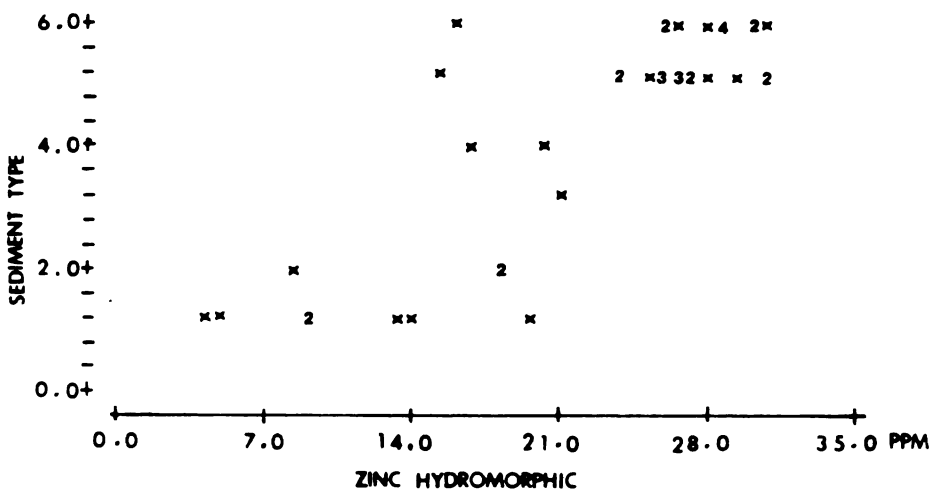
6.0+
4.0+
2.0+
0.0+
SEDIMENT TYPE
0.0
7.0
14.0
21.0
28.0
35.0 PPM
ZINC HYDROMORPHIC

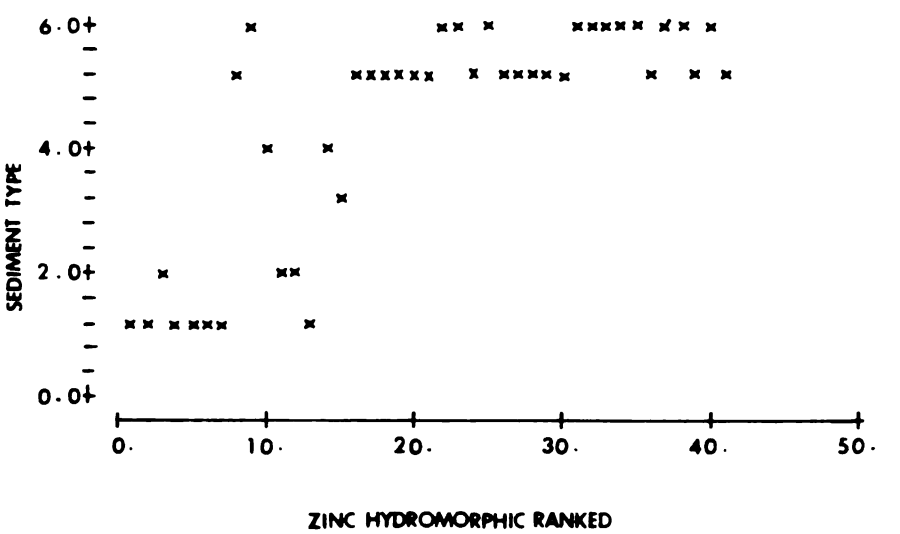
6.0+
4.0+
2.0+
0.0+
SEDIMENT TYPE
0.
10.
20.
30.
40.
50.
ZINC HYDROMORPHIC RANKED

type over the shelf. The dependency of metal concentration on grain-type is supported by the works of Gupta and Chen (1975), Loring (1979). On the Amazon Continental Shelf, grain-type appears to control metal concentration.

These results suggest that physical processes (mechanical deposition as a function of sediment type and shelf hydrodynamics) are mainly responsible for the distribution of metals on the shelf.

In an attempt to eliminate the effect of grain-type on metal concentrations when interpretating partitioning data, ratioed concentrations were studied. By using ratios, other possible controls (biogenic and geochemical) on metal distributions in shelf sediments can be deduced (Long and Gephart, 1982).

Ratios of metal concentration to Al were used to study metal distribution independent of biogenic effects (Sholkovitz and Price, 1980). Figures 18 and 19 are concentration maps of Zn residual/Al residual and Zn hydromorphic/Al total, respectively. Both maps show a strong dependency on grain-type and suggests that biogenic controls on the distribution of Zn in the shelf sediment is minor.

Zn, Ba/Fe + Mn oxide ratios were also utilized. The Fe + Mn oxide ratios were chosen because of the dependency of the oxide fraction on grain-type and by utilizing the ratio, normalization with respect to grain-type dependency was sought (Tessier et al., 1982). Figure 20 is a concentration map of Zn oxide/Fe + Mn oxide. The Zn oxide ratio has a uniform distribution across the shelf. Figure 21 is of Ba oxide/Fe + Mn oxide. The Ba oxide ratio has a high concentration (dump) at the mouth of the river and values decrease away from the coast. Figure 21 could be related to salinity, as the river waters mix with the oceans a

Figure 18. Contour map of the ratio zinc in the detrital fraction divided by aluminum in the detrital fraction in the surface (Ø-5 cm) sediments of the Amazon Continental Shelf.

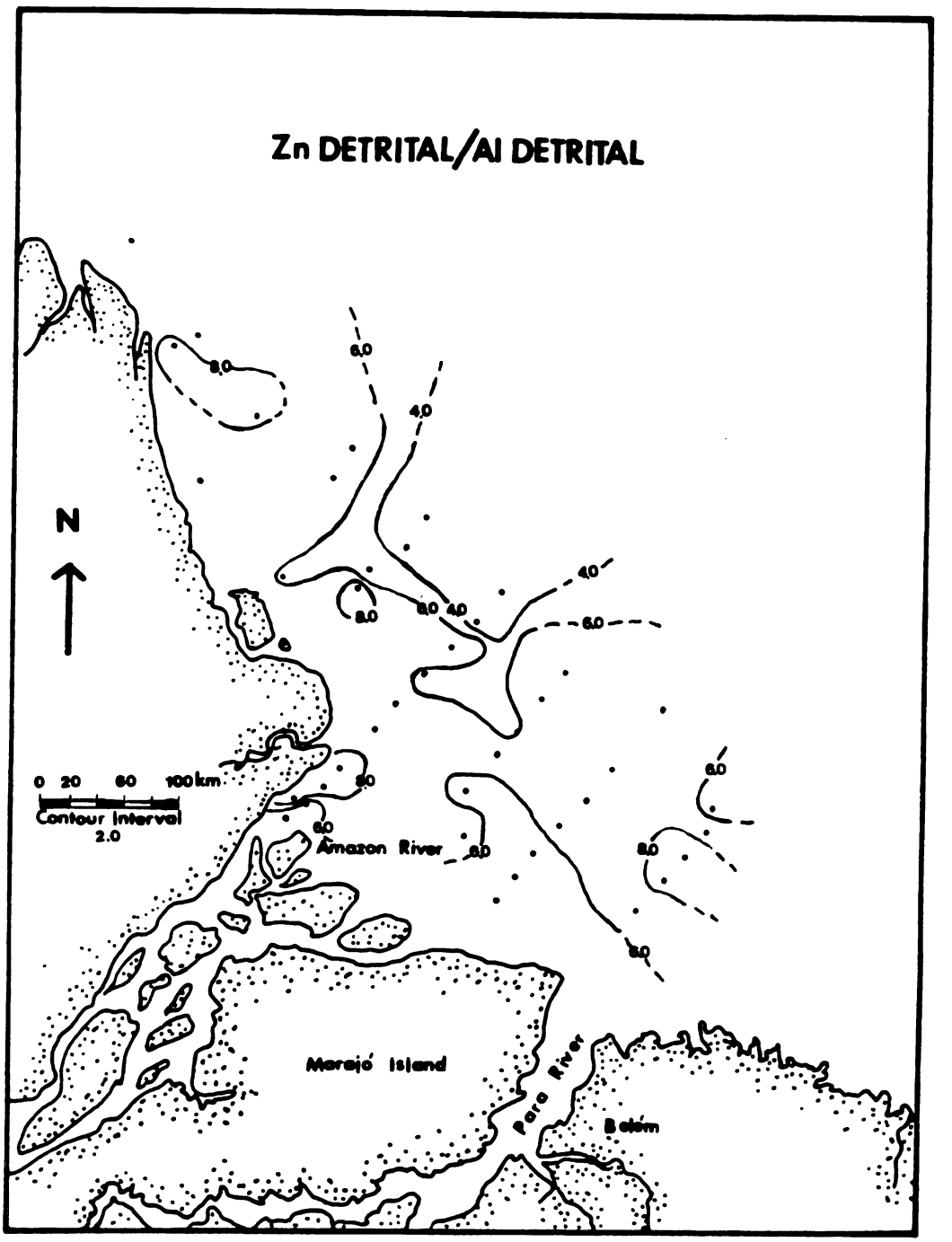
Zn DETRITAL/Al DETRITAL
N
0 20 60 100km
Contour Interval
2.0
8.0
6.0
4.0
Amazon River
Marajó Island
Para River
Belém

Figure 19. Contour map of the ratio hydromorphic zinc concentration divided by total aluminum concentration in the surface (0-5 cm) sediments of the Amazon Continental Shelf.

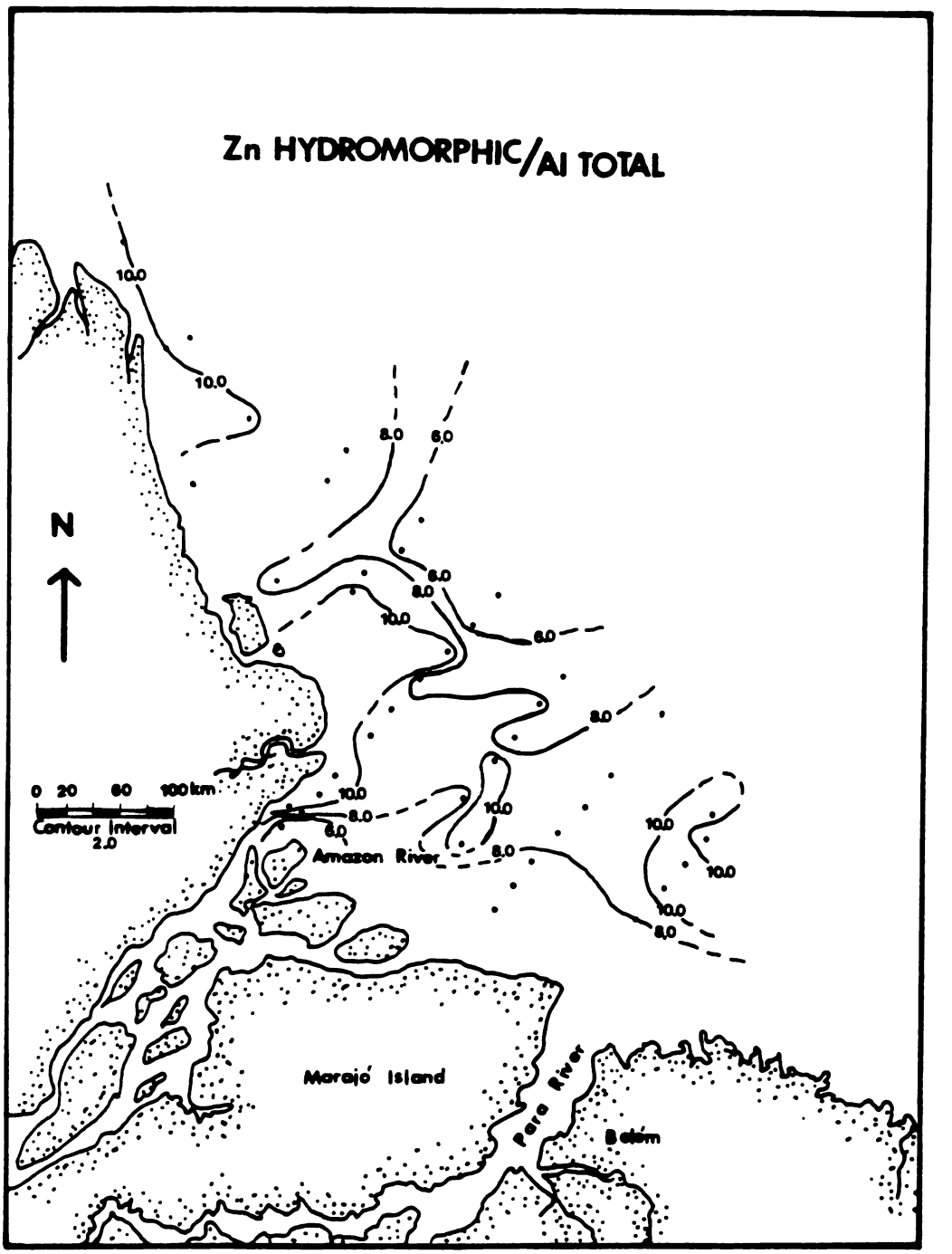
Zn HYDROMORPHIC/Al TOTAL
N
0 20 60 100 km
Contour Interval
2.0
10.0
8.0
6.0
Amazon River
Marajó Island
Pará River
Belém

Figure 20. Contour map of the ratio zinc in the oxide fraction divided by iron and manganese in the oxide fraction in the surface (Ø-5 cm) sediments of the Amazon Continental Shelf.

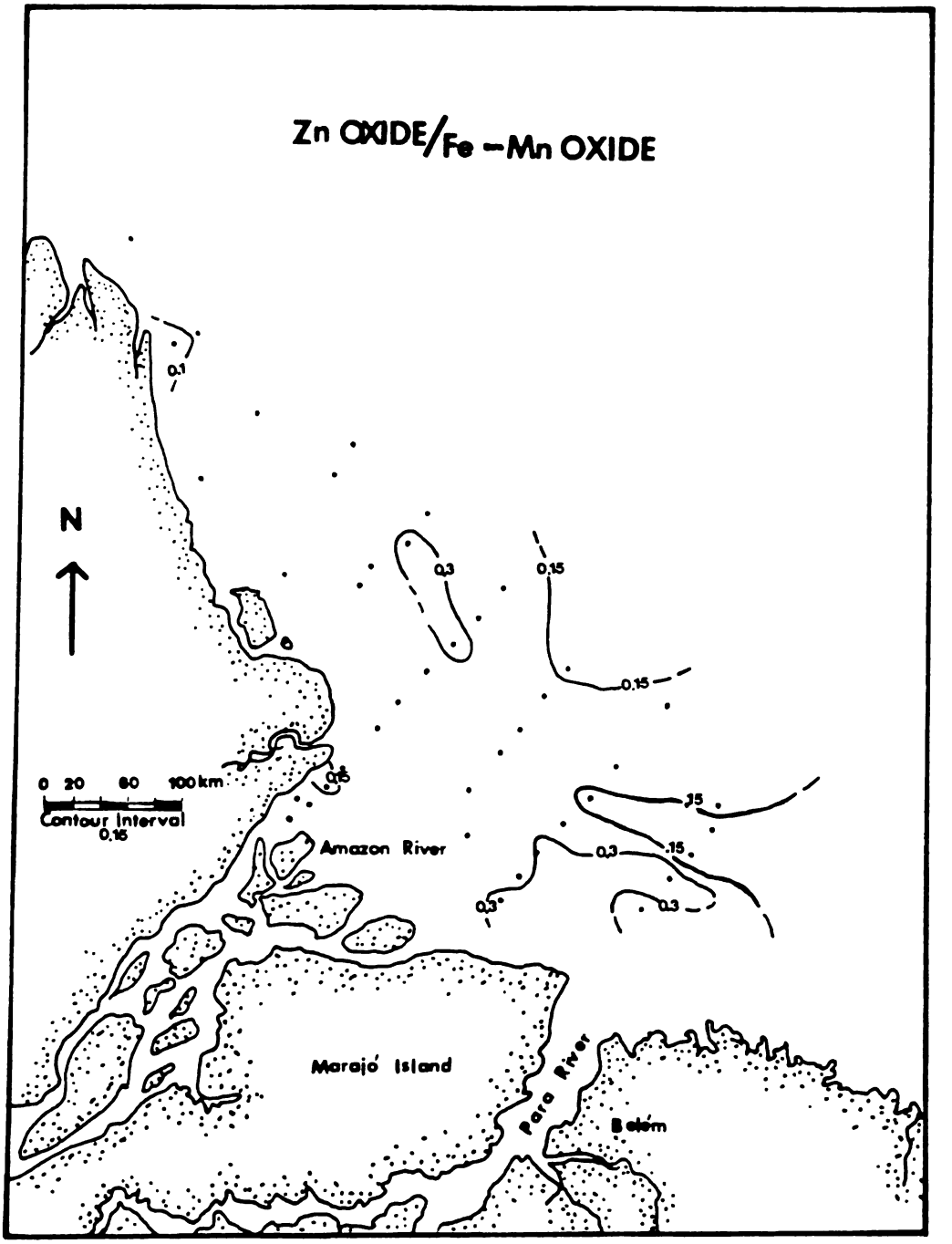
Zn OXIDE/Fe -Mn OXIDE
N
0.1
0.3
0.15
0.15
0.15
.15
0.3
.15
0.3
0.3
0 20 60 100 km
Contour interval
0.15
Amazon River
Marajó Island
Pará River
Belém

Figure 21. Contour map of the ratio barium in the oxide fraction divided by iron and manganese in the oxide fraction in the surface (Ø-5 cm) sediments of the Amazon Continental Shelf.

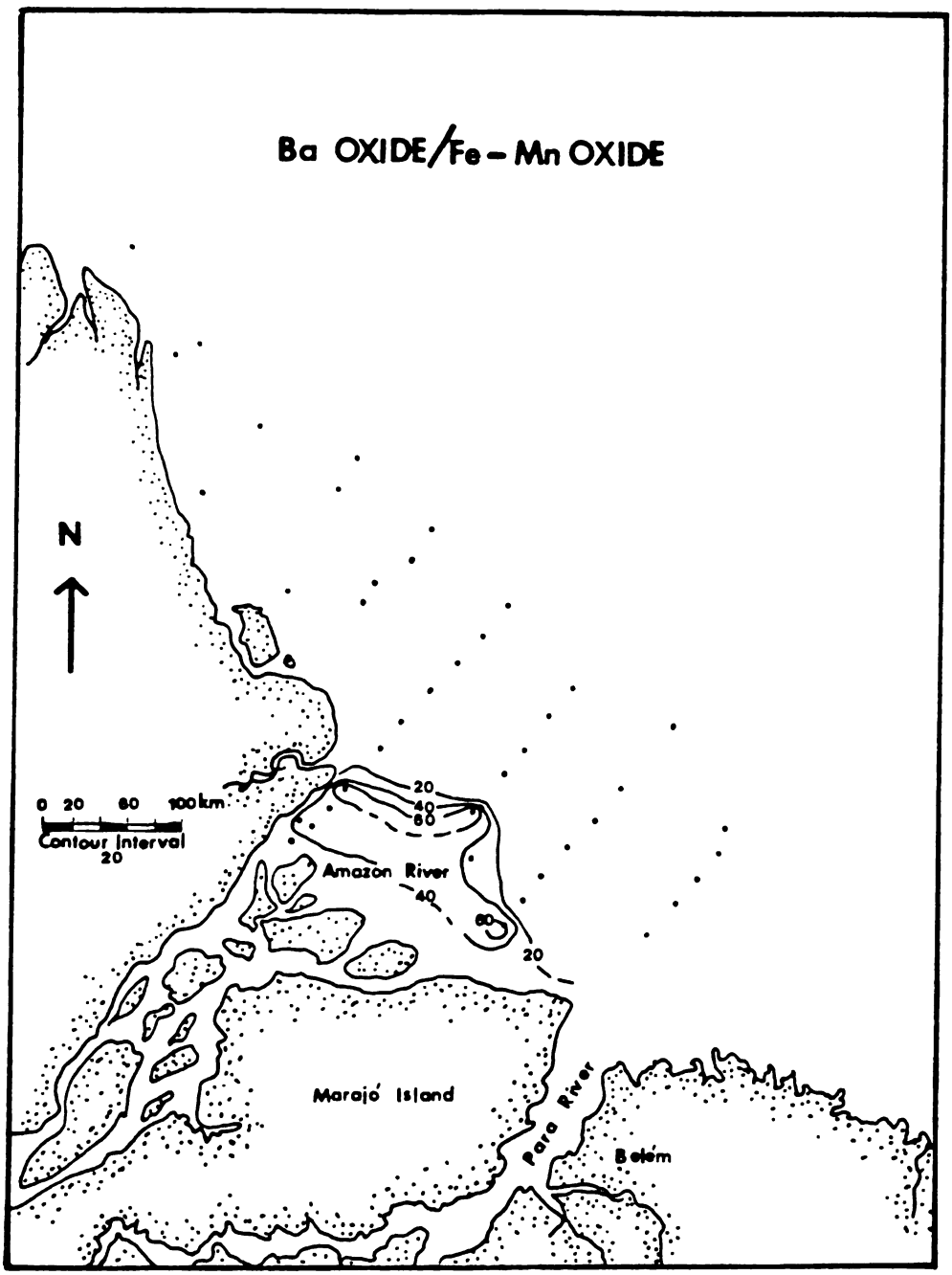
Ba OXIDE/Fe – Mn OXIDE
N
0 20 60 100km
Contour Interval
20
20
40
60
Amazon River
40
60
20
Marajó Island
Para River
Belém

drop in terrigenous sediment load occurs before 3 0/00 salinity (Milliman et al., 1975) (Figure 3). Both maps (Figures 20 and 21) no longer show the strict grain-type dependency for the distribution of the metal in the sediment, each map having a slightly different distribution pattern.

Figures 22 and 23 show Zn hydromorphic/Zn residual and Ba hydromorphic/Ba residual, respectively. Both Figures (22 and 23) display an increase in hydromorphic/detrital ratios as one moves in a direction across the shelf, away from the coast. Also observed in Figure 22 is the high ratio Zn values associated with sediments of Types 1 and 2 (sands). These Figures suggest that either the hydromorphic fraction is a source for metals to seawater resulting in a decrease in hydromorphic fraction or that metal is repartitioned from the hydromorphic fraction to the detrital resulting in an increase in residual fraction to account for observed ratio trends.

Diagenesis of Metals in Amazon Shelf Sediments:

Sediment samples were taken as a function of depth at locations 10 and 42 (Figure 1). Core 42 and core 10 were found to have similar trends and therefore only core 10 will be discussed. Metal concentrations versus depth profiles are in Figures 24-31 for core 10. Figure 24 shows sediment type for samples with depth. Figure 25 is a plot of Cr concentration with depth and shows that the organic and oxide phases are of minor importance in controlling Cr concentration and have a constant value throughout the core. Chromium concentrations in the detrital phase, however, show several fluctuations. There is a decrease at 50 cm (silt composition), an increase at 220 cm (clay composition), a

Figure 22. Contour map of the ratio zinc in the hydromorphic fraction divided by zinc in the detrital fraction in the surface (Ø-5 cm) sediments of the Amazon Continental Shelf.

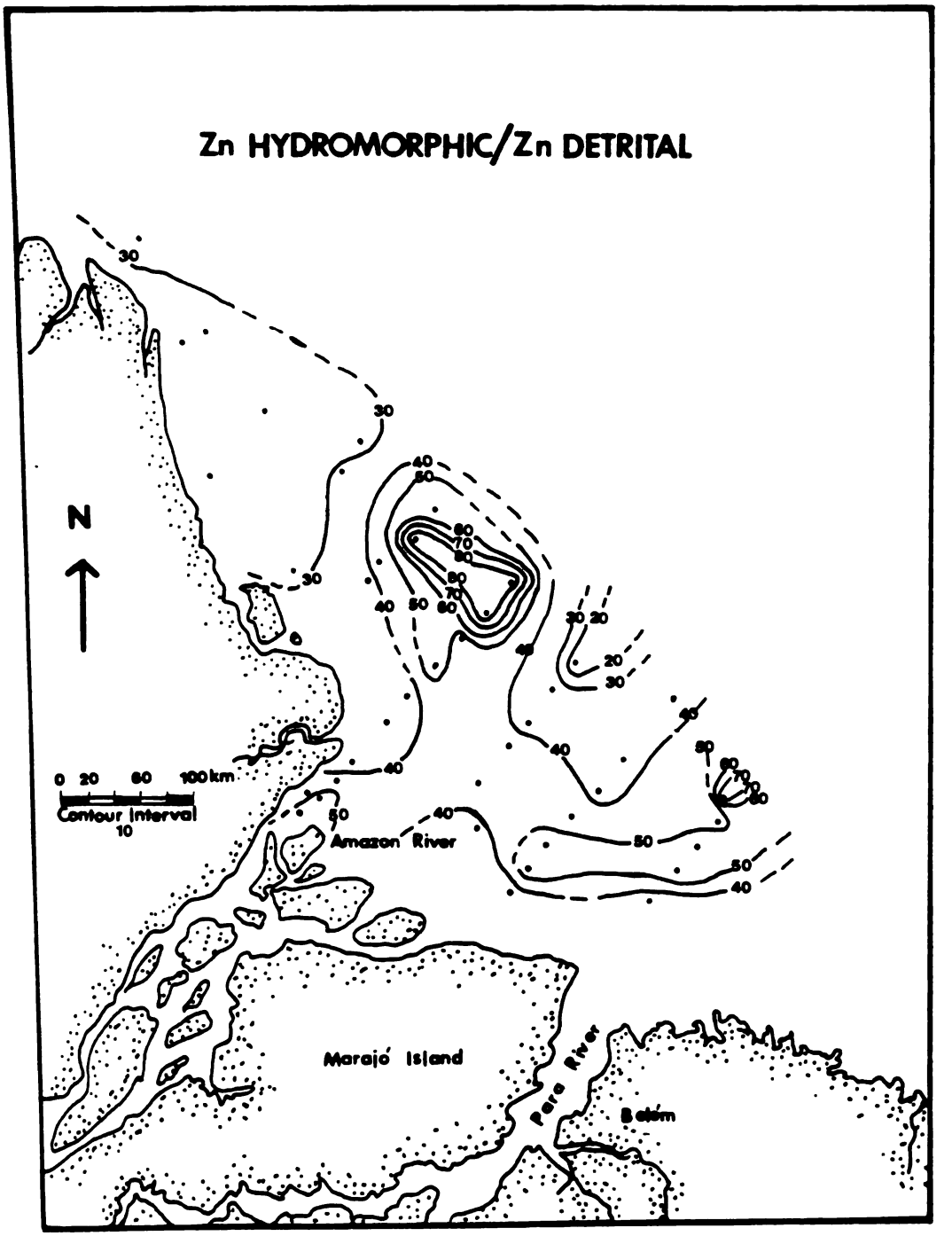
Zn HYDROMORPHIC/Zn DETRITAL
N
0 20 60 100 km
Contour Interval
10
Amazon River
Marajó Island
Pará River
Belém

Figure 23. Contour map of the ratio barium in the hydromorphic fraction divided by barium in the detrital fraction.

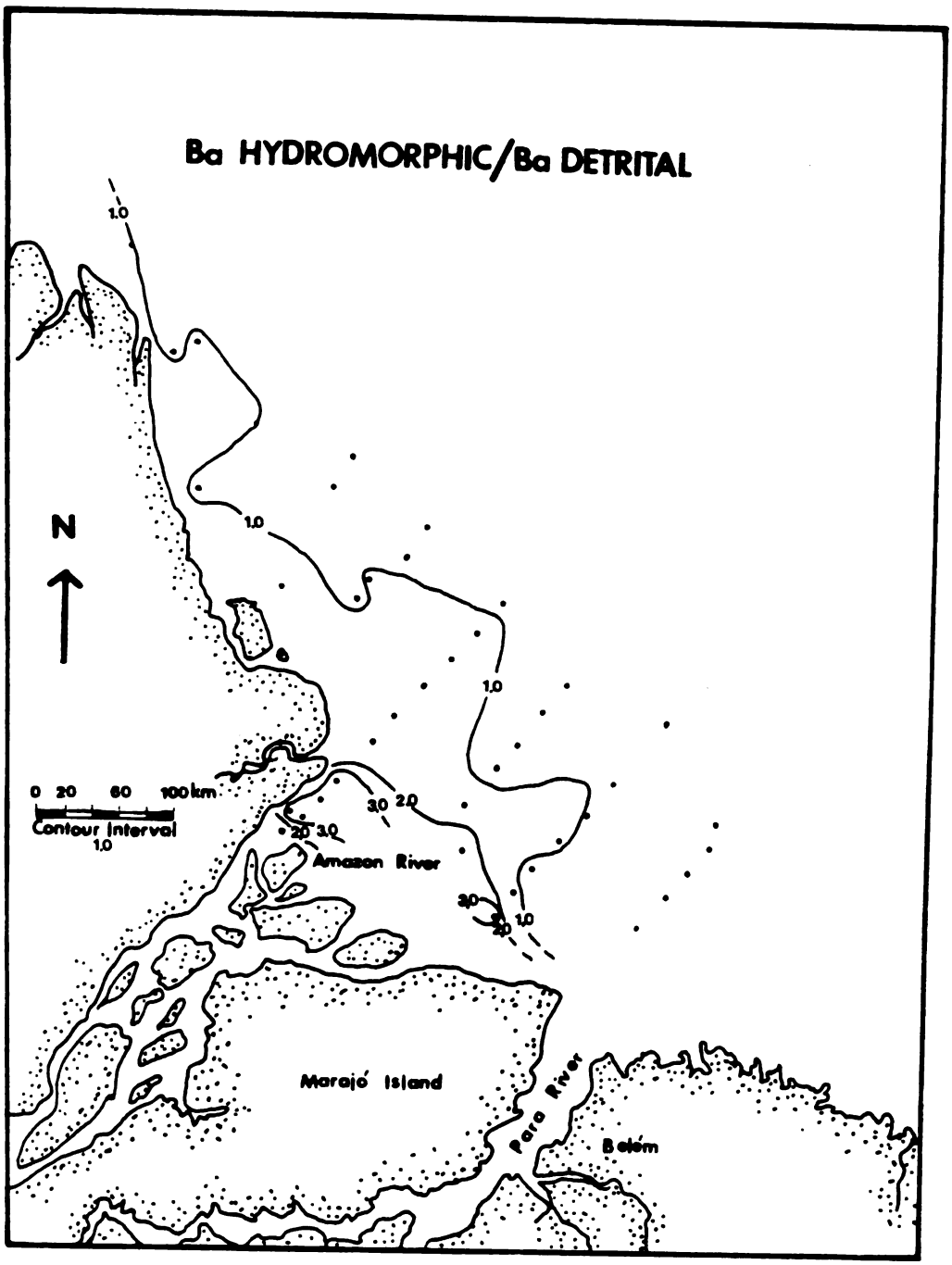
Ba HYDROMORPHIC/Ba DETRITAL
1.0
1.0
1.0
N
0 20 60 100km
Contour Interval
1.0
3.0
2.0
2.0
3.0
Amazon River
3.0
2.0
1.0
Marajó Island
Para River
Belém

Figure 24. Sediment type with depth for core 10 (Nittrouer et al., 1983).

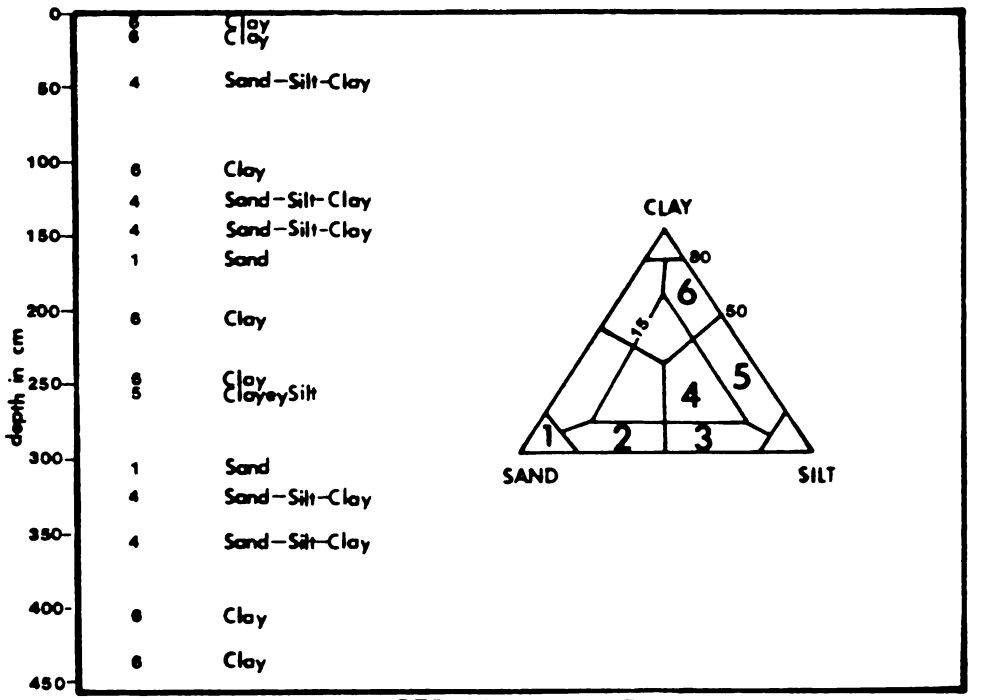

SEDIMENT TYPE
CORE 10

Figure 25. Concentration of chromium with depth in core 10.

Symbol key:

■ ORG - organic fraction

▲ OXD - oxide fraction

● RES - detrital fraction

\- TOT - total Cr concentration

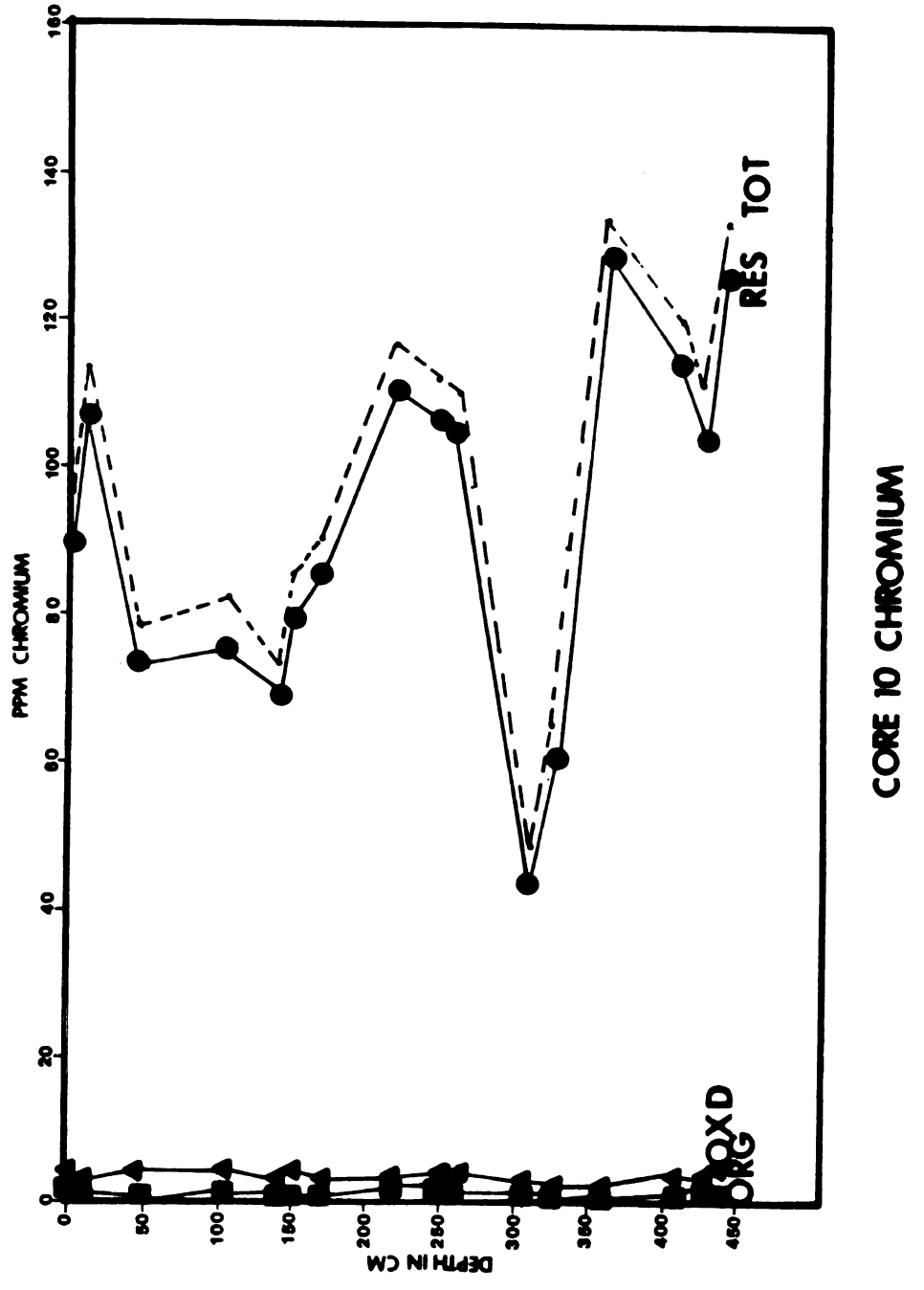
CORE 10 CHROMIUM
PPM CHROMIUM
DEPTH IN CM
RES TOT
OXD
ORG
0
20
40
60
80
100
120
140
160
0
50
100
150
200
250
300
350
400
450

decrease at 310 cm (sand), and an increase at 350 cm (silt composition). This suggests for Cr that the detrital fraction is grain-type dependent.

Iron concentration versus depth (Figure 26) shows relatively constant concentration values for Fe in the oxide and detrital phases. However, a slight decrease of Fe in these fractions is observed at 360 cm where a compositional change from sand-silt-clay to silty-clay occurs. The exchangeable, and organic phases show a fluctuation in Fe concentration at 100 cm; the exchangeable phase increases while the organic phase decreases. At 200 cm there is a decrease in Fe concentration and at 350 cm, another decrease in both exchangeable and organic phases. These changes in concentration reflect changes in composition. (Type 4 has a higher concentration value than Type 6). This suggests that for Fe, grain-type plays a significant part in metal concentration.

Mn concentration with depth (Figure 27) shows that the amount of Mn in the exchangeable, residual and organic fractions is fairly constant with depth. Manganese in the oxide fraction (the major phase of Mn in the sediment) changes with depth as a function of sediment type. The highest concentration values are in the sand-silty-clay composition, the lower concentrations appear in the sand and silty-clay compositions. Thus, for Mn, the concentration changes with depth and nature of its partitioning suggests that Mn concentration is grain-type dependent and that the total Mn concentration pattern reflects the Mn oxide pattern.

Figure 28 is a plot of Zn concentration versus depth. The Zn plot shows that concentrations in the organic and oxide phases are constant

Figure 26. Concentration of iron with depth in core 10.

Symbol key:

O EX - exchangeable fraction

■ ORG - organic fraction

▲ OXD - oxide fraction

● RES - detrital fraction

\- TOT - total Fe concentration

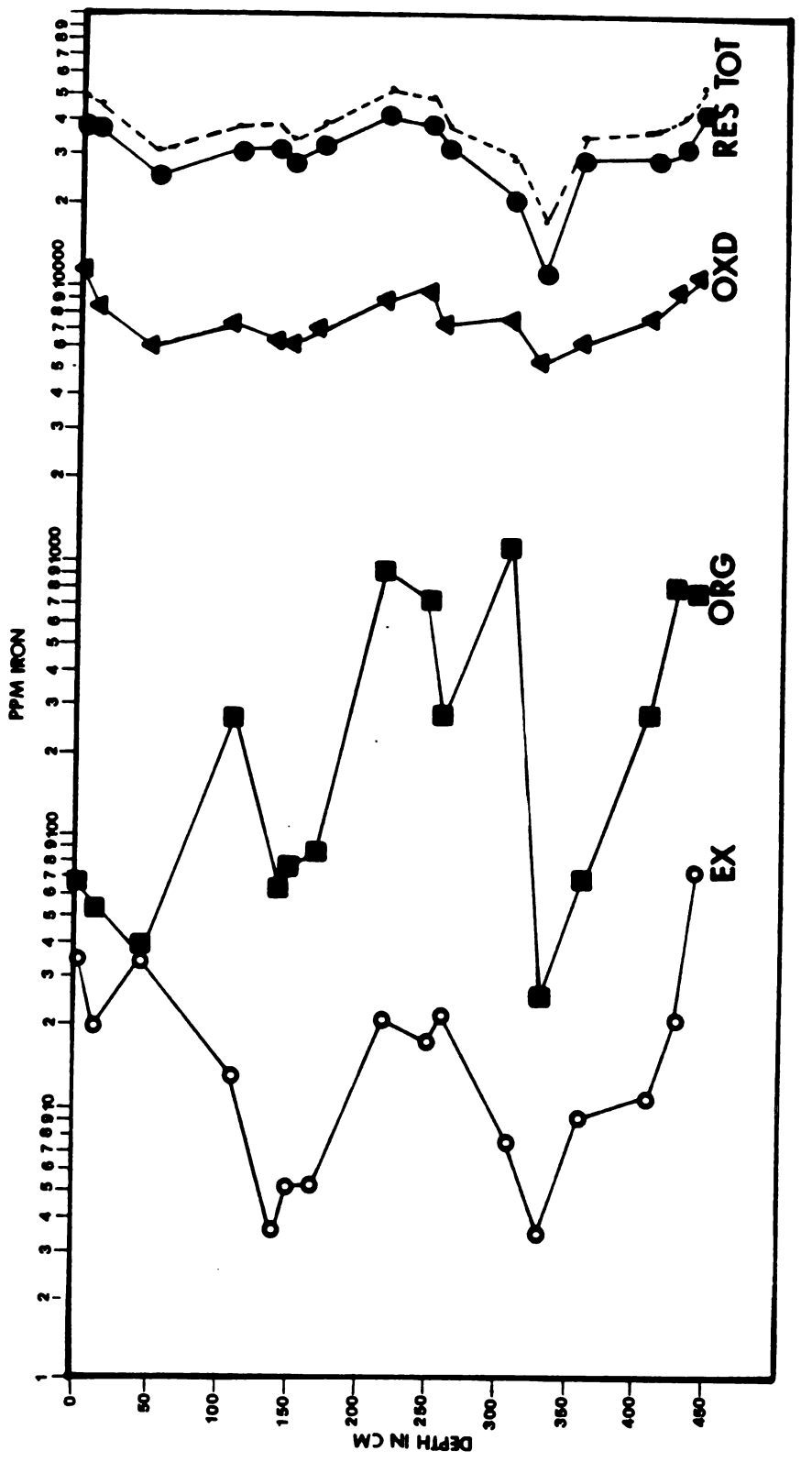

CORE 10 IRON

Figure 27. Concentration of manganese with depth in core 10.

Symbol key:

o EX - exchangeable fraction

■ ORG - organic fraction

▲ OXD - oxide fraction

● RES - detrital fraction

- TOT - total Mn concentration

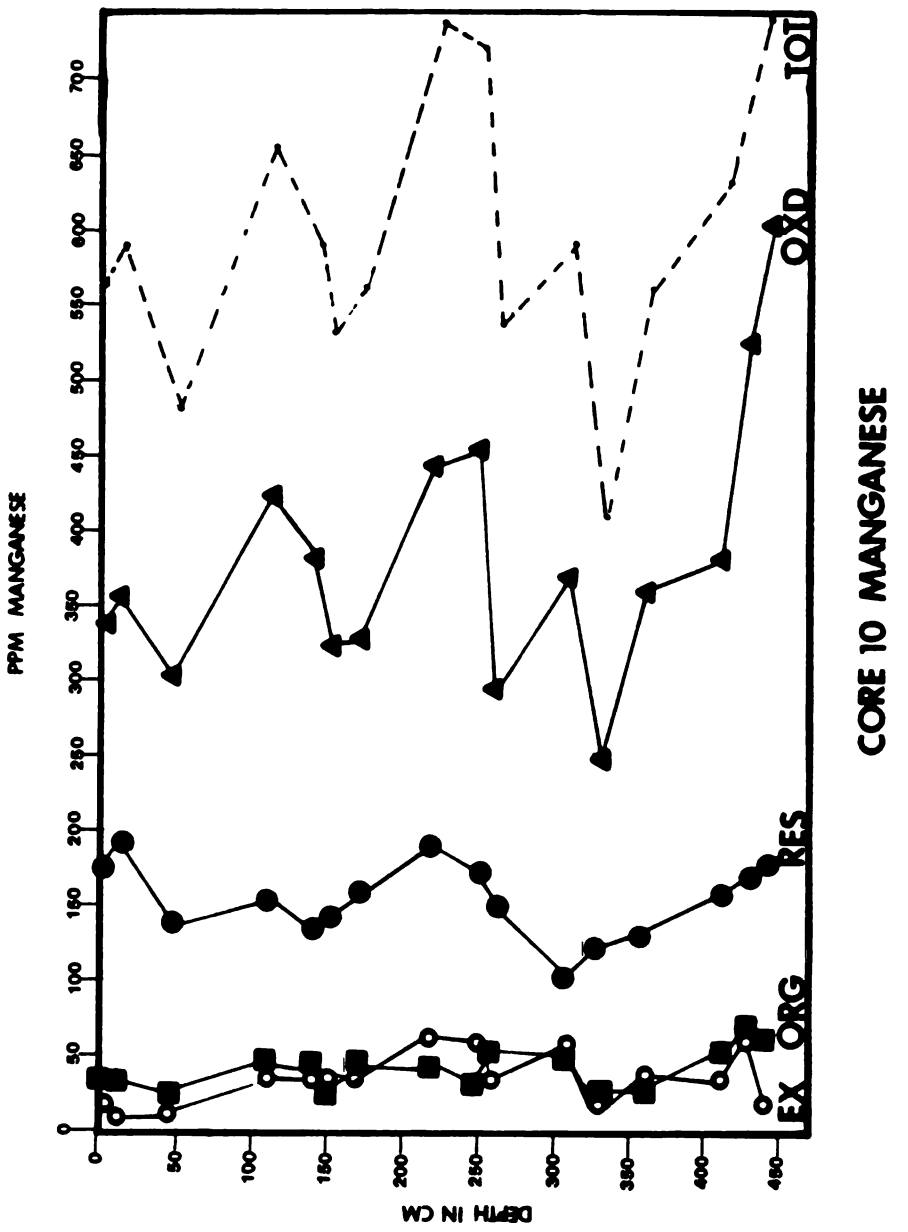
PPM MANGANESE
DEPTH IN CM
TOT
OXD
RES
ORG
EX
CORE 10 MANGANESE

Figure 28. Concentration of zinc with depth in core 10.

Symbol key:

■ ORG - organic fraction

▲ OXD - oxide fraction

● RES - detrital fraction

\- TOT - total Zn concentration

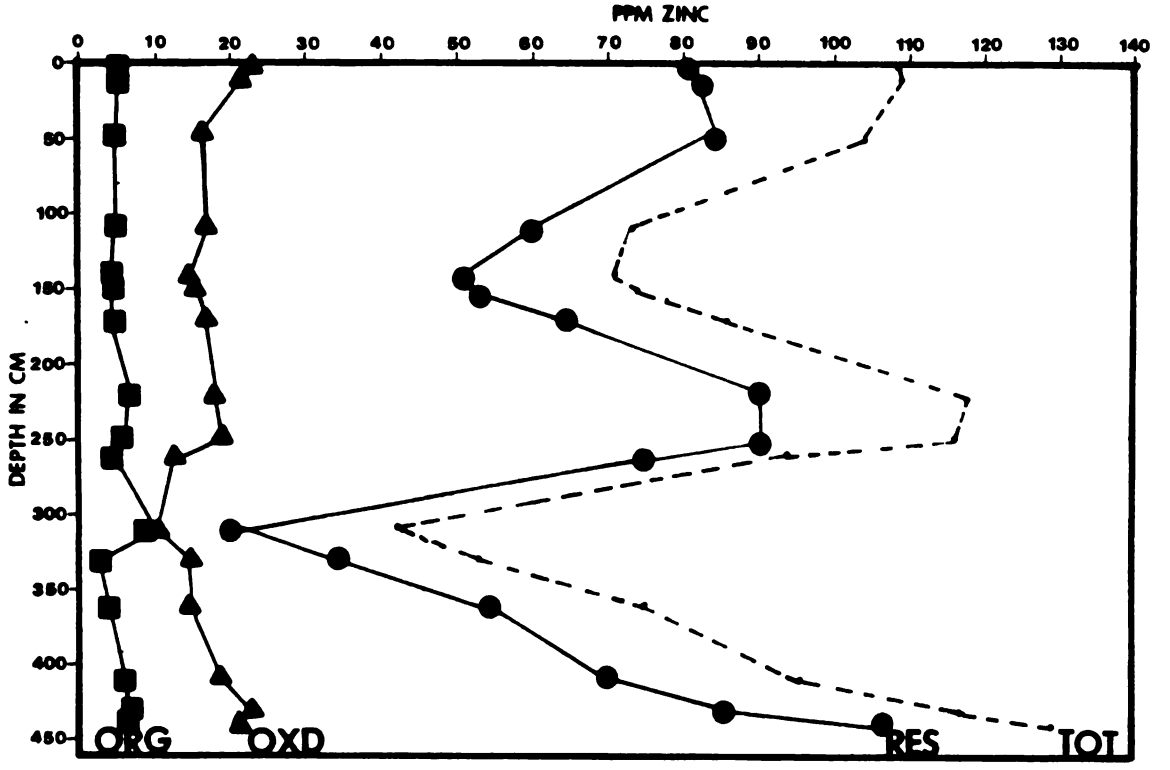
PPM ZINC
0
10
20
30
40
50
60
70
80
90
100
110
120
130
140
DEPTH IN CM
0
50
100
150
200
250
300
350
400
450
ORG
OXD
RES
TOT

CORE 10 ZINC

with depth except at 330 cm. There is a decrease of Zn in the organic phase and an increase of Zn in the oxide phase. There are two fluctuations of Zn in the residual phase with depth: at 150 cm and at 310 cm. Both depths show a decrease in detrital concentration of Zn. At 150 cm and 310 cm depths the sediment composition changes to the sand (Type 1). Other compositional changes (sand-silty-clay and silty-clays) appear to have no discernable effect on concentrations of Zn in the sediment.

Figure 29 is a plot of Cu concentration with depth. Copper in the oxide fraction appears constant with depth and is relatively small. The organic fraction also is constant with depth except for an increase at 300 cm. The organic fraction increases drastically due to encountering a grain-type compositional change at this point. Copper in the detrital fraction is of dominate control on its concentration in these sediments and fluctuates throughout the sediment core. The Cu detrital fraction appear to be controlled by the sediment type (higher concentration values are associated with clay type sediment and lower concentration values are associated with sand type composition).

Figures 30 and 31, nickel and barium concentrations with depth, respectively, show similar grain-type dependencies. The organic and oxide fraction are relatively unimportant and remain constant with depth. Little repartitioning occurs with depth. The detrital fraction has two major low level concentration points at 150 cm and 300 cm for both barium and nickel profiles. These low level concentration points correspond to a sand grain-type (Type 1). High concentration levels correspond to a clay grain-type (Type 5 and Type 6). Nickel and barium

Figure 29. Concentration of copper with depth in core 10.

Symbol key:

■ ORG - organic fraction

▲ OXD - oxide fraction

● RES - detrital fraction

\- TOT - total Cu concentration

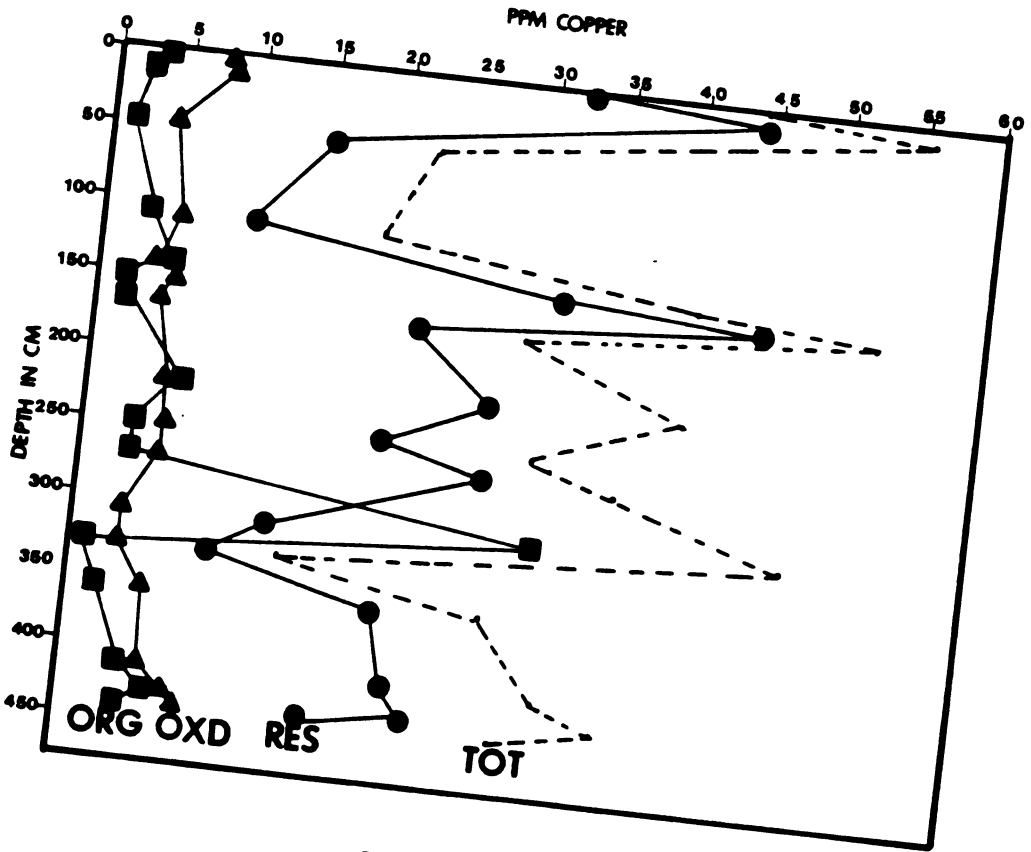

CORE 10 COPPER

Figure 30. Concentration of nickel with depth in core 10.

Symbol key:

■ ORG - organic fraction

▲ OXD - oxide fraction

● RES - detrital fraction

\- TOT - total Ni concentration

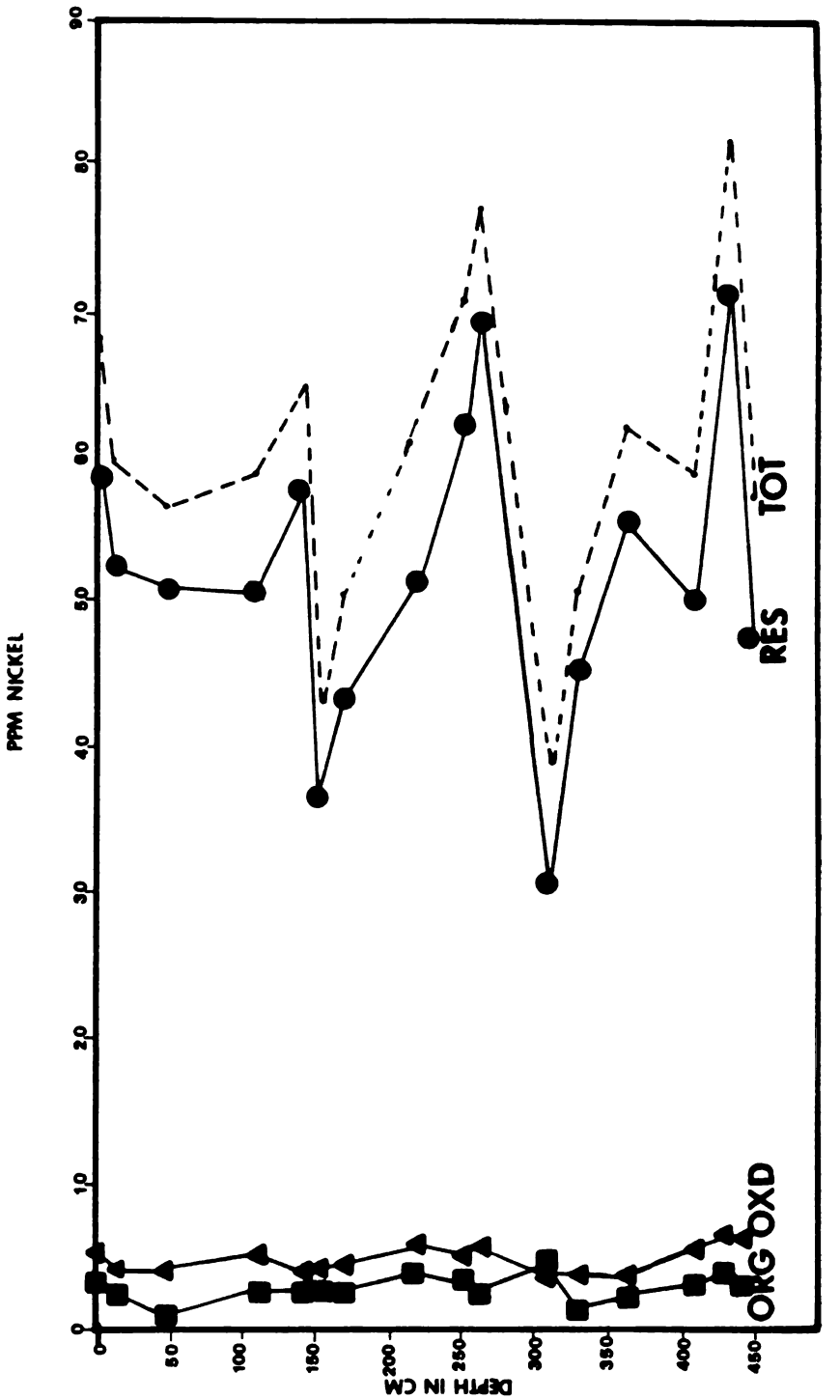
PPM NICKEL
DEPTH IN CM
RES
TOT
ORG
OXD
CORE 10 NICKEL

Figure 31. Concentration of barium with depth in core 10.

Symbol key:

● RES - detrital fraction

\- TOT - total Ba concentration

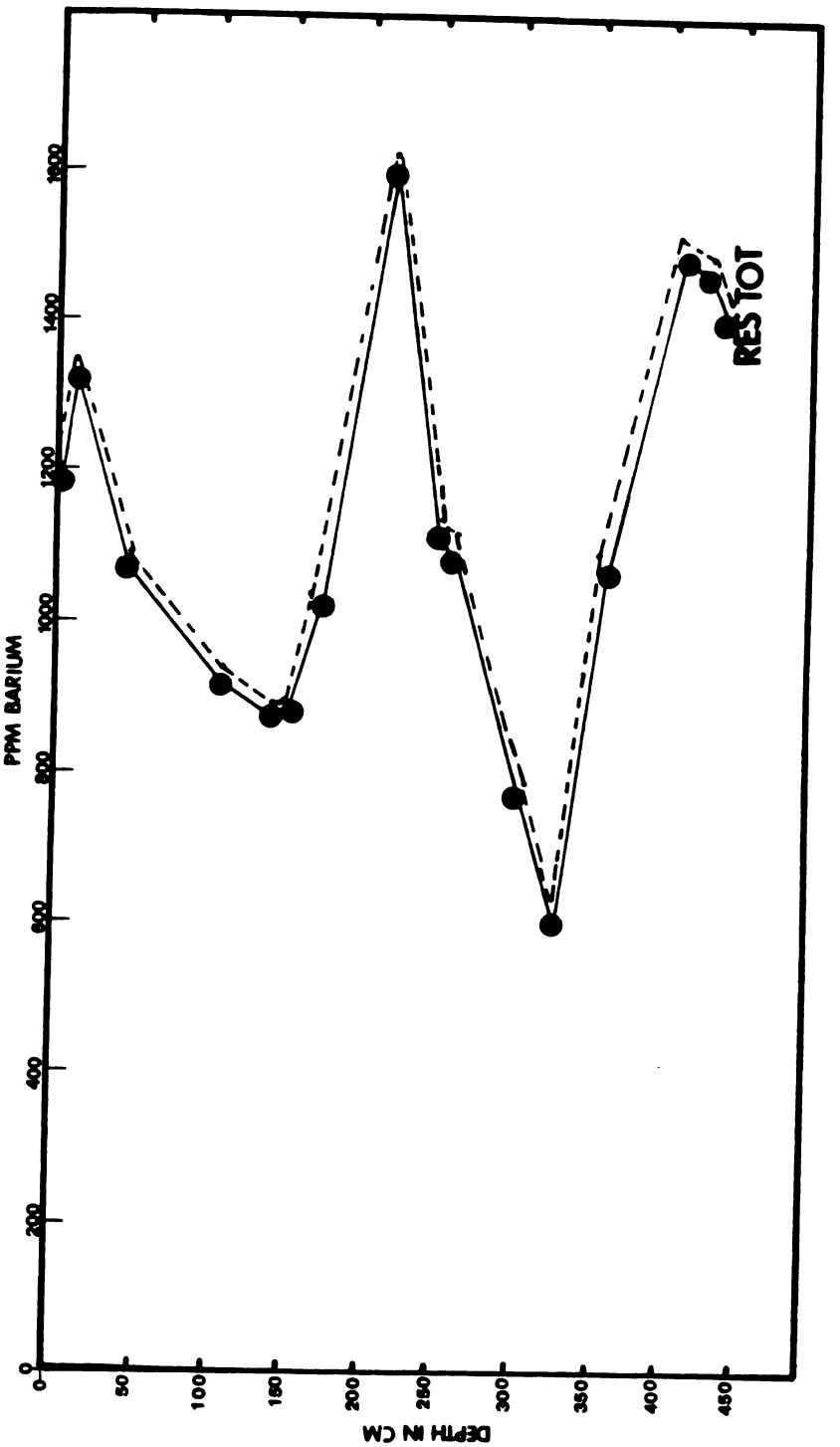
CORE 10 BARIUM
RES TOT
PPM BARIUM
DEPTH IN CM
0
200
400
600
800
1000
1200
1400
1600
0
50
100
150
200
250
300
350
400
450

concentrations with depth are, therefore, grain-type dependent and show little repartitioning.

In general, there exists a relationship between sediment type and concentration of the detrital fraction. The hydromorphic phase is more independent of sediment type with depth than they are at the surface (excluding Mn oxide fraction). The relative importance of the hydromorphic phases in sequestering metal does not indicate major repartitioning of the metals with depth within the hydromorphic fraction.

These observations can be interpreted to indicate that to a depth of 450 cm on the shelf, the metal concentrations in the sediment are dependent on sediment type. However, the relatively high amount of Mn in the Fe-Mn oxide fraction results in the profile of total Mn concentration with depth to be independent of sediment type as the Mn in the oxide fraction gets redistributed.

Core 10 sediments are also considered oxic throughout the core length. The lack of decreasing metal concentration in the oxide phase and no observable oxidized sediment zone enrichment for Ni, Fe, Mn, and Co which is expected when reducing conditions are encountered [Addy et al., 1976; Holmes and Martin, 1978; Heath and Dymond, 1981]. These observations lead to the conclusion that core 10 does not encounter a reducing environment and is therefore considered oxic throughout the core.

Source:

Partitioning data for the surface (0-5 cm) shelf sediments were arranged in a Q-mode and R-mode factor analysis array. The data was factored in raw form and in transformed form (i.e., natural log matrix) (Loring, 1982). The B-matrix for factor analysis of raw R-mode,

transformed R-mode, transformed R-mode PA1, raw Q-mode, and transformed Q-mode PA1 appear in Appendix III. Q-mode will be discussed below. The results of R-mode factor analysis will not be discussed, however the data appears in Appendix III. PA1 (principal factoring iteration) was employed because one factor dominated. PA1 may extract other variables which cannot be determined by other factor methods (Statistical Package for the Social Sciences, 1975).

The B-matrix is the influence of each end member on the total metals found in each sediment sample (Bopp and Biggs, 1981). Q-mode factor analysis, both raw and transformed PA1 forms, show high communality (i.e., squared multiple correlation) of about .9 and has one factor accounting for greater than 90% factor influence on the shelf. In conclusion, only one factor appears to be controlling the source of trace metals to the shelf sediments. This factor is interpreted to indicate that the Amazon River is the dominant source. Other factors accounting for an anthropogenic source or a biogenic source are undetectable. A hydrothermal source is also undetectable, which is in support with past work (Dymond and Heath, 1982).

CONCLUSIONS

This research examined the chemical partitioning of Fe, Mn, Zn, Cu, Pb, Ni, Cr, Co, Ba and Al among four theoretical phases within continental shelf sediments and soils from Belèm. The conclusions of this study are:

(1) The Amazon River is dominate over all other sources of trace metals to shelf sediments.

(2) Significant repartitioning of metals in sediment occurs when sediments move from a river to an ocean environment.

(3) The suspended load sediment of the river can be a potential source of metals to seawater, when the sediment enter seawater. The order of importance for this source decreases in the sequence Ni>Co>Fe>Cr.

(4) Metal concentrations and distribution in and on the shelf are mainly dependent on the grain-type of the sediment.

(5) Amazon shelf sediments do not encounter reducing conditions to a depth of 450 cm.

(6) Little repartitioning of metals in the sediment occurs with depth.

REFERENCES

Figure 29. Concentration of copper with depth in core 10.

Symbol key:

■ ORG - organic fraction

▲ OXD - oxide fraction

● RES - detrital fraction

\- TOT - total Cu concentration

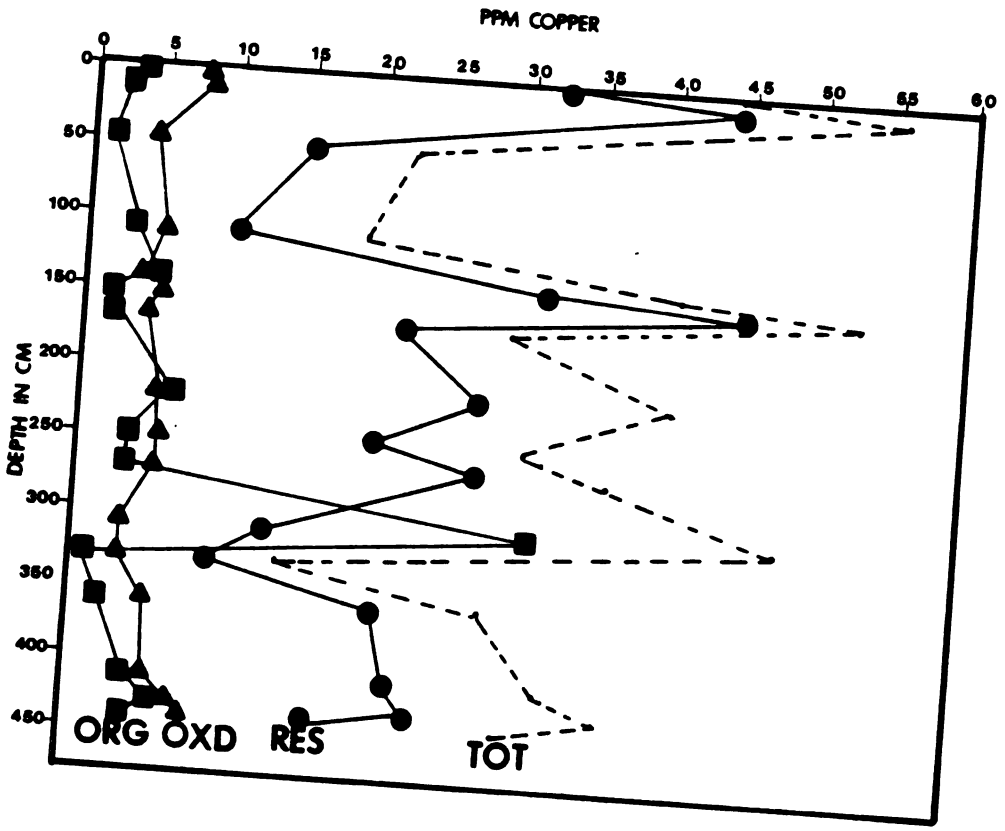

CORE 10 COPPER

Figure 30. Concentration of nickel with depth in core 10.

Symbol key:

■ ORG - organic fraction

▲ OXD - oxide fraction

● RES - detrital fraction

\- TOT - total Ni concentration

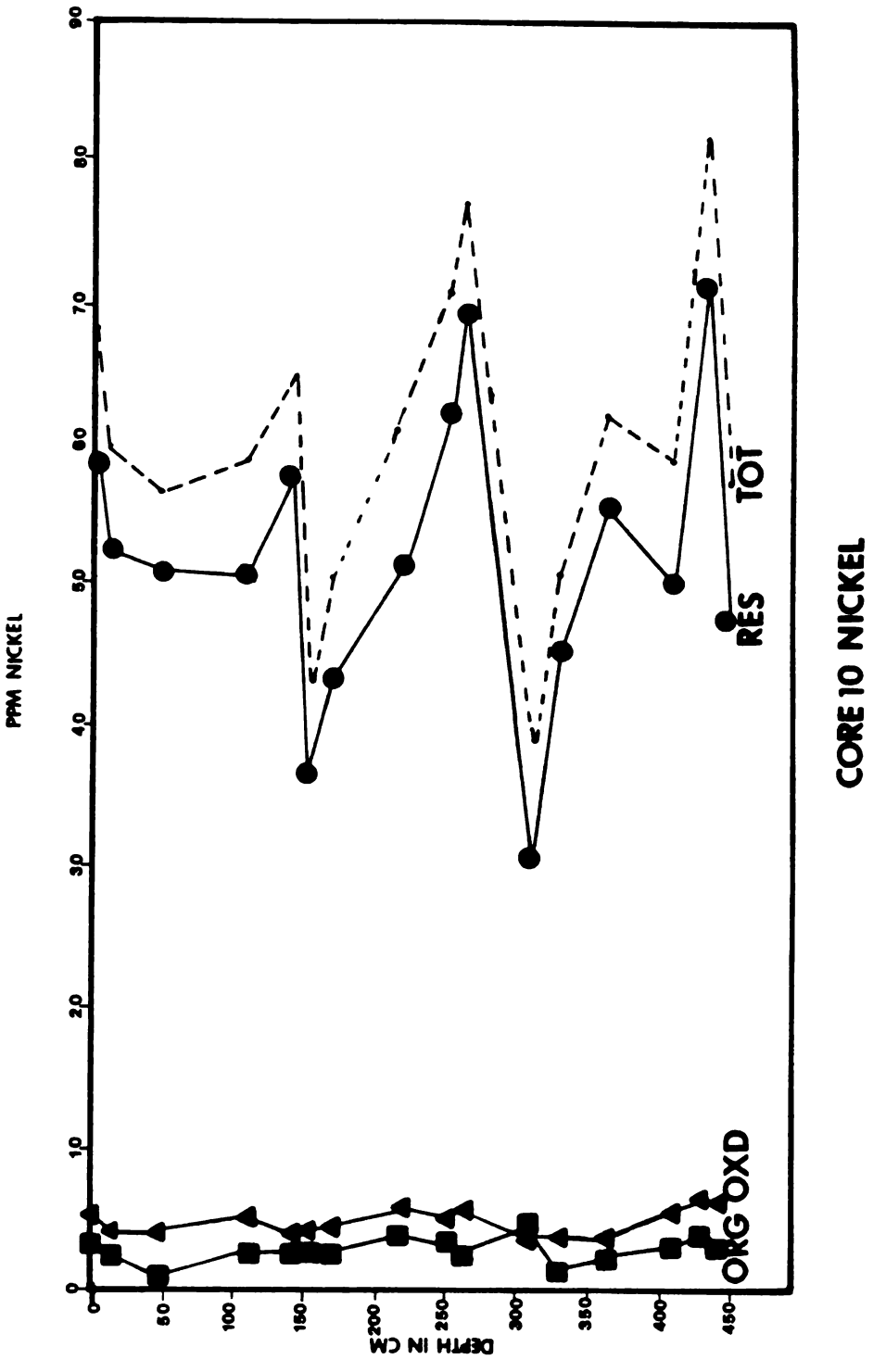
CORE 10 NICKEL
PPM NICKEL
DEPTH IN CMS
TOT
RES
OXD
ORG
0
10
20
30
40
50
60
70
80
90
0
50
100
150
200
250
300
350
400
450

Figure 31. Concentration of barium with depth in core 10.

Symbol key:

● RES - detrital fraction

\- TOT - total Ba concentration

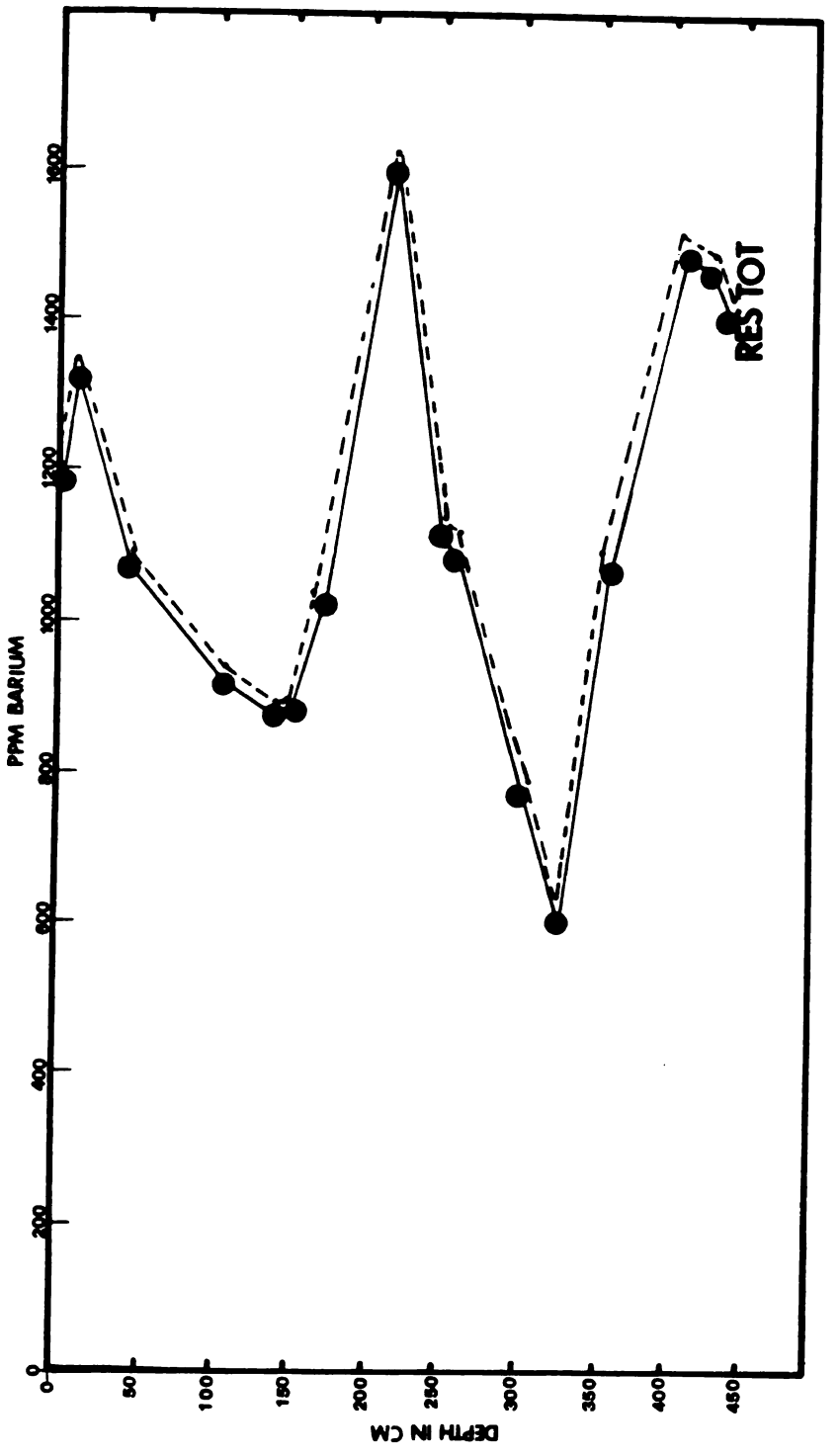

CORE 10 BARIUM

concentrations with depth are, therefore, grain-type dependent and show little repartitioning.

In general, there exists a relationship between sediment type and concentration of the detrital fraction. The hydromorphic phase is more independent of sediment type with depth than they are at the surface (excluding Mn oxide fraction). The relative importance of the hydromorphic phases in sequestering metal does not indicate major repartitioning of the metals with depth within the hydromorphic fraction.

These observations can be interpreted to indicate that to a depth of 450 cm on the shelf, the metal concentrations in the sediment are dependent on sediment type. However, the relatively high amount of Mn in the Fe-Mn oxide fraction results in the profile of total Mn concentration with depth to be independent of sediment type as the Mn in the oxide fraction gets redistributed.

Core 10 sediments are also considered oxic throughout the core length. The lack of decreasing metal concentration in the oxide phase and no observable oxidized sediment zone enrichment for Ni, Fe, Mn, and Co which is expected when reducing conditions are encountered [Addy et al., 1976; Holmes and Martin, 1978; Heath and Dymond, 1981]. These observations lead to the conclusion that core 10 does not encounter a reducing environment and is therefore considered oxic throughout the core.

Source:

Partitioning data for the surface (0-5 cm) shelf sediments were arranged in a Q-mode and R-mode factor analysis array. The data was factored in raw form and in transformed form (i.e., natural log matrix) (Loring, 1982). The B-matrix for factor analysis of raw R-mode,

transformed R-mode, transformed R-mode PA1, raw Q-mode, and transformed Q-mode PA1 appear in Appendix III. Q-mode will be discussed below. The results of R-mode factor analysis will not be discussed, however the data appears in Appendix III. PA1 (principal factoring iteration) was employed because one factor dominated. PA1 may extract other variables which cannot be determined by other factor methods (Statistical Package for the Social Sciences, 1975).

The B-matrix is the influence of each end member on the total metals found in each sediment sample (Bopp and Biggs, 1981). Q-mode factor analysis, both raw and transformed PA1 forms, show high communality (i.e., squared multiple correlation) of about .9 and has one factor accounting for greater than 90% factor influence on the shelf. In conclusion, only one factor appears to be controlling the source of trace metals to the shelf sediments. This factor is interpreted to indicate that the Amazon River is the dominant source. Other factors accounting for an anthropogenic source or a biogenic source are undetectable. A hydrothermal source is also undetectable, which is in support with past work (Dymond and Heath, 1982).

CONCLUSIONS

This research examined the chemical partitioning of Fe, Mn, Zn, Cu, Pb, Ni, Cr, Co, Ba and Al among four theoretical phases within continental shelf sediments and soils from Belèm. The conclusions of this study are:

(1) The Amazon River is dominate over all other sources of trace metals to shelf sediments.

(2) Significant repartitioning of metals in sediment occurs when sediments move from a river to an ocean environment.

(3) The suspended load sediment of the river can be a potential source of metals to seawater, when the sediment enter seawater. The order of importance for this source decreases in the sequence Ni>Co>Fe>Cr.

(4) Metal concentrations and distribution in and on the shelf are mainly dependent on the grain-type of the sediment.

(5) Amazon shelf sediments do not encounter reducing conditions to a depth of 450 cm.

(6) Little repartitioning of metals in the sediment occurs with depth.

REFERENCES

REFERENCES

Addy S. K., Presley B.J. and Ewing M. (1976) Distribution of manganese, iron and other trace elements in a core from the Northwest Atlantic. J. Sed. Pet. 46, (4), 813-818.

Bender M., Broecker W., Gornitz V., Middel U., Kay R., Sun S.S. and Biscaye P. (1971) Geochemistry of 3 cores from the East Pacific Rise. Earth and Planet. Sci. Lett. 12, 425-433.

Bischoff J.L. and Dickson F.W. (1975) Seawater-basalt interaction at 200°C and 500 bars: Implications for origin of seafloor heavy-metal deposits and regulation of seawater chemistry. Earth and Planet. Sci. Lett. 25, 385-397.

Bonatti E., Fisher D.E., Joensuu O. and Rydell H.S. (1971) Post depositional mobility of some transition elements, phosphorus, uranium, and thorium in deep sea sediments. Geochim. Cosmochim. Acta 35, 189-201.

Bopp F. III and Biggs R.B. (1981) Metals in estuarine sediments: Factor analysis and its environmental significance. Science 214, 441-443.

Bopp F. III (1981) Ph.D. Thesis: University of Delaware, 1-179.

Brannon J.M., Rose J.R., Engler R.M. and Smith I. (1977) The distribution of heavy metals in sediment fractions from Mobil Bay, Alabama. Chemistry of Marine Sediments, (ed. T.F. Yen), 125-149.

Brooks R.R., Presley B.J. and Kaplan I.P. (1968) Trace elements in the interstitial waters of marine sediments. Geochim. Cosmochim. Acta 32, 397-414.

Brumsack H.J. (1980) Geochemistry of cretaceous black shales from the Atlantic Ocean. Chem. Geol. 31, 1-25.

Corliss J.B., Dymond J., Gordon L.I., Edmond J.M., Von Herzen R.P., Ballard R.D., Green K., Williams D., Bainbridge A., Crane K., and Van Andel T.H. (1979) Submarine thermal springs on the Galapagos rift. Science 203, (4385), 1073-1083.

Cosma B., Drago M., Tucci S., Piccazzo M. and Scarponi G. (1979) Heavy metals in Ligurian Sea sediments: Distribution of Cr, Cu, Ni and Mn in superficial sediments. Mar. Chem. 8, 125-142.

DeMaster D. (1982) Personal communication. North Carolina State University.

Demina L.L., Gordeyev V.V. and Formina L.S. (1978) Forms of occurrence of Fe, Mn, Zn, and Cu in river water and suspended matter, and their variation in the zone of mixing of river and seawater. (As exemplified by Rivers of the Black Sea, Sea of Azov, and Caspian Sea Basins). Geochem. Intl. 15, (4), 146-163.

Drever J.I. (1982) The Geochemistry of National Waters, Prentice-Hall, Inc., 163-165.

Dymond J. (1981) Geochemistry of nazca plate surface sediments: An evaluation of hydrothermal, biogenic, detrital, and hydrogenous sources. Geol. Soc. Amer. 154, 133-173.

Dymond J., Corliss J.B., Cobler R., Muratii C.M., Chou C. and Conard R. Composition and origin of sediments recovered by deep drilling of sediment mounds, Galapagos Spreading Center. 377-385.

Edmond J.M. (1981) Hydrothermal activity at mid-ocean ridge axes. Nature 290, (5802) 87-88.

Edmond J.M., Craig H., Gordon L.I. and Holland H.D. (1979) Chemistry of hydrothermal waters at 21°N on the East Pacific Rise. EOS 60, (46), 864.

Edmond J.M., Measures C., McDuff R.E., Chan L.H., Collier R., Grant B., Gordon L.I. and Corliss J.B. (1979) Ridge crest hydrothermal activity and the balances of the major and minor elements in the ocean: The Galapagos data. Earth Planet. Sci. Lett. 46, 1-18.

Edmond J.M., Von Damm K.L, McDuff R.E. and Measures C.I. (1982) Chemistry of hot springs on the East Pacific Rise and their effluent disposal. Nature 297, 187-191.

Eisma D. and Van Der Mavel H.W. (1971) Marine muds along the Guyana Coast and their origin from the Amazon Basin. Contrib. Mineralogy and Petrology 31, 321-334.

Folk R.L. (1974) Petrology of sedimentary rocks. Hemphill Publ. Co. 182.

Gaudette H.E., Flight, W.R., Toner, L. and Floger, D.W. (1974) An inexpensive titration method for the determination of organic carbon in recent sediments. J. Sed. Pet. 44, (1), 249-253.

Gephart C.J. (1982) Relative importance of iron-oxide, manganese-oxide, and organic material on the adsorption of chromium in natural water sediment systems. MS Thesis, Michigan State University.

Gibbs R.J. (1965) The Geochemistry of the Amazon River Basin. Ph.D. Thesis, University of California, San Diego.

Gibbs R.J. (1967) The geochemistry of the Amazon River system: Part I the factors that control the salinity and the composition and concentration of the suspended solids. Geol. Soc. Amer. Bull. 78, 1203-1232.

Gibbs R.J. (1976) Amazon River sediment transport in the Atlantic Ocean. Geology 4, 45-48.

Gibbs R.J. (1977) Transport phases of transition metals in the Amazon and Yukon Rivers. Geol. Soc. Amer. Bull. 88, 829-843.

Grupta S.K. and Chen K.Y. (1975) Partitioning of trace metals in selective chemical fractions on nearshore sediments. Environ. Letters 10, (2), 129-158.

Harding S.C. and Brown H.S. (1976) Distribution of selected trace elements in sediments of Pamlico River, Estuary, North Carolina. Environ. Geol. 1, (3), 181-190.

Heath G.R. and Dymond J. (1981) Metalliferous-sediment deposition in time and space: East Pacific Rise and Bauer Basin Northern Nazca Plate. Nazca Plate: Crustal Formation and Andean Convergence. 175-197.

Hoffmann J.A.J. (1975) Climatic Atlas of South America WMO: Hungary.

Holeman J.N. (1968) The sediment yield of major rivers of the world. Water Resources Research 4, 737-747.

Holmes C.W. and Martin E.A. (1978) Migration of anthropogenically induced trace metals (barium and lead) in a continental shelf environment. Amer. Chem. Society 672-676.

Imbrie J. and Van Andel T.H. (1964) Factor analysis of heavy-mineral data. Geol. Soc. Amer. Bull. 75, 1131-1156.

Kerlinger F.N. (1973) Foundations of behavioral research. Holt, Rinehart and Winston, Inc., New York. 582-692.

Kharkar D.P., Turekian K.L. and Bertine K.K. (1968) Stream supply of dissolved silver, molybdenum, antimony, selenium, chromium, cobalt, rubidium and cesium to the oceans. Geochim. Cosmochim. Acta 32, 285-298.

Kitano Y., Sakata M. and Matsumoto E. (1980) Partitioning of heavy metals into mineral and organic fractions in a sediment core from Tokyo Bay. Geochim. Cosmochim. Acta 44, 1279-1285.

Krauskopf K.B. (1956) Factors controlling the concentration of 13 rare metals in seawater. Geochim. Cosmochim. Acta 9, 1-32B.

Kuehl S.A., Nittrouer C.A. and DeMaster D.J. (1982) Modern sediment accumulation and strata formation on the Amazon Continental Shelf. Marine Geology 49, 279-300.

Long D.T. and Gephart C.J. (1982) Relative importance of iron-oxide, manganese-oxide, and organic material on the adsorption of chromium in natural water sediment systems. Proceeding from October Geological Society of America National Conference.

Loring D.H. (1976) The distribution and partition of zinc, copper, and lead in the sediments of the Saguenary Fjord. Can. J. Earth Sci. 13, 960-971.

Loring D.H. (1976b) Distribution and partition of cobalt, nickel, chromium, and vanadium in the sediments of the Saguenary Fjord. Can. J. Earth Sci. 13, 1706-1718.

Loring D.H. (1979) Geochemistry of cobalt, nickel, chromium and vanadium in the sediments of the estuary and open Gulf of St. Lawrence. Can. J. Earth Sci. 16, 1197-1209.

Loring D.H. (1982) Geochemical factors controlling the accumulation and dispersal of heavy metals in the Bay of Fundy Sediments. Can. J. Earth Sci. 19, (5), 930-944.

Luoma S.M. and Bryan G.W. (1981) A statistical assessment of the form of trace metals in oxidized estuarine sediments emloying chemical extractants. The Science of the Total Environment 17, 165-196.

Marchig V. and Gundlach H. (1982) Iron-rich metalliferous sediments on the East Pacific Rise: Prototype of undifferentiated metalliferous sediments on divergent plate boundaries. Earth Planet. Sci. Lett. 58, 361-382.

Martin J.M. and Meybeck M. (1979) Elemental mass-balance of material carried by major world rivers. Marine Chem. 7, 173-206.

Meade R.H., Curtis W., DoVale C.M., Edmond J.M., Nordin C.F. Jr. and Rodrigues F.M. Costa. (1979) Sediment loads in the Amazon River. Nature 278, 161-163.

Milliman J.D., Summerhayes C.P. and Barretto H.T. (1975) Oceanography and suspended matters off the Amazon River February - March 1973. J. Sed. Petrol. 45, 189-206.

Morozov N.P. (1979) Trace-element migration - form relationships for rivers, estuaries, seas, and oceans. Geochem. Intl. 16, (4), 161-164.

Nelsen T.A. (1981) The application of Q-mode factor analysis to suspended particulate matter studies: Examples from the New York Bright Apex. Marine Geology 39, 15-31.

Nittrouer C.A., DeMaster D.J. and Kowsmann R.O. (1981) The deltaic nature of Amazon shelf sedimentation as revealed by high resolution seismic reflection studies. EOS 62, (17), 303.

Nittrouer C.A., Sharara M.T. and DeMaster D.J. (1983) Variations of sediment texture on the Amazon Continental Shelf. J. Sed. Pet. 53, (1), 179-191.

Ottman R.E. (1968) Reconnaissance investigations of the discharge and water quality of the Amazon River. U.S.G.S. Circ. 552, 16.

Parks J.M. (1970) Fortran IV Program for Q-Mode cluster analysis on distance function with printed dendrogram. Computer Contribution 46. State Geological Survey, The University of Kansas.

Perkin Elmer Atomic Absorption Spectroscopy Instruction Book (1973).

Ryther J.J., Menzel D.W., Corwin N. (1967) Influence of the Amazon River outflow on the ecology of the western Tropical Atlantic I. hydrography and nutrient chemistry. J. Mar. Res. 25, 69-83.

Schmidt G.F. (1972) Amounts of suspended solids and dissolved substances in the middle reaches of the Amazon over the course of one year. Amazoniana 3, (11) 208-223.

Schultz D.J. and Turekian K.K. (1965) The investigation of the geographical and vertical distribution of several trace elements in seawater using neutron activation analysis. Geochim. Cosmochim. Acta 29, 259-313.

Sholkovitz E.R. (1976) Flocculation of dissolved organic and inorganic matter during the mixing of river water and seawater. Geochim. Cosmochim. Acta 40, 831-845.

Sholkovitz E.R. and Price N.B. (1980) The major element chemistry of suspended matter in the Amazon Estuary. Geochim. Cosmochim. Acta 44, 163-171.

Stallard R.F. (1980) Major element geochemistry of the Amazon River system. PhD. Thesis: Woods Hole Oceanographic Institution and Massachusetts Inst. of Technology, 1-366.

Statistical package for the social sciences (1975) (eds. Nie H.H., Hull C.H., Jenkins J.G., Steinbrenner K. and Bent D.H.) McGraw-Hill Book Co. 468-508.

Tessier A., Campbell P.G.C. and Bisson M. (1979) Sequential extraction procedure for the speculation of particulate trace metals. Anal. Chem. 51, (7).

Tessier A., Campbell P.G.C. and Bisson M. (1982) Particulate trace metal speciation in stream sediments and relationships by grain size: Implications for geochemical exploration. J. Chem. Exp. 16, 77-104.

Turekian K.K. and Imbric J. (1966) The distribution of trace elements in deep-sea sediments of the Atlantic Ocean. Earth Planet. Sci. Lett. 1, 161-168.

Walkley A. and Black I.A. (1934) An examination of the Degthareff method for determining soil organic matter and a proposed modification of the chronic acid titration method. Soil Sci. 27, 29-38.

Windom H.L., Beck K.C. and Smith R. (1971) Transport of trace metals to the Atlantic Ocean by Three Southeastern Rivers. Southeastern Geology 12, (3), 169-181.

Yen T.F. and Tang J.I.S. (1977) Chemical aspects of marine sediments. In Chemistry of Marine Sediments (ed. T.F. Yen), 1-38.

APPENDICES

APPENDIX I
CHEMICAL PARTITIONING DATA

APPENDIX I

A = Sample Location

B = Processed prior to receiving sample (1 = yes; 2 = no)

C = Bioturbated (1 = yes; 2 = no)

D = Sample sediment type (Type 1-6 see triangular diagram) (Nittrouer et al., 1983).

E = Sediment accumulate rate based on Pb-210 data (Nittrouer et al., 1983).

F = Depth in cm (low)

G = Depth in cm (high)

H = Total organic carbon

I = Exchangable fraction in ppm

J = Fe-Mn oxide fraction in ppm

K = Organic fraction in ppm

L = Residual fraction in ppm

M = Total metal concentration in ppm (Addition of I - L values)

-- = Missing data

99 = Missing data

80 = Soils taken at Belem'

81-85 = Soil horizons

All samples sieved in less than .212 mm sieve prior to analysis.

BARIUM

A	B	C	D	E	F	G	H	I	J	K	L	M
2.	2.	1.	5.	2.	0.0	2.0	.190	0.000	7.020	2.867	1529.000	1538.900
3.	1.	1.	5.	2.	0.0	1.0	0.000	0.000	.030	.325	196.900	197.260
4.	2.	1.	1.	2.	0.0	5.0	0.000	0.000	.090	.340	132.000	132.430
5.	1.	1.	1.	2.	0.0	1.0	0.000	0.000	0.000	.253	45.375	45.628
6.	1.	1.	1.	2.	0.0	1.0	0.000	0.000	0.000	.185	70.125	70.310
7.	1.	1.	1.	2.	0.0	1.0	0.000	0.000	.543	.320	492.250	493.110
9.	2.	1.	5.	2.	0.0	2.0	0.000	0.000	2.853	5.610	1645.600	1654.100
10.	2.	1.	6.	2.	0.0	2.0	0.000	0.000	8.009	4.112	1208.200	1220.300
10.	2.	1.	6.	99.	10.0	12.0	0.000	0.000	8.720	4.940	1332.100	1345.800
10.	2.	1.	4.	99.	45.0	47.0	0.000	0.000	7.060	4.813	1076.200	1088.100
10.	2.	1.	6.	99.	109.0	110.0	.100	0.000	4.700	3.475	926.750	934.920
10.	2.	1.	4.	99.	138.0	140.0	.100	0.000	3.160	3.207	880.000	886.370
10.	2.	1.	4.	99.	148.0	150.0	.250	0.000	4.420	2.940	887.700	895.060
10.	2.	1.	1.	99.	168.0	170.0	.100	0.000	4.900	2.867	1026.300	1034.100
10.	2.	1.	6.	99.	218.0	220.0	.150	0.000	6.740	3.893	1607.400	1618.000
10.	2.	1.	6.	99.	248.0	250.0	.220	0.000	8.440	4.990	1115.400	1128.800
10.	2.	1.	5.	99.	258.0	260.0	.190	0.000	7.677	3.740	1098.200	1109.600
10.	2.	1.	1.	99.	308.0	310.0	0.000	0.000	2.390	.995	774.130	777.510
10.	2.	1.	4.	99.	328.0	330.0	.100	0.000	3.730	1.980	605.000	610.710
10.	2.	1.	4.	99.	358.0	360.0	0.000	0.000	3.540	2.940	1083.500	1090.100
10.	2.	1.	5.	99.	408.0	413.0	.100	0.000	8.533	3.967	1496.000	1508.500
10.	2.	1.	6.	99.	428.0	430.0	.100	0.000	7.140	4.340	1471.800	1483.300
10.	2.	1.	6.	99.	439.0	440.0	0.000	0.000	8.960	5.215	1408.000	1422.200
11.	1.	1.	5.	2.	0.0	1.0	.310	0.000	8.647	4.152	1014.800	1027.500
12.	1.	1.	5.	2.	0.0	1.0	.050	0.000	8.260	4.530	1481.700	1494.500
13.	1.	1.	5.	2.	0.0	1.0	.200	0.000	10.730	4.268	1478.600	1493.600
14.	2.	1.	5.	2.	0.0	2.0	.150	0.000	45.430	8.990	1633.500	1687.900
15.	1.	2.	5.	3.	0.0	1.0	.200	0.000	22.660	5.295	1315.600	1343.600
16.	1.	2.	5.	3.	0.0	1.0	.150	0.000	9.490	6.440	1029.900	1045.800
17.	1.	2.	5.	3.	0.0	1.0	.200	0.000	7.227	3.507	1708.300	1719.000
18.	1.	2.	6.	3.	0.0	1.0	.150	0.000	7.130	4.196	1291.100	1302.500
19.	1.	2.	6.	3.	0.0	1.0	.260	0.000	5.930	4.800	1196.300	1207.000
20.	2.	1.	6.	2.	0.0	2.0	0.000	0.000	6.250	4.067	1742.100	1752.400
25.	1.	1.	3.	3.	0.0	1.0	0.000	0.000	4.860	2.427	969.100	976.390
26.	1.	2.	1.	3.	0.0	1.0	0.000	0.000	6.630	2.293	809.880	818.800
27.	1.	2.	2.	3.	0.0	1.0	0.000	99.000	5.600	2.550	574.750	582.900
28.	2.	2.	5.	1.	0.0	5.0	0.000	0.000	10.310	3.464	995.500	1009.300
29.	2.	2.	5.	1.	0.0	2.0	.100	0.000	11.378	7.133	1505.200	1523.700
30.	2.	2.	1.	1.	0.0	5.0	0.000	0.000	8.347	1.730	852.500	862.580
31.	1.	2.	2.	1.	0.0	1.0	0.000	0.000	25.300	3.900	698.500	727.700
32.	2.	2.	2.	1.	0.0	5.0	.100	0.000	27.400	5.605	1060.400	1093.400
33.	2.	2.	1.	1.	0.0	2.0	0.000	0.000	19.930	1.780	567.880	589.590
34.	2.	2.	5.	1.	0.0	5.0	0.000	0.000	55.440	11.135	1579.900	1646.500
35.	2.	2.	5.	1.	0.0	1.0	.050	0.000	13.973	4.853	1398.100	1416.900
36.	1.	2.	5.	3.	0.0	1.0	.200	0.000	7.996	4.255	1482.300	1494.500
37.	1.	2.	5.	3.	0.0	1.0	.200	0.000	7.910	4.807	1100.000	1112.700
38.	1.	2.	4.	3.	0.0	1.0	0.000	0.000	3.860	1.380	745.250	750.490
39.	1.	2.	4.	3.	0.0	1.0	.100	0.000	2.720	2.855	1137.100	1142.700
42.	2.	2.	6.	3.	0.0	5.0	.290	0.000	6.630	4.047	1235.300	1246.000
42.	2.	99.	99.	99.	40.0	45.0	.220	0.000	5.307	3.755	1370.900	1379.900
42.	2.	99.	99.	99.	108.0	110.0	.150	0.000	7.300	5.890	1678.600	1691.800
42.	2.	99.	99.	99.	168.0	170.0	0.000	0.000	6.410	4.816	1465.800	1477.000
42.	2.	99.	99.	99.	308.0	310.0	0.000	0.000	6.440	4.725	1584.000	1595.200
42.	2.	99.	99.	99.	361.0	370.0	.240	0.000	.653	1.555	908.600	910.810
42.	2.	99.	99.	99.	411.0	419.0	0.000	0.000	2.120	1.020	1106.400	1109.600
42.	2.	99.	99.	99.	556.0	563.0	.190	0.000	5.450	2.616	842.600	850.670
43.	2.	2.	6.	3.	0.0	2.0	.100	0.000	1.453	2.760	1338.300	1342.500

BARRIUM (cont'd.)

A	B	C	D	E	F	G	H	I	J	K	L	M
46.	2.	2.	6.	3.	0.0	5.0	0.000	0.000	8.910	4.730	954.250	967.890
46.	2.	99.	99.	99.	5.0	10.0	.250	0.000	8.320	4.445	1431.400	1444.100
46.	2.	99.	99.	99.	10.0	15.0	.270	0.000	9.300	5.185	1469.600	1484.100
46.	2.	99.	99.	99.	15.0	20.0	.150	0.000	7.193	4.465	1145.100	1156.800
46.	2.	99.	99.	99.	20.0	25.0	.250	0.000	5.960	5.360	1482.300	1493.600
46.	2.	99.	99.	99.	25.0	30.0	.050	0.000	7.396	6.380	1634.900	1648.700
46.	2.	99.	99.	99.	30.0	35.0	.200	0.000	6.310	4.475	863.500	874.290
46.	2.	99.	99.	99.	35.0	40.0	.150	0.000	8.260	4.460	1553.800	1566.500
46.	2.	99.	99.	99.	40.0	45.0	.190	0.000	8.973	5.475	1285.900	1300.300
46.	2.	99.	99.	99.	45.0	50.0	.240	0.000	8.880	4.795	1049.100	1062.800
47.	1.	2.	6.	3.	0.0	1.0	.260	0.000	6.867	5.300	1347.500	1359.700
50.	1.	1.	6.	3.	0.0	1.0	.260	0.000	6.260	5.190	1098.900	1110.400
55.	1.	1.	6.	1.	0.0	1.0	.200	0.000	6.570	4.450	1086.300	1097.300
56.	2.	2.	6.	1.	0.0	2.0	.100	0.000	4.190	4.285	1652.800	1661.200
57.	2.	1.	6.	3.	0.0	2.0	0.000	0.000	6.080	4.045	971.080	981.210
80.	2.	99.	99.	99.	0.0	2.0	.300	0.000	1.285	.267	90.750	92.302
80.	2.	99.	99.	99.	2.0	4.4	.710	0.000	1.110	.067	61.600	62.777
80.	2.	99.	99.	99.	4.4	7.5	.500	0.000	1.345	.100	86.625	88.070
80.	2.	99.	99.	99.	7.5	11.1	.050	0.000	1.047	.047	39.875	40.969
80.	2.	99.	99.	99.	11.1	15.0	.150	0.000	.812	.047	19.250	20.109
80.	2.	99.	99.	99.	15.0	23.0	.100	0.000	.428	.020	15.125	15.573
80.	2.	99.	99.	99.	23.0	31.0	.100	0.000	.270	0.000	35.750	36.020
81.	2.	99.	99.	99.	99.0	99.0	2.970	0.000	2.280	.460	198.000	200.740
82.	2.	99.	99.	99.	99.0	99.0	.940	0.000	2.424	.380	314.880	317.680
83.	2.	99.	99.	99.	99.0	99.0	.890	0.000	2.280	.487	214.500	217.270
84.	2.	99.	99.	99.	99.0	99.0	1.140	0.000	2.675	1.540	384.070	388.280
85.	2.	99.	99.	99.	99.0	99.0	.660	0.000	2.520	.447	342.380	345.340

COPPER

A	B	C	D	E	F	G	H	I	J	K	L	M
2.	2.	1.	5.	2.	0.0	2.0	.190	.200	5.713	2.007	29.333	37.253
3.	1.	1.	5.	2.	0.0	1.0	0.000	.337	6.847	2.480	8.750	18.414
4.	2.	1.	1.	2.	0.0	5.0	0.000	.203	1.000	.200	28.000	29.403
5.	1.	1.	1.	2.	0.0	1.0	0.000	0.000	.427	.327	14.600	15.354
6.	1.	1.	1.	2.	0.0	1.0	0.000	.653	9.247	.760	18.167	28.850
7.	1.	1.	1.	2.	0.0	1.0	0.000	2.920	7.080	14.000	16.200	40.200
9.	2.	1.	5.	2.	0.0	2.0	0.000	.093	4.267	1.660	35.500	41.520
10.	2.	1.	6.	2.	0.0	2.0	0.000	.460	7.913	3.533	32.333	44.236
10.	2.	1.	6.	99.	10.0	12.0	0.000	.227	8.147	2.793	44.236	55.403
10.	2.	1.	4.	99.	45.0	47.0	0.000	.387	4.433	1.473	15.833	22.383
10.	2.	1.	6.	99.	109.0	110.0	.100	.210	5.333	3.467	10.000	19.010
10.	2.	1.	4.	99.	138.0	140.0	.100	0.000	4.607	4.867	31.500	40.974
10.	2.	1.	4.	99.	148.0	150.0	.250	0.000	5.300	2.200	45.500	53.000
10.	2.	1.	1.	99.	168.0	170.0	.100	0.000	4.573	2.620	22.000	29.193
10.	2.	1.	6.	99.	218.0	220.0	.150	.053	5.567	6.107	28.750	40.477
10.	2.	1.	6.	99.	248.0	250.0	.220	0.000	5.893	3.807	20.667	30.367
10.	2.	1.	5.	99.	258.0	260.0	.190	.308	5.927	3.307	27.333	36.875
10.	2.	1.	1.	99.	308.0	310.0	0.000	0.000	3.667	31.813	13.083	48.563
10.	2.	1.	4.	99.	328.0	330.0	.100	.113	3.580	1.000	9.500	14.193
10.	2.	1.	4.	99.	358.0	360.0	0.000	0.000	5.127	2.093	21.000	28.263
10.	2.	1.	5.	99.	408.0	413.0	.100	0.000	5.593	4.693	22.417	32.703
10.	2.	1.	6.	99.	428.0	430.0	.100	.227	7.007	5.993	23.583	36.810
10.	2.	1.	6.	99.	439.0	440.0	0.000	.300	8.193	4.587	16.833	29.913
11.	1.	1.	5.	2.	0.0	1.0	.310	0.000	4.680	1.760	296.670	303.110
12.	1.	1.	5.	2.	0.0	1.0	.050	0.000	4.353	2.460	20.833	27.586
13.	1.	1.	5.	2.	0.0	1.0	.200	0.000	4.547	1.927	229.670	236.140
14.	2.	1.	5.	2.	0.0	2.0	.150	0.000	3.993	3.105	22.833	29.931
15.	1.	2.	5.	3.	0.0	1.0	.200	0.000	10.707	3.560	25.667	39.934
16.	1.	2.	5.	3.	0.0	1.0	.150	0.000	5.580	2.307	48.333	56.220
17.	1.	2.	5.	3.	0.0	1.0	.200	.370	15.733	7.140	20.000	43.243
18.	1.	2.	6.	3.	0.0	1.0	.150	.265	7.800	2.653	26.583	37.301
19.	1.	2.	6.	3.	0.0	1.0	.260	0.000	13.407	3.353	128.330	145.090
20.	2.	1.	6.	2.	0.0	2.0	0.000	.010	6.767	2.253	30.333	39.363
25.	1.	1.	3.	3.	0.0	1.0	0.000	.227	2.473	1.600	22.250	40.950
26.	1.	2.	1.	3.	0.0	1.0	0.000	0.000	3.000	1.427	56.167	60.594
27.	1.	2.	2.	3.	0.0	1.0	0.000	99.000	3.733	1.140	18.643	23.516
28.	2.	2.	5.	1.	0.0	5.0	0.000	.180	3.667	.913	12.500	17.260
29.	2.	2.	5.	1.	0.0	2.0	.100	0.000	5.953	3.120	28.583	37.656
30.	2.	2.	1.	1.	0.0	5.0	0.000	.620	.947	.513	12.250	14.330
31.	1.	2.	2.	1.	0.0	1.0	0.000	.617	2.107	2.520	27.167	32.411
32.	2.	2.	2.	1.	0.0	5.0	.100	.495	3.667	4.100	15.000	23.262
33.	2.	2.	1.	1.	0.0	2.0	0.000	.080	1.747	.140	7.100	9.067
34.	2.	2.	5.	1.	0.0	5.0	0.000	.400	5.513	1.980	25.917	33.810
35.	2.	2.	5.	1.	0.0	1.0	.050	.100	5.960	2.667	22.083	30.810
36.	1.	2.	5.	3.	0.0	1.0	.200	.240	12.347	3.947	50.000	66.534
37.	1.	2.	5.	3.	0.0	1.0	.200	.300	6.733	3.507	24.417	34.957
38.	1.	2.	4.	3.	0.0	1.0	0.000	.250	15.133	.367	13.500	29.250
39.	1.	2.	4.	3.	0.0	1.0	.100	0.000	1.660	1.353	18.750	21.763
42.	2.	2.	6.	3.	0.0	5.0	.290	.120	10.240	4.647	35.667	50.674
42.	2.	99.	99.	99.	40.0	45.0	.220	.120	7.193	3.153	24.333	34.879
42.	2.	99.	99.	99.	108.0	110.0	.150	.210	10.653	3.820	28.250	42.933
42.	2.	99.	99.	99.	168.0	170.0	0.000	.210	9.033	4.127	20.750	34.120
42.	2.	99.	99.	99.	308.0	310.0	0.000	0.000	8.187	5.080	33.333	46.600
42.	2.	99.	99.	99.	361.0	370.0	.240	.050	1.093	1.013	18.100	20.253
42.	2.	99.	99.	99.	411.0	419.0	0.000	0.000	5.340	1.260	13.500	20.100
42.	2.	99.	99.	99.	556.0	563.0	.190	0.000	5.607	3.353	11.900	20.860
43.	2.	2.	6.	3.	0.0	2.0	.100	.100	9.640	2.533	33.583	45.856

COPPER (cont'd)

A	B	C	D	E	F	G	H	I	J	K	L	M
46.	2.	2.	6.	3.	0.0	5.0	0.000	.300	6.973	3.733	31.167	42.173
46.	2.	99.	99.	99.	5.0	10.0	.250	.110	7.487	3.280	24.667	35.544
46.	2.	99.	99.	99.	10.0	15.0	.270	.080	9.247	3.027	23.167	35.521
46.	2.	99.	99.	99.	15.0	20.0	.150	0.000	7.660	3.027	31.167	41.854
46.	2.	99.	99.	99.	20.0	25.0	.250	.250	8.387	3.367	215.500	227.500
46.	2.	99.	99.	99.	25.0	30.0	.050	.040	6.787	3.013	36.917	46.757
46.	2.	99.	99.	99.	30.0	35.0	.200	0.000	6.240	2.660	21.333	30.233
46.	2.	99.	99.	99.	35.0	40.0	.150	.290	7.647	4.720	167.830	180.490
46.	2.	99.	99.	99.	40.0	45.0	.190	.047	8.507	5.740	16.250	30.544
46.	2.	99.	99.	99.	45.0	50.0	.240	.073	8.233	4.327	67.000	79.633
47.	1.	2.	6.	3.	0.0	1.0	.260	0.000	10.687	4.400	30.000	45.087
50.	1.	1.	6.	3.	0.0	1.0	.260	.343	17.953	4.747	135.330	158.380
55.	1.	1.	6.	1.	0.0	1.0	.200	0.000	9.700	5.780	60.833	76.313
56.	2.	2.	6.	1.	0.0	2.0	.100	.300	9.960	5.140	35.667	51.067
57.	2.	1.	6.	3.	0.0	2.0	0.000	.323	25.420	22.353	40.083	88.179
80.	2.	99.	99.	99.	0.0	2.0	.300	.907	1.987	12.347	18.167	33.408
80.	2.	99.	99.	99.	2.0	4.4	.710	.710	1.247	8.353	2.500	12.810
80.	2.	99.	99.	99.	4.4	7.5	.500	.577	1.327	8.960	3.333	14.197
80.	2.	99.	99.	99.	7.5	11.1	.050	2.827	.987	17.980	4.000	25.794
80.	2.	99.	99.	99.	11.1	15.0	.150	1.553	7.080	10.127	8.750	27.510
80.	2.	99.	99.	99.	15.0	23.0	.100	7.780	16.287	10.993	43.833	78.893
80.	2.	99.	99.	99.	23.0	31.0	.100	1.310	3.053	2.073	6.200	12.636
81.	2.	99.	99.	99.	99.0	99.0	2.970	.203	.193	2.040	7.750	10.186
82.	2.	99.	99.	99.	99.0	99.0	.940	.253	.633	1.247	12.200	14.333
83.	2.	99.	99.	99.	99.0	99.0	.890	.367	.593	1.753	12.600	15.313
84.	2.	99.	99.	99.	99.0	99.0	1.140	0.000	.650	1.060	14.083	15.793
85.	2.	99.	99.	99.	99.0	99.0	.660	.310	1.260	1.513	14.800	17.883

IRON

A	B	C	D	E	F	G	H	I	J	K	L	M
2.	2.	1.	5.	2.	0.0	2.0	.190	4.173	6800.000	56.047	33900.000	40760.000
3.	1.	1.	5.	2.	0.0	1.0	0.000	5.520	2780.000	16.700	10275.000	13077.000
4.	2.	1.	1.	2.	0.0	5.0	0.000	4.610	1953.300	17.613	2716.700	4692.200
5.	1.	1.	1.	2.	0.0	1.0	0.000	1.510	2120.000	24.680	2983.300	5129.500
6.	1.	1.	1.	2.	0.0	1.0	0.000	27.560	3466.000	7.433	5990.800	9491.800
7.	1.	1.	1.	2.	0.0	1.0	0.000	7.115	1814.000	7.707	41592.000	43420.000
9.	2.	1.	5.	2.	0.0	2.0	0.000	29.253	6980.000	47.213	34217.000	41273.000
10.	2.	1.	6.	2.	0.0	2.0	0.000	35.093	11840.000	64.340	37508.000	49448.000
10.	2.	1.	6.	99.	10.0	12.0	0.000	20.100	8600.000	56.167	37717.000	46393.000
10.	2.	1.	4.	99.	45.0	47.0	0.000	34.453	6026.700	35.673	25842.000	31938.000
10.	2.	1.	6.	99.	109.0	110.0	.100	13.687	7100.000	266.800	31017.000	38397.000
10.	2.	1.	4.	99.	138.0	140.0	.100	3.987	6493.300	64.953	31775.000	38337.000
10.	2.	1.	4.	99.	148.0	150.0	.250	5.103	6120.000	78.947	28600.000	34804.000
10.	2.	1.	1.	99.	168.0	170.0	.100	5.110	7020.000	85.973	32400.000	39511.000
10.	2.	1.	6.	99.	218.0	220.0	.150	21.163	9353.300	916.370	41048.000	51339.000
10.	2.	1.	6.	99.	248.0	250.0	.220	17.860	9900.000	713.700	39717.000	50348.000
10.	2.	1.	5.	99.	258.0	260.0	.190	22.747	7480.000	278.530	32117.000	39898.000
10.	2.	1.	1.	99.	308.0	310.0	0.000	7.337	7806.700	1118.300	20800.000	29726.000
10.	2.	1.	4.	99.	328.0	330.0	.100	3.640	5266.700	25.053	11950.000	17245.000
10.	2.	1.	4.	99.	358.0	360.0	0.000	9.107	6280.000	69.353	29600.000	35958.000
10.	2.	1.	5.	99.	408.0	413.0	.100	11.600	7960.000	288.290	29783.000	38043.000
10.	2.	1.	6.	99.	428.0	430.0	.100	21.750	9900.000	826.110	31767.000	42515.000
10.	2.	1.	6.	99.	439.0	440.0	0.000	71.960	10907.000	796.810	41683.000	53459.000
11.	1.	1.	5.	2.	0.0	1.0	.310	5.473	6793.300	44.640	27550.000	34393.000
12.	1.	1.	5.	2.	0.0	1.0	.050	21.210	5453.300	50.925	24875.000	30400.000
13.	1.	1.	5.	2.	0.0	1.0	.200	10.753	6086.700	49.480	24142.000	30288.000
14.	2.	1.	5.	2.	0.0	2.0	.150	9.227	6133.300	80.285	29933.000	36156.000
15.	1.	2.	5.	3.	0.0	1.0	.200	28.483	9360.000	82.073	37433.000	46904.000
16.	1.	2.	5.	3.	0.0	1.0	.150	13.420	957.480	57.126	34883.000	35911.000
17.	1.	2.	5.	3.	0.0	1.0	.200	26.930	7920.000	58.433	34450.000	42455.000
18.	1.	2.	6.	3.	0.0	1.0	.150	10.927	7593.300	59.700	33925.000	41589.000
19.	1.	2.	6.	3.	0.0	1.0	.260	13.010	8160.000	56.660	39175.000	47405.000
20.	2.	1.	6.	2.	0.0	2.0	0.000	22.657	7693.300	64.605	44558.000	52339.000
25.	1.	1.	3.	3.	0.0	1.0	0.000	1.400	5840.000	37.807	23133.000	29013.000
26.	1.	2.	1.	3.	0.0	1.0	0.000	9.447	5286.700	29.893	19333.000	24659.000
27.	1.	2.	2.	3.	0.0	1.0	0.000	99.000	3786.700	13.360	26550.000	30350.000
28.	2.	2.	5.	1.	0.0	5.0	0.000	4.338	6706.700	27.653	22992.000	29730.000
29.	2.	2.	5.	1.	0.0	2.0	.100	15.903	7826.700	81.235	39317.000	47240.000
30.	2.	2.	1.	1.	0.0	5.0	0.000	35.050	3266.700	11.533	16367.000	19680.000
31.	1.	2.	2.	1.	0.0	1.0	0.000	2.093	5380.000	90.975	27875.000	33348.000
32.	2.	2.	2.	1.	0.0	5.0	.100	22.553	6666.700	258.370	29367.000	36314.000
33.	2.	2.	1.	1.	0.0	2.0	0.000	9.097	3451.800	9.067	12558.000	16028.000
34.	2.	2.	5.	1.	0.0	5.0	0.000	27.283	7566.700	69.513	35625.000	43288.000
35.	2.	2.	5.	1.	0.0	1.0	.050	11.400	7246.700	59.093	32900.000	40217.000
36.	1.	2.	5.	3.	0.0	1.0	.200	12.527	7653.300	59.600	39667.000	47392.000
37.	1.	2.	5.	3.	0.0	1.0	.200	33.837	7733.300	94.507	34594.000	42456.000
38.	1.	2.	4.	3.	0.0	1.0	0.000	6.070	3473.300	13.293	17783.000	21276.000
39.	1.	2.	4.	3.	0.0	1.0	.100	9.427	5100.000	33.980	22700.000	27843.000
42.	2.	2.	6.	3.	0.0	5.0	.290	8.003	8306.700	77.733	46192.000	54584.000
42.	2.	99.	99.	99.	40.0	45.0	.220	24.920	8140.000	72.933	47900.000	56138.000
42.	2.	99.	99.	99.	108.0	110.0	.150	34.125	8826.700	249.570	45017.000	54127.000
42.	2.	99.	99.	99.	168.0	170.0	0.000	19.637	9113.300	682.670	46083.000	55899.000
42.	2.	99.	99.	99.	308.0	310.0	0.000	36.767	1458.000	720.370	44542.000	46757.000
42.	2.	99.	99.	99.	361.0	370.0	.240	10.655	5046.700	49.100	39583.000	44690.000
42.	2.	99.	99.	99.	411.0	419.0	0.000	3.643	3306.700	23.073	27317.000	30650.000
42.	2.	99.	99.	99.	556.0	563.0	.190	8.137	7973.300	319.920	29192.000	37493.000
43.	2.	2.	6.	3.	0.0	2.0	.100	86.713	7313.300	64.460	38192.000	45656.000

IRON (cont'd.)

A	B	C	D	E	F	G	H	I	J	K	L	M
46.	2.	2.	6.	3.	0.0	5.0	0.000	35.670	9040.000	88.373	42050.000	51214.000
46.	2.	99.	99.	99.	5.0	10.0	.250	18.048	7446.700	56.827	36350.000	43872.000
46.	2.	99.	99.	99.	10.0	15.0	.270	15.683	7680.000	71.805	38675.000	46442.000
46.	2.	99.	99.	99.	15.0	20.0	.150	34.590	7853.300	38.593	44892.000	52818.000
46.	2.	99.	99.	99.	20.0	25.0	.250	74.133	7293.300	79.240	45383.000	52830.000
46.	2.	99.	99.	99.	25.0	30.0	.050	33.613	8693.300	82.810	48167.000	56976.000
46.	2.	99.	99.	99.	30.0	35.0	.200	22.940	8093.300	92.745	42050.000	50259.000
46.	2.	99.	99.	99.	35.0	40.0	.150	17.385	8326.700	328.690	44750.000	53423.000
46.	2.	99.	99.	99.	40.0	45.0	.190	18.165	8980.000	353.070	43017.000	52368.000
46.	2.	99.	99.	99.	45.0	50.0	.240	13.407	8233.300	340.530	42217.000	50804.000
47.	1.	2.	6.	3.	0.0	1.0	.260	27.935	7586.700	88.840	45208.000	52912.000
50.	1.	1.	6.	3.	0.0	1.0	.260	11.927	7713.300	69.913	46150.000	53945.000
55.	1.	1.	6.	1.	0.0	1.0	.200	21.290	11200.000	221.470	44350.000	55793.000
56.	2.	2.	6.	1.	0.0	2.0	.100	12.217	12740.000	832.170	45333.000	58918.000
57.	2.	1.	6.	3.	0.0	2.0	0.000	15.003	9013.300	88.640	43083.000	52200.000
80.	2.	99.	99.	99.	0.0	2.0	.300	60.787	314.530	8.580	1558.300	1942.200
80.	2.	99.	99.	99.	2.0	4.4	.710	47.162	328.130	6.610	1828.600	2210.500
80.	2.	99.	99.	99.	4.4	7.5	.500	34.697	314.670	8.667	1175.000	1533.000
80.	2.	99.	99.	99.	7.5	11.1	.050	60.193	513.870	5.413	700.000	1279.500
80.	2.	99.	99.	99.	11.1	15.0	.150	16.903	231.730	3.320	633.330	885.290
80.	2.	99.	99.	99.	15.0	23.0	.100	9.070	37.270	.340	83.330	130.010
80.	2.	99.	99.	99.	23.0	31.0	.100	2.353	12.207	0.000	342.500	357.060
81.	2.	99.	99.	99.	99.0	99.0	2.970	34.583	692.000	20.040	5350.000	6096.600
82.	2.	99.	99.	99.	99.0	99.0	.940	24.393	862.670	8.213	6700.000	7595.300
83.	2.	99.	99.	99.	99.0	99.0	.890	15.680	823.330	8.933	5516.700	6364.600
84.	2.	99.	99.	99.	99.0	99.0	1.140	17.147	1000.000	8.053	6333.300	7358.500
85.	2.	99.	99.	99.	99.0	99.0	.660	7.247	1075.300	4.920	6891.700	7979.200

COBALT

A	B	C	D	E	F	G	H	I	J	K	L	M
2.	2.	1.	5.	2.	0.0	2.0	.190	0.000	2.800	.900	47.400	51.100
3.	1.	1.	5.	2.	0.0	1.0	0.000	0.000	.914	.270	35.100	36.284
4.	2.	1.	1.	2.	0.0	5.0	0.000	0.000	.324	.090	40.667	41.081
5.	1.	1.	1.	2.	0.0	1.0	0.000	0.000	.343	.180	44.000	44.523
6.	1.	1.	1.	2.	0.0	1.0	0.000	0.000	.475	.060	37.100	37.635
7.	1.	1.	1.	2.	0.0	1.0	0.000	0.000	.765	.093	36.400	37.258
9.	2.	1.	5.	2.	0.0	2.0	0.000	0.000	1.157	1.091	48.400	50.640
10.	2.	1.	6.	2.	0.0	2.0	0.000	0.000	1.454	1.160	39.900	42.514
10.	2.	1.	6.	99.	10.0	12.0	0.000	0.000	1.552	1.170	46.000	48.722
10.	2.	1.	4.	99.	45.0	47.0	0.000	0.000	2.550	.810	47.000	50.360
10.	2.	1.	6.	99.	109.0	110.0	.100	0.000	1.420	1.267	50.500	53.187
10.	2.	1.	4.	99.	138.0	140.0	.100	0.000	.787	1.030	39.500	41.317
10.	2.	1.	4.	99.	148.0	150.0	.250	.055	2.787	.980	44.625	48.447
10.	2.	1.	1.	99.	168.0	170.0	.100	0.000	.997	1.085	41.625	43.707
10.	2.	1.	6.	99.	218.0	220.0	.150	0.000	1.675	1.790	55.125	58.590
10.	2.	1.	6.	99.	248.0	250.0	.220	.005	1.255	1.713	57.250	60.223
10.	2.	1.	5.	99.	258.0	260.0	.190	0.000	2.347	1.160	51.125	54.632
10.	2.	1.	1.	99.	308.0	310.0	0.000	0.000	.783	1.000	43.000	44.783
10.	2.	1.	4.	99.	328.0	330.0	.100	0.000	1.117	.800	36.200	38.117
10.	2.	1.	4.	99.	358.0	360.0	0.000	.015	.943	.800	56.250	58.008
10.	2.	1.	5.	99.	408.0	413.0	.100	.040	1.909	1.453	48.375	51.777
10.	2.	1.	6.	99.	428.0	430.0	.100	0.000	2.017	1.935	43.750	47.702
10.	2.	1.	6.	99.	439.0	440.0	0.000	0.000	3.140	1.633	48.875	53.648
11.	1.	1.	5.	2.	0.0	1.0	.310	0.000	1.518	1.150	46.200	48.868
12.	1.	1.	5.	2.	0.0	1.0	.050	0.000	1.930	.913	39.875	42.718
13.	1.	1.	5.	2.	0.0	1.0	.200	0.000	1.830	1.310	49.000	52.140
14.	2.	1.	5.	2.	0.0	2.0	.150	.020	4.240	1.207	50.875	56.342
15.	1.	2.	5.	3.	0.0	1.0	.200	.140	.687	1.260	47.900	49.987
16.	1.	2.	5.	3.	0.0	1.0	.150	.010	.653	1.090	45.250	47.003
17.	1.	2.	5.	3.	0.0	1.0	.200	0.000	1.071	1.200	40.375	42.646
18.	1.	2.	6.	3.	0.0	1.0	.150	.030	1.723	1.200	45.000	47.953
19.	1.	2.	6.	3.	0.0	1.0	.260	.400	.882	1.110	54.200	56.592
20.	2.	1.	6.	2.	0.0	2.0	0.000	.155	2.340	1.593	56.750	60.838
25.	1.	1.	3.	3.	0.0	1.0	0.000	0.000	3.210	.890	44.125	48.215
26.	1.	2.	1.	3.	0.0	1.0	0.000	.020	3.320	.730	43.667	47.917
27.	1.	2.	2.	3.	0.0	1.0	0.000	99.000	3.120	.420	47.750	51.290
28.	2.	2.	5.	1.	0.0	5.0	0.000	.070	2.720	.800	40.125	43.715
29.	2.	2.	5.	1.	0.0	2.0	.100	0.000	2.360	1.505	47.500	51.375
30.	2.	2.	1.	1.	0.0	5.0	0.000	.400	1.777	.210	47.000	49.387
31.	1.	2.	2.	1.	0.0	1.0	0.000	0.000	4.113	.547	37.625	42.285
32.	2.	2.	2.	1.	0.0	5.0	.100	.035	4.540	.807	41.875	47.257
33.	2.	2.	1.	1.	0.0	2.0	0.000	0.000	1.083	.167	44.000	45.250
34.	2.	2.	5.	1.	0.0	5.0	0.000	.420	1.898	1.300	57.500	61.118
35.	2.	2.	5.	1.	0.0	1.0	.050	0.000	2.893	1.160	43.625	47.678
36.	1.	2.	5.	3.	0.0	1.0	.200	0.000	1.520	1.310	50.000	52.830
37.	1.	2.	5.	3.	0.0	1.0	.200	0.000	1.197	1.410	33.125	35.732
38.	1.	2.	4.	3.	0.0	1.0	0.000	0.000	2.728	.520	37.875	41.123
39.	1.	2.	4.	3.	0.0	1.0	.100	0.000	1.710	.600	51.100	53.410
42.	2.	2.	6.	3.	0.0	5.0	.290	0.000	1.000	1.570	48.625	51.195
42.	2.	99.	99.	99.	40.0	45.0	.220	.475	1.694	7.860	45.500	55.529
42.	2.	99.	99.	99.	108.0	110.0	.150	0.000	1.311	1.610	42.625	45.546
42.	2.	99.	99.	99.	168.0	170.0	0.000	.070	4.800	1.773	46.250	52.893
42.	2.	99.	99.	99.	308.0	310.0	0.000	0.000	3.660	2.460	45.900	52.020
42.	2.	99.	99.	99.	361.0	370.0	.240	0.000	2.620	.670	52.800	56.090
42.	2.	99.	99.	99.	411.0	419.0	0.000	0.000	3.227	.560	51.583	55.370
42.	2.	99.	99.	99.	556.0	563.0	.190	0.000	1.653	1.340	53.250	56.243
43.	2.	2.	6.	3.	0.0	2.0	.100	0.000	5.428	1.060	52.125	58.613

COBALT (cont'd.)

A	B	C	D	E	F	G	H	I	J	K	L	M
46.	2.	2.	6.	3.	0.0	5.0	0.000	.035	1.711	1.920	43.375	45.241
46.	2.	99.	99.	99.	5.0	10.0	.250	0.000	4.060	1.420	44.375	49.855
46.	2.	99.	99.	99.	10.0	15.0	.270	.040	1.825	1.230	53.700	56.795
46.	2.	99.	99.	99.	15.0	20.0	.150	.035	.914	1.750	52.250	54.949
46.	2.	99.	99.	99.	20.0	25.0	.250	0.000	1.007	1.547	45.400	47.954
46.	2.	99.	99.	99.	25.0	30.0	.050	0.000	1.870	1.710	50.500	54.080
46.	2.	99.	99.	99.	30.0	35.0	.200	0.000	.876	1.800	48.375	51.051
46.	2.	99.	99.	99.	35.0	40.0	.150	0.000	1.576	2.067	48.500	52.143
46.	2.	99.	99.	99.	40.0	45.0	.190	0.000	2.638	1.840	58.500	62.978
46.	2.	99.	99.	99.	45.0	50.0	.240	0.000	5.060	1.893	50.200	57.153
47.	1.	2.	6.	3.	0.0	1.0	.260	0.000	2.063	1.455	57.750	61.268
50.	1.	1.	6.	3.	0.0	1.0	.260	.180	1.604	1.207	49.500	52.491
55.	1.	1.	6.	1.	0.0	1.0	.200	.743	1.169	1.420	48.500	51.832
56.	2.	2.	6.	1.	0.0	2.0	.100	0.000	6.633	1.767	59.125	67.525
57.	2.	1.	6.	3.	0.0	2.0	0.000	0.000	1.680	1.490	57.250	60.420
80.	2.	99.	99.	99.	0.0	2.0	.300	0.000	0.000	0.000	48.750	48.750
80.	2.	99.	99.	99.	2.0	4.4	.710	0.000	0.000	0.000	41.625	41.625
80.	2.	99.	99.	99.	4.4	7.5	.500	.400	0.000	0.000	50.250	50.650
80.	2.	99.	99.	99.	7.5	11.1	.050	.010	0.000	0.000	49.000	49.010
80.	2.	99.	99.	99.	11.1	15.0	.150	0.000	0.000	0.000	45.250	45.250
80.	2.	99.	99.	99.	15.0	23.0	.100	0.000	0.000	0.000	45.625	45.625
80.	2.	99.	99.	99.	23.0	31.0	.100	0.000	0.000	0.000	38.667	38.667
81.	2.	99.	99.	99.	99.0	99.0	2.970	0.000	0.000	0.000	38.000	38.000
82.	2.	99.	99.	99.	99.0	99.0	.940	0.000	0.000	0.000	37.800	37.800
83.	2.	99.	99.	99.	99.0	99.0	.890	0.000	.020	.030	30.500	30.550
84.	2.	99.	99.	99.	99.0	99.0	1.140	0.000	.040	.010	35.600	35.650
85.	2.	99.	99.	99.	99.0	99.0	.660	0.000	.103	0.000	50.500	50.603

MANGANESE

A	B	C	D	E	F	G	H	I	J	K	L	M
2.	2.	1.	5.	2.	0.0	2.0	.190	2.357	309.270	31.680	176.000	519.300
3.	1.	1.	5.	2.	0.0	1.0	0.000	5.537	97.867	4.120	27.666	135.190
4.	2.	1.	1.	2.	0.0	5.0	0.000	2.630	19.600	.813	26.250	49.293
5.	1.	1.	1.	2.	0.0	1.0	0.000	1.647	18.267	.767	33.666	54.347
6.	1.	1.	1.	2.	0.0	1.0	0.000	2.247	28.733	1.287	23.916	56.183
7.	1.	1.	1.	2.	0.0	1.0	0.000	2.533	23.000	.940	998.080	1024.600
9.	2.	1.	5.	2.	0.0	2.0	0.000	4.587	245.070	27.513	184.830	462.000
10.	2.	1.	6.	2.	0.0	2.0	0.000	17.210	342.330	35.107	173.080	567.730
10.	2.	1.	6.	99.	10.0	12.0	0.000	6.063	357.600	34.973	192.170	590.800
10.	2.	1.	4.	99.	45.0	47.0	0.000	10.917	305.600	26.460	139.750	482.730
10.	2.	1.	6.	99.	109.0	110.0	.100	35.233	426.670	43.260	154.250	659.410
10.	2.	1.	4.	99.	138.0	140.0	.100	34.033	384.130	34.727	139.080	591.970
10.	2.	1.	4.	99.	148.0	150.0	.250	34.467	326.670	28.767	142.670	532.570
10.	2.	1.	1.	99.	168.0	170.0	.100	38.733	330.670	33.460	161.000	563.860
10.	2.	1.	6.	99.	218.0	220.0	.150	46.633	445.530	61.527	192.170	745.860
10.	2.	1.	6.	99.	248.0	250.0	.220	36.733	458.270	60.887	175.000	730.890
10.	2.	1.	5.	99.	258.0	260.0	.190	53.700	298.400	32.460	155.500	540.060
10.	2.	1.	1.	99.	308.0	310.0	0.000	51.833	372.130	60.760	108.400	593.130
10.	2.	1.	4.	99.	328.0	330.0	.100	16.127	251.470	16.907	127.130	411.670
10.	2.	1.	4.	99.	358.0	360.0	0.000	31.133	363.270	36.460	134.250	565.110
10.	2.	1.	5.	99.	408.0	413.0	.100	51.900	386.330	39.847	160.670	638.750
10.	2.	1.	6.	99.	428.0	430.0	.100	67.667	528.070	64.787	177.580	838.110
10.	2.	1.	6.	99.	439.0	440.0	0.000	20.937	606.730	62.747	180.170	870.580
11.	1.	1.	5.	2.	0.0	1.0	.310	81.100	221.000	21.387	166.080	489.570
12.	1.	1.	5.	2.	0.0	1.0	.050	68.500	250.200	21.967	172.920	513.580
13.	1.	1.	5.	2.	0.0	1.0	.200	56.867	229.200	18.867	165.830	470.770
14.	2.	1.	5.	2.	0.0	2.0	.150	18.870	391.470	40.940	194.000	645.280
15.	1.	2.	5.	3.	0.0	1.0	.200	80.267	391.550	36.087	175.670	683.570
16.	1.	2.	5.	3.	0.0	1.0	.150	136.130	355.000	31.413	190.500	713.050
17.	1.	2.	5.	3.	0.0	1.0	.200	101.070	269.870	27.067	191.580	589.580
18.	1.	2.	6.	3.	0.0	1.0	.150	171.200	322.730	34.360	194.330	722.630
19.	1.	2.	6.	3.	0.0	1.0	.260	225.720	323.200	33.340	186.580	768.840
20.	2.	1.	6.	2.	0.0	2.0	0.000	14.700	366.670	46.467	213.580	641.420
25.	1.	1.	3.	3.	0.0	1.0	0.000	48.300	198.470	18.413	167.170	432.350
26.	1.	2.	1.	3.	0.0	1.0	0.000	36.400	186.200	13.687	116.920	353.200
27.	1.	2.	2.	3.	0.0	1.0	0.000	99.000	126.730	6.993	322.000	455.730
28.	2.	2.	5.	1.	0.0	5.0	0.000	103.730	139.330	11.933	144.920	399.920
29.	2.	2.	5.	1.	0.0	2.0	.100	22.393	427.200	58.247	183.250	691.090
30.	2.	2.	1.	1.	0.0	5.0	0.000	46.800	42.200	4.493	150.500	243.990
31.	1.	2.	2.	1.	0.0	1.0	0.000	17.590	200.400	12.373	388.920	619.280
32.	2.	2.	2.	1.	0.0	5.0	.100	345.990	122.200	16.053	279.250	763.490
33.	2.	2.	1.	1.	0.0	2.0	0.000	10.037	179.400	5.660	140.000	335.100
34.	2.	2.	5.	1.	0.0	5.0	0.000	815.970	215.000	24.380	230.420	1285.800
35.	2.	2.	5.	1.	0.0	1.0	.050	1.830	347.200	41.453	180.500	570.980
36.	1.	2.	5.	3.	0.0	1.0	.200	148.930	409.200	43.293	178.420	779.840
37.	1.	2.	5.	3.	0.0	1.0	.200	166.830	361.600	44.473	189.250	762.160
38.	1.	2.	4.	3.	0.0	1.0	0.000	12.853	114.670	8.040	116.670	252.230
39.	1.	2.	4.	3.	0.0	1.0	.100	29.633	231.470	17.853	142.250	421.200
42.	2.	2.	6.	3.	0.0	5.0	.290	18.970	409.530	55.533	186.580	670.620
42.	2.	99.	99.	99.	40.0	45.0	.220	33.233	525.530	67.533	189.750	816.050
42.	2.	99.	99.	99.	108.0	110.0	.150	66.600	671.670	87.895	188.340	1014.500
42.	2.	99.	99.	99.	168.0	170.0	0.000	57.833	691.400	86.880	191.170	1027.300
42.	2.	99.	99.	99.	308.0	310.0	0.000	59.567	658.200	95.567	182.500	995.830
42.	2.	99.	99.	99.	361.0	370.0	.240	2.718	168.870	11.440	269.000	452.030
42.	2.	99.	99.	99.	411.0	419.0	0.000	2.103	113.070	8.587	191.750	315.510
42.	2.	99.	99.	99.	556.0	563.0	.190	117.000	318.930	35.320	148.830	620.080
43.	2.	2.	6.	3.	0.0	2.0	.100	43.033	511.130	63.287	184.670	802.120

MANGANESE (cont'd.)

A	B	C	D	E	F	G	H	I	J	K	L	M
46.	2.	2.	6.	3.	0.0	5.0	0.000	286.390	347.600	47.260	172.000	853.250
46.	2.	99.	99.	99.	5.0	10.0	.250	158.800	265.400	33.513	188.250	645.960
46.	2.	99.	99.	99.	10.0	15.0	.270	159.370	298.300	37.660	197.000	692.330
46.	2.	99.	99.	99.	15.0	20.0	.150	157.170	547.730	63.400	190.000	958.300
46.	2.	99.	99.	99.	20.0	25.0	.250	13.230	554.000	77.873	192.330	837.440
46.	2.	99.	99.	99.	25.0	30.0	.050	44.333	525.400	77.420	205.580	852.740
46.	2.	99.	99.	99.	30.0	35.0	.200	53.933	396.400	56.693	205.830	712.860
46.	2.	99.	99.	99.	35.0	40.0	.150	5.057	613.800	86.420	192.830	898.110
46.	2.	99.	99.	99.	40.0	45.0	.190	89.067	603.070	83.327	177.670	953.130
46.	2.	99.	99.	99.	45.0	50.0	.240	66.200	552.330	75.987	190.750	885.270
47.	1.	2.	6.	3.	0.0	1.0	.260	143.930	469.130	66.200	191.000	870.270
50.	1.	1.	6.	3.	0.0	1.0	.260	109.400	521.730	57.593	195.000	883.730
55.	1.	1.	6.	1.	0.0	1.0	.200	207.610	396.670	40.580	185.000	829.850
56.	2.	2.	6.	1.	0.0	2.0	.100	19.677	721.270	89.947	174.670	1005.600
57.	2.	1.	6.	3.	0.0	2.0	0.000	12.613	492.600	63.800	184.670	753.680
80.	2.	99.	99.	99.	0.0	2.0	.300	3.813	0.000	.800	34.667	39.280
80.	2.	99.	99.	99.	2.0	4.4	.710	1.750	.002	.054	37.584	39.390
80.	2.	99.	99.	99.	4.4	7.5	.500	3.543	.001	.153	40.583	44.280
80.	2.	99.	99.	99.	7.5	11.1	.050	.507	0.000	.573	25.333	26.413
80.	2.	99.	99.	99.	11.1	15.0	.150	.340	0.000	.453	32.333	33.103
80.	2.	99.	99.	99.	15.0	23.0	.100	2.970	0.000	.567	30.000	33.537
80.	2.	99.	99.	99.	23.0	31.0	.100	2.327	0.000	1.200	46.250	49.777
81.	2.	99.	99.	99.	99.0	99.0	2.970	5.293	.017	.160	47.333	52.803
82.	2.	99.	99.	99.	99.0	99.0	.940	3.080	.025	.180	38.750	42.035
83.	2.	99.	99.	99.	99.0	99.0	.890	1.483	.015	.353	48.000	49.851
84.	2.	99.	99.	99.	99.0	99.0	1.140	2.200	.020	.520	49.750	52.490
85.	2.	99.	99.	99.	99.0	99.0	.660	1.483	.040	.553	36.722	38.798

ZINC

A	B	C	D	E	F	G	H	I	J	K	L	M
2.	2.	1.	5.	2.	0.0	2.0	.190	0.00000	21.15300	4.53300	75.50800	101.19000
3.	1.	1.	5.	2.	0.0	1.0	0.000	0.00000	13.45300	2.07300	30.00000	45.52600
4.	2.	1.	1.	2.	0.0	5.0	0.000	.01700	3.81300	.92700	9.03300	13.79000
5.	1.	1.	1.	2.	0.0	1.0	0.000	0.00000	3.39300	1.10700	10.61700	15.11700
6.	1.	1.	1.	2.	0.0	1.0	0.000	0.00000	7.66000	1.49300	9.16700	18.32000
7.	1.	1.	1.	2.	0.0	1.0	0.000	.25300	12.38000	1.56700	61.16700	75.36700
9.	2.	1.	5.	2.	0.0	2.0	0.000	0.00000	21.04000	4.80000	76.24800	102.09000
10.	2.	1.	6.	2.	0.0	2.0	0.000	.21700	23.28700	5.50000	80.49900	109.50000
10.	2.	1.	6.	99.	10.0	12.0	0.000	0.00000	21.63300	5.30700	82.58400	109.52000
10.	2.	1.	4.	99.	45.0	47.0	0.000	.03000	16.17300	4.26700	84.50000	104.97000
10.	2.	1.	6.	99.	109.0	110.0	.100	0.00000	17.49300	5.44700	60.33300	73.27300
10.	2.	1.	4.	99.	138.0	140.0	.100	0.00000	15.54700	4.85300	51.16700	71.56700
10.	2.	1.	4.	99.	148.0	150.0	.250	0.00000	16.28000	4.86700	53.49900	74.64600
10.	2.	1.	1.	99.	168.0	170.0	.100	0.00000	17.83300	4.92700	64.16500	86.92500
10.	2.	1.	6.	99.	218.0	220.0	.150	.02000	20.68700	7.54700	90.41500	118.67000
10.	2.	1.	6.	99.	248.0	250.0	.220	0.00000	19.71300	6.82000	90.25000	116.78000
10.	2.	1.	5.	99.	258.0	260.0	.190	0.00000	13.80300	5.76700	75.08200	94.65200
10.	2.	1.	1.	99.	308.0	310.0	0.000	0.00000	11.69300	10.89300	20.16700	42.75300
10.	2.	1.	4.	99.	328.0	330.0	.100	0.00000	15.18700	3.48000	34.33400	53.00100
10.	2.	1.	4.	99.	358.0	360.0	0.000	0.00000	15.88000	4.66000	55.41700	75.95700
10.	2.	1.	5.	99.	408.0	413.0	.100	0.00000	19.13300	6.48600	70.66700	96.28600
10.	2.	1.	6.	99.	428.0	430.0	.100	0.00000	23.09300	7.79300	86.22500	117.11000
10.	2.	1.	6.	99.	439.0	440.0	0.000	.03300	22.30700	7.10700	107.25000	129.59000
11.	1.	1.	5.	2.	0.0	1.0	.310	.15000	19.98000	4.74700	58.00000	82.87700
12.	1.	1.	5.	2.	0.0	1.0	.050	0.00000	21.48000	5.27300	53.08300	79.75600
13.	1.	1.	5.	2.	0.0	1.0	.200	.38300	18.73300	4.56700	42.66700	66.35000
14.	2.	1.	5.	2.	0.0	2.0	.150	.34700	20.56700	5.73300	69.91600	96.56300
15.	1.	2.	5.	3.	0.0	1.0	.200	2.31700	22.00000	6.29300	80.84300	111.45000
16.	1.	2.	5.	3.	0.0	1.0	.150	.32300	21.79300	5.23300	66.91700	94.26600
17.	1.	2.	5.	3.	0.0	1.0	.200	.30000	24.06000	6.76700	70.50000	101.63000
18.	1.	2.	6.	3.	0.0	1.0	.150	.11700	21.16700	5.28700	73.58300	100.15000
19.	1.	2.	6.	3.	0.0	1.0	.260	.20800	22.96700	5.52000	84.16700	112.86000
20.	2.	1.	6.	2.	0.0	2.0	0.000	0.00000	10.72000	5.44700	93.91600	110.08000
25.	1.	1.	3.	3.	0.0	1.0	0.000	.05300	16.46000	4.62700	34.83000	55.97000
26.	1.	2.	1.	3.	0.0	1.0	0.000	0.00000	15.78700	3.82700	21.51600	41.13000
27.	1.	2.	2.	3.	0.0	1.0	0.000	99.00000	13.68700	4.24000	36.75000	54.67700
28.	2.	2.	5.	1.	0.0	5.0	0.000	.84000	19.24000	3.65300	43.91500	67.64800
29.	2.	2.	5.	1.	0.0	2.0	.100	0.00000	21.72000	6.04000	89.33300	117.09000
30.	2.	2.	1.	1.	0.0	5.0	0.000	1.73000	8.95300	2.32700	22.58300	35.59300
31.	1.	2.	2.	1.	0.0	1.0	0.000	.11500	14.14000	3.81100	38.16700	56.23300
32.	2.	2.	2.	1.	0.0	5.0	.100	2.80700	15.63300	4.08000	43.33300	51.85300
33.	2.	2.	1.	1.	0.0	2.0	0.000	1.87470	5.20000	1.77300	21.33300	30.15300
34.	2.	2.	5.	1.	0.0	5.0	0.000	1.37300	18.97300	5.46700	68.75000	94.56300
35.	2.	2.	5.	1.	0.0	1.0	.050	0.00000	21.38700	5.13300	77.83300	104.35000
36.	1.	2.	5.	3.	0.0	1.0	.200	0.00000	21.84700	5.60700	89.24900	116.70000
37.	1.	2.	5.	3.	0.0	1.0	.200	0.00000	22.01300	7.07300	66.74800	95.83400
38.	1.	2.	4.	3.	0.0	1.0	0.000	.08300	13.52700	3.20000	20.41700	37.22700
39.	1.	2.	4.	3.	0.0	1.0	.100	.03000	15.46000	4.61300	36.08300	56.18600
42.	2.	2.	6.	3.	0.0	5.0	.290	0.00000	20.48700	5.48700	104.58000	130.56000
42.	2.	99.	99.	99.	40.0	45.0	.220	0.00000	19.71300	5.88000	101.33000	126.93000
42.	2.	99.	99.	99.	108.0	110.0	.150	0.00000	21.00000	6.71300	102.83000	130.55000
42.	2.	99.	99.	99.	168.0	170.0	0.000	0.00000	20.98700	7.04700	104.42000	132.45000
42.	2.	99.	99.	99.	308.0	310.0	0.000	0.00000	21.30000	7.58700	104.17000	133.05000
42.	2.	99.	99.	99.	361.0	370.0	.240	0.00000	7.78700	2.96700	67.91600	78.67000
42.	2.	99.	99.	99.	411.0	419.0	0.000	0.00000	8.60700	3.03300	41.49800	53.13800
42.	2.	99.	99.	99.	556.0	563.0	.190	0.00000	20.36000	5.90700	68.41600	94.68300
43.	2.	2.	6.	3.	0.0	2.0	.100	0.00000	21.78000	4.10000	78.38300	104.26000

ZINC (cont'd.)

A	B	C	D	E	F	G	H	I	J	K	L	M
46.	2.	2.	6.	3.	0.0	5.0	0.000	.83700	21.09300	6.14700	95.25000	123.33000
46.	2.	99.	99.	99.	5.0	10.0	.250	.31300	22.66700	5.43300	83.93100	112.34000
46.	2.	99.	99.	99.	10.0	15.0	.270	.94000	24.24700	5.59300	84.71600	115.50000
46.	2.	99.	99.	99.	15.0	20.0	.150	.13700	23.46700	5.74700	96.08300	125.43000
46.	2.	99.	99.	99.	20.0	25.0	.250	.27000	23.14700	6.08700	100.33000	129.84000
46.	2.	99.	99.	99.	25.0	30.0	.050	0.00000	21.70000	6.30000	104.92000	132.92000
46.	2.	99.	99.	99.	30.0	35.0	.200	0.00000	22.72000	6.48000	106.58000	135.78000
46.	2.	99.	99.	99.	35.0	40.0	.150	0.00000	22.48000	7.20700	92.72700	122.41000
46.	2.	99.	99.	99.	40.0	45.0	.190	0.00000	22.74000	7.30000	99.41700	129.46000
46.	2.	99.	99.	99.	45.0	50.0	.240	0.00000	21.98700	7.25300	97.41500	126.66000
47.	1.	2.	6.	3.	0.0	1.0	.260	.01300	22.36000	6.48000	101.79000	130.64000
50.	1.	1.	6.	3.	0.0	1.0	.260	.01700	23.18700	5.64700	98.91700	127.92000
55.	1.	1.	6.	1.	0.0	1.0	.200	0.00000	23.48000	6.34000	102.92000	132.74000
56.	2.	2.	6.	1.	0.0	2.0	.100	.04800	23.26700	7.06000	106.92000	137.29000
57.	2.	1.	6.	3.	0.0	2.0	0.000	.05000	23.80000	6.77300	96.25000	126.87000
80.	2.	99.	99.	99.	0.0	2.0	.300	2.68700	2.07300	.42000	2.58300	7.76300
80.	2.	99.	99.	99.	2.0	4.4	.710	1.66000	.92700	.35300	5.41600	8.35600
80.	2.	99.	99.	99.	4.4	7.5	.500	3.39300	1.40700	.38000	2.41600	7.59600
80.	2.	99.	99.	99.	7.5	11.1	.050	4.14000	4.85300	.61500	1.25000	10.85800
80.	2.	99.	99.	99.	11.1	15.0	.150	2.35500	3.86000	.41300	11.16700	17.79500
80.	2.	99.	99.	99.	15.0	23.0	.100	4.00700	5.15300	.92700	.91600	11.00300
80.	2.	99.	99.	99.	23.0	31.0	.100	1.82700	1.70000	.32000	2.25000	6.09700
81.	2.	99.	99.	99.	99.0	99.0	2.970	3.03700	1.62700	.54700	19.33300	24.54400
82.	2.	99.	99.	99.	99.0	99.0	.940	1.68000	1.81300	.49300	14.08100	18.06700
83.	2.	99.	99.	99.	99.0	99.0	.890	1.24300	1.60000	.40000	22.50000	25.74300
84.	2.	99.	99.	99.	99.0	99.0	1.140	.80800	1.70700	.48000	16.25000	19.24500
85.	2.	99.	99.	99.	99.0	99.0	.660	.92800	1.92000	.50000	10.74800	14.09600

NICKEL

A	B	C	D	E	F	G	H	I	J	K	L	M
2.	2.	1.	5.	2.	0.0	2.0	.190	.030	4.130	2.547	64.750	71.457
3.	1.	1.	5.	2.	0.0	1.0	0.000	.087	1.700	2.030	23.800	27.617
4.	2.	1.	1.	2.	0.0	5.0	0.000	.110	.940	.293	38.700	40.043
5.	1.	1.	1.	2.	0.0	1.0	0.000	.055	1.490	.360	33.000	34.905
6.	1.	1.	1.	2.	0.0	1.0	0.000	.060	1.340	.260	41.750	43.410
7.	1.	1.	1.	2.	0.0	1.0	0.000	.098	1.727	.250	32.000	34.075
9.	2.	1.	5.	2.	0.0	2.0	0.000	.283	5.727	2.620	48.625	57.255
10.	2.	1.	6.	2.	0.0	2.0	0.000	0.000	5.520	3.587	58.700	67.807
10.	2.	1.	6.	99.	10.0	12.0	0.000	.142	4.370	2.727	52.500	59.739
10.	2.	1.	4.	99.	45.0	47.0	0.000	.150	4.140	.893	51.375	56.558
10.	2.	1.	6.	99.	109.0	110.0	.100	.055	5.150	2.787	50.875	58.867
10.	2.	1.	4.	99.	138.0	140.0	.100	.025	4.013	2.780	57.800	64.618
10.	2.	1.	4.	99.	148.0	150.0	.250	.248	4.210	2.500	36.500	43.458
10.	2.	1.	1.	99.	168.0	170.0	.100	.036	4.500	2.827	43.250	50.613
10.	2.	1.	6.	99.	218.0	220.0	.150	.090	5.960	3.960	51.250	61.260
10.	2.	1.	6.	99.	248.0	250.0	.220	.098	5.060	3.220	62.250	70.628
10.	2.	1.	5.	99.	258.0	260.0	.190	.050	5.412	2.667	69.250	77.379
10.	2.	1.	1.	99.	308.0	310.0	0.000	.046	3.970	4.273	30.667	38.956
10.	2.	1.	4.	99.	328.0	330.0	.100	.052	3.870	1.300	45.500	50.722
10.	2.	1.	4.	99.	358.0	360.0	0.000	.182	3.860	2.400	55.700	62.147
10.	2.	1.	5.	99.	408.0	413.0	.100	.100	5.510	2.980	50.375	58.965
10.	2.	1.	6.	99.	428.0	430.0	.100	.024	6.550	3.850	71.500	81.924
10.	2.	1.	6.	99.	439.0	440.0	0.000	.062	6.430	3.243	47.375	57.110
11.	1.	1.	5.	2.	0.0	1.0	.310	.108	3.570	2.410	55.750	61.838
12.	1.	1.	5.	2.	0.0	1.0	.050	0.000	4.150	3.953	49.500	57.603
13.	1.	1.	5.	2.	0.0	1.0	.200	.076	3.770	2.430	45.500	51.776
14.	2.	1.	5.	2.	0.0	2.0	.150	.088	5.250	2.987	53.643	61.968
15.	1.	2.	5.	3.	0.0	1.0	.200	.495	3.030	4.160	52.900	60.585
16.	1.	2.	5.	3.	0.0	1.0	.150	.025	3.040	3.415	49.125	55.605
17.	1.	2.	5.	3.	0.0	1.0	.200	.125	2.650	15.060	58.625	76.460
18.	1.	2.	6.	3.	0.0	1.0	.150	.092	3.695	2.930	82.750	89.467
19.	1.	2.	6.	3.	0.0	1.0	.260	.330	3.010	3.947	51.800	59.087
20.	2.	1.	6.	2.	0.0	2.0	0.000	.184	4.320	3.350	70.250	78.104
25.	1.	1.	3.	3.	0.0	1.0	0.000	.012	7.807	2.680	46.333	56.832
26.	1.	2.	1.	3.	0.0	1.0	0.000	.092	4.210	1.850	44.875	51.027
27.	1.	2.	2.	3.	0.0	1.0	0.000	99.000	7.100	9.250	44.250	60.600
28.	2.	2.	5.	1.	0.0	5.0	0.000	.384	3.750	1.470	51.100	56.704
29.	2.	2.	5.	1.	0.0	2.0	.100	.005	6.270	3.220	52.000	61.495
30.	2.	2.	1.	1.	0.0	5.0	0.000	.340	1.790	.580	53.875	56.585
31.	1.	2.	2.	1.	0.0	1.0	0.000	.157	3.850	1.712	44.750	50.469
32.	2.	2.	2.	1.	0.0	5.0	.100	.927	6.457	2.987	39.625	49.996
33.	2.	2.	1.	1.	0.0	2.0	0.000	.260	1.685	.460	35.167	37.572
34.	2.	2.	5.	1.	0.0	5.0	0.000	.490	5.533	3.420	58.250	67.693
35.	2.	2.	5.	1.	0.0	1.0	.050	.107	7.400	2.870	76.750	87.127
36.	1.	2.	5.	3.	0.0	1.0	.200	.416	4.408	3.460	56.500	64.784
37.	1.	2.	5.	3.	0.0	1.0	.200	.357	3.072	6.050	51.625	61.104
38.	1.	2.	4.	3.	0.0	1.0	0.000	.097	6.513	1.080	45.250	52.940
39.	1.	2.	4.	3.	0.0	1.0	.100	.105	4.760	2.260	43.625	50.750
42.	2.	2.	6.	3.	0.0	5.0	.290	.542	4.210	3.600	47.125	55.477
42.	2.	99.	99.	99.	40.0	45.0	.220	.878	4.880	3.750	54.125	63.633
42.	2.	99.	99.	99.	108.0	110.0	.150	.508	4.713	5.273	52.625	63.119
42.	2.	99.	99.	99.	168.0	170.0	0.000	.012	6.510	3.507	66.250	76.279
42.	2.	99.	99.	99.	308.0	310.0	0.000	.190	8.487	4.730	49.125	62.532
42.	2.	99.	99.	99.	361.0	370.0	.240	.096	7.816	2.400	48.250	58.562
42.	2.	99.	99.	99.	411.0	419.0	0.000	.072	18.664	1.707	68.750	89.193
42.	2.	99.	99.	99.	556.0	563.0	.190	.080	5.150	2.927	49.750	57.907
43.	2.	2.	6.	3.	0.0	2.0	.100	.050	10.410	2.930	76.500	89.890

NICKEL (cont'd.)

A	B	C	D	E	F	G	H	I	J	K	L	M
46.	2.	2.	6.	3.	0.0	5.0	0.000	.485	5.247	3.870	67.500	77.102
46.	2.	99.	99.	99.	5.0	10.0	.250	.144	16.160	6.470	51.500	74.274
46.	2.	99.	99.	99.	10.0	15.0	.270	.344	4.355	3.067	45.875	53.641
46.	2.	99.	99.	99.	15.0	20.0	.150	.122	4.447	3.750	54.000	62.319
46.	2.	99.	99.	99.	20.0	25.0	.250	.037	5.340	3.413	64.700	73.490
46.	2.	99.	99.	99.	25.0	30.0	.050	.008	11.524	7.260	73.625	92.417
46.	2.	99.	99.	99.	30.0	35.0	.200	.025	4.170	3.570	46.000	53.765
46.	2.	99.	99.	99.	35.0	40.0	.150	.223	6.730	5.770	56.375	69.098
46.	2.	99.	99.	99.	40.0	45.0	.190	.245	7.287	3.480	60.500	71.512
46.	2.	99.	99.	99.	45.0	50.0	.240	.098	6.600	4.040	95.250	105.990
47.	1.	2.	6.	3.	0.0	1.0	.260	.566	8.096	3.293	74.750	86.705
50.	1.	1.	6.	3.	0.0	1.0	.260	.410	4.880	3.193	56.625	65.108
55.	1.	1.	6.	1.	0.0	1.0	.200	.532	4.800	4.547	83.250	93.129
56.	2.	2.	6.	1.	0.0	2.0	.100	.167	9.580	3.320	78.500	91.567
57.	2.	1.	6.	3.	0.0	2.0	0.000	.310	5.730	3.480	46.300	55.820
80.	2.	99.	99.	99.	0.0	2.0	.300	.075	0.000	.080	31.375	31.530
80.	2.	99.	99.	99.	2.0	4.4	.710	.122	0.000	.067	34.250	34.439
80.	2.	99.	99.	99.	4.4	7.5	.500	.472	0.000	.120	25.125	25.719
80.	2.	99.	99.	99.	7.5	11.1	.050	.040	0.000	0.000	46.333	46.373
80.	2.	99.	99.	99.	11.1	15.0	.150	.192	0.000	0.000	45.500	45.692
80.	2.	99.	99.	99.	15.0	23.0	.100	.226	0.000	.007	38.250	38.483
80.	2.	99.	99.	99.	23.0	31.0	.100	.232	0.000	.030	50.250	50.512
81.	2.	99.	99.	99.	99.0	99.0	2.970	.277	0.000	.220	37.000	37.497
82.	2.	99.	99.	99.	99.0	99.0	.940	.066	0.000	.140	43.833	44.039
83.	2.	99.	99.	99.	99.0	99.0	.890	.182	0.000	.070	53.250	53.502
84.	2.	99.	99.	99.	99.0	99.0	1.140	.265	0.000	.853	21.375	22.493
85.	2.	99.	99.	99.	99.0	99.0	.660	.140	0.000	.093	38.250	38.483

LEAD

A	B	C	D	E	F	G	H	I	J	K	L	M
2.	2.	1.	5.	2.	0.0	2.0	.1900	0.000	0.000	.860	0.000	.860
3.	1.	1.	5.	2.	0.0	1.0	0.0000	0.000	.125	.920	0.000	1.045
4.	2.	1.	1.	2.	0.0	5.0	0.0000	0.000	0.000	.060	16.000	16.060
5.	1.	1.	1.	2.	0.0	1.0	0.0000	0.000	0.000	.040	1.590	16.300
6.	1.	1.	1.	2.	0.0	1.0	0.0000	0.000	0.000	1.170	.840	2.010
7.	1.	1.	1.	2.	0.0	1.0	0.0000	0.000	0.000	1.400	8.500	9.900
9.	2.	1.	5.	2.	0.0	2.0	0.0000	0.000	0.000	.770	4.750	5.520
10.	2.	1.	6.	2.	0.0	2.0	0.0000	0.000	0.000	1.850	9.170	11.020
10.	2.	1.	6.	99.	10.0	12.0	0.0000	0.000	0.000	1.090	0.000	1.090
10.	2.	1.	4.	99.	45.0	47.0	0.0000	0.000	0.000	.990	2.250	3.240
10.	2.	1.	6.	99.	109.0	110.0	.1000	0.000	0.000	.650	3.670	4.320
10.	2.	1.	4.	99.	138.0	140.0	.1000	0.000	0.000	.960	4.920	5.880
10.	2.	1.	4.	99.	148.0	150.0	.2500	0.000	0.000	.670	0.000	.670
10.	2.	1.	1.	99.	168.0	170.0	.1000	0.000	0.000	.580	0.000	.580
10.	2.	1.	6.	99.	218.0	220.0	.1500	0.000	0.000	.360	2.080	2.440
10.	2.	1.	6.	99.	248.0	250.0	.2200	0.000	0.000	.530	1.920	2.450
10.	2.	1.	5.	99.	258.0	260.0	.1900	0.000	0.000	.530	8.750	9.280
10.	2.	1.	1.	99.	308.0	310.0	0.0000	0.000	0.000	8.370	7.000	15.370
10.	2.	1.	4.	99.	328.0	330.0	.1000	0.000	0.000	.780	4.300	5.080
10.	2.	1.	4.	99.	358.0	360.0	0.0000	0.000	0.000	.780	3.900	4.680
10.	2.	1.	5.	99.	408.0	413.0	.1000	0.000	0.000	.400	0.000	.400
10.	2.	1.	6.	99.	428.0	430.0	.1000	0.000	0.000	.560	9.670	10.230
10.	2.	1.	6.	99.	439.0	440.0	0.0000	0.000	0.000	.420	0.000	.420
11.	1.	1.	5.	2.	0.0	1.0	.3100	0.000	0.000	.900	2.750	3.650
12.	1.	1.	5.	2.	0.0	1.0	.0500	0.000	0.000	.104	0.000	.104
13.	1.	1.	5.	2.	0.0	1.0	.2000	0.000	0.000	.890	0.000	.890
14.	2.	1.	5.	2.	0.0	2.0	.1500	0.000	.020	1.110	0.000	1.130
15.	1.	2.	5.	3.	0.0	1.0	.2000	0.000	0.000	1.060	0.000	1.060
16.	1.	2.	5.	3.	0.0	1.0	.1500	0.000	0.000	.950	5.420	6.370
17.	1.	2.	5.	3.	0.0	1.0	.2000	0.000	0.000	3.220	8.250	11.470
18.	1.	2.	6.	3.	0.0	1.0	.1500	0.000	0.000	1.250	0.000	1.250
19.	1.	2.	6.	3.	0.0	1.0	.2600	0.000	0.000	2.290	3.000	5.290
20.	2.	1.	6.	2.	0.0	2.0	0.0000	0.000	0.000	1.230	5.355	6.565
25.	1.	1.	3.	3.	0.0	1.0	0.0000	0.000	0.000	1.080	4.400	5.480
26.	1.	2.	1.	3.	0.0	1.0	0.0000	0.000	0.000	1.070	1.165	2.335
27.	1.	2.	2.	3.	0.0	1.0	0.0000	99.000	1.550	2.460	.500	4.510
28.	2.	2.	5.	1.	0.0	5.0	0.0000	0.000	0.000	.770	0.000	.770
29.	2.	2.	5.	1.	0.0	2.0	.1000	0.000	0.000	1.250	0.000	1.250
30.	2.	2.	1.	1.	0.0	5.0	0.0000	0.000	1.990	.870	0.000	2.860
31.	1.	2.	2.	1.	0.0	1.0	0.0000	0.000	.630	.940	6.585	8.155
32.	2.	2.	2.	1.	0.0	5.0	.1000	0.000	.740	1.230	.500	2.470
33.	2.	2.	1.	1.	0.0	2.0	0.0000	0.000	0.000	.720	0.000	.720
34.	2.	2.	5.	1.	0.0	5.0	0.0000	0.000	0.000	1.080	0.000	1.080
35.	2.	2.	5.	1.	0.0	1.0	.0500	0.000	0.000	1.100	4.917	6.017
36.	1.	2.	5.	3.	0.0	1.0	.2000	0.000	0.000	2.970	3.333	6.303
37.	1.	2.	5.	3.	0.0	1.0	.2000	0.000	0.000	1.490	0.000	1.490
38.	1.	2.	4.	3.	0.0	1.0	0.0000	0.000	.280	1.060	0.000	1.340
39.	1.	2.	4.	3.	0.0	1.0	.1000	0.000	0.000	.760	0.000	.760
42.	2.	2.	6.	3.	0.0	5.0	.2900	0.000	0.000	1.780	7.785	9.565
42.	2.	99.	99.	99.	40.0	45.0	.2200	0.000	0.000	1.690	15.250	16.940
42.	2.	99.	99.	99.	108.0	110.0	.1500	0.000	0.000	1.170	0.000	1.170
42.	2.	99.	99.	99.	168.0	170.0	0.0000	0.000	0.000	.550	1.085	1.635
42.	2.	99.	99.	99.	308.0	310.0	0.0000	0.000	0.000	.630	2.915	3.545
42.	2.	99.	99.	99.	361.0	370.0	.2400	0.000	6.667	.230	0.000	6.897
42.	2.	99.	99.	99.	411.0	419.0	0.0000	0.000	9.500	.200	1.170	10.870
42.	2.	99.	99.	99.	556.0	563.0	.1900	0.000	0.000	.610	7.875	8.485
43.	2.	2.	6.	3.	0.0	2.0	.1000	0.000	0.000	1.730	0.000	1.730

LEAD (cont'd.)

A	B	C	D	E	F	G	H	I	J	K	L	M
46.	2.	2.	6.	3.	0.0	5.0	0.0000	0.000	0.000	1.690	6.700	8.430
46.	2.	99.	99.	99.	5.0	10.0	.2500	0.000	0.000	1.730	0.000	1.730
46.	2.	99.	99.	99.	10.0	15.0	.2700	0.000	0.000	1.080	0.000	1.080
46.	2.	99.	99.	99.	15.0	20.0	.1500	0.000	0.000	1.450	0.000	1.450
46.	2.	99.	99.	99.	20.0	25.0	.2500	0.000	0.000	1.690	0.000	1.690
46.	2.	99.	99.	99.	25.0	30.0	.0500	0.000	0.000	1.970	0.000	1.970
46.	2.	99.	99.	99.	30.0	35.0	.2000	0.000	0.000	1.320	7.665	8.985
46.	2.	99.	99.	99.	35.0	40.0	.1500	0.000	0.000	.880	5.915	6.795
46.	2.	99.	99.	99.	40.0	45.0	.1900	0.000	0.000	.620	5.500	6.120
46.	2.	99.	99.	99.	45.0	50.0	.2400	0.000	0.000	.830	2.000	2.830
47.	1.	2.	6.	3.	0.0	1.0	.2600	0.000	0.000	1.980	3.250	5.230
50.	1.	1.	6.	3.	0.0	1.0	.2600	0.000	0.000	2.800	11.400	14.200
55.	1.	1.	6.	1.	0.0	1.0	.2000	0.000	0.000	1.230	12.415	13.645
56.	2.	2.	6.	1.	0.0	2.0	.1000	0.000	0.000	.740	0.000	.740
57.	2.	1.	6.	3.	0.0	2.0	0.0000	0.000	0.000	1.800	1.000	2.800
80.	2.	99.	99.	99.	0.0	2.0	.3000	0.000	.129	5.010	0.000	5.139
80.	2.	99.	99.	99.	2.0	4.4	.7100	0.000	2.280	4.950	0.000	7.230
80.	2.	99.	99.	99.	4.4	7.5	.5000	0.000	4.713	5.100	0.000	9.813
80.	2.	99.	99.	99.	7.5	11.1	.0500	0.000	4.460	5.247	0.000	9.707
80.	2.	99.	99.	99.	11.1	15.0	.1500	0.000	4.793	4.550	0.000	9.343
80.	2.	99.	99.	99.	15.0	23.0	.1000	0.000	2.546	2.280	3.000	7.826
80.	2.	99.	99.	99.	23.0	31.0	.1000	0.000	3.340	1.360	15.145	19.845
81.	2.	99.	99.	99.	99.0	99.0	2.9700	0.000	0.000	.660	0.000	.660
82.	2.	99.	99.	99.	99.0	99.0	.9400	0.000	0.000	.640	0.000	.640
83.	2.	99.	99.	99.	99.0	99.0	.8900	0.000	.050	.860	6.335	7.195
84.	2.	99.	99.	99.	99.0	99.0	1.1400	0.000	0.000	.910	0.000	.910
85.	2.	99.	99.	99.	99.0	99.0	.6600	0.000	.430	.520	0.000	.950

CHROMIUM

A	B	C	D	E	F	G	H	I	J	K	L	M
2.	2.	1.	5.	2.	0.0	2.0	.190	.170	4.487	1.213	105.500	111.370
3.	1.	1.	5.	2.	0.0	1.0	0.000	.140	4.167	.607	19.000	23.914
4.	2.	1.	1.	2.	0.0	5.0	0.000	.130	5.400	.407	36.375	42.312
5.	1.	1.	1.	2.	0.0	1.0	0.000	.150	5.553	.540	21.500	27.743
6.	1.	1.	1.	2.	0.0	1.0	0.000	.150	6.510	.673	13.000	20.333
7.	1.	1.	1.	2.	0.0	1.0	0.000	.075	6.335	.310	56.300	63.020
9.	2.	1.	5.	2.	0.0	2.0	0.000	.110	3.730	.960	84.500	89.300
10.	2.	1.	6.	2.	0.0	2.0	0.000	.075	4.353	2.687	89.700	96.815
10.	2.	1.	6.	99.	10.0	12.0	0.000	.170	3.710	1.253	108.000	113.130
10.	2.	1.	4.	99.	45.0	47.0	0.000	.180	4.170	.700	73.900	78.950
10.	2.	1.	6.	99.	109.0	110.0	.100	.050	4.700	1.380	75.875	82.005
10.	2.	1.	4.	99.	138.0	140.0	.100	.040	3.280	1.000	69.100	73.420
10.	2.	1.	4.	99.	148.0	150.0	.250	.085	4.520	1.138	79.585	85.328
10.	2.	1.	1.	99.	168.0	170.0	.100	.065	3.800	1.073	85.875	90.813
10.	2.	1.	6.	99.	218.0	220.0	.150	.070	3.770	1.970	111.880	117.690
10.	2.	1.	6.	99.	248.0	250.0	.220	.090	4.020	2.110	106.340	112.560
10.	2.	1.	5.	99.	258.0	260.0	.190	.097	4.127	1.287	105.250	110.760
10.	2.	1.	1.	99.	308.0	310.0	0.000	.055	3.770	1.007	44.000	48.832
10.	2.	1.	4.	99.	328.0	330.0	.100	.040	2.680	.587	61.750	65.057
10.	2.	1.	4.	99.	358.0	360.0	0.000	.015	2.980	.940	129.670	133.600
10.	2.	1.	5.	99.	408.0	413.0	.100	.020	4.213	1.810	114.800	120.840
10.	2.	1.	6.	99.	428.0	430.0	.100	.026	3.720	3.067	104.750	111.560
10.	2.	1.	6.	99.	439.0	440.0	0.000	0.000	4.410	2.173	126.670	133.250
11.	1.	1.	5.	2.	0.0	1.0	.310	0.000	3.487	.980	97.000	101.470
12.	1.	1.	5.	2.	0.0	1.0	.050	.025	3.670	4.073	83.250	91.018
13.	1.	1.	5.	2.	0.0	1.0	.200	.015	3.520	1.410	95.875	100.820
14.	2.	1.	5.	2.	0.0	2.0	.150	.020	3.690	1.907	110.090	115.700
15.	1.	2.	5.	3.	0.0	1.0	.200	.050	3.630	4.930	118.750	127.360
16.	1.	2.	5.	3.	0.0	1.0	.150	0.000	2.950	1.310	107.630	111.890
17.	1.	2.	5.	3.	0.0	1.0	.200	.080	3.827	5.540	110.000	119.450
18.	1.	2.	6.	3.	0.0	1.0	.150	.020	3.920	1.300	114.500	119.740
19.	1.	2.	6.	3.	0.0	1.0	.260	.083	2.860	1.900	102.130	106.970
20.	2.	1.	6.	2.	0.0	2.0	0.000	.035	4.160	1.510	131.200	136.910
25.	1.	1.	3.	3.	0.0	1.0	0.000	.005	3.053	1.140	54.335	58.533
26.	1.	2.	1.	3.	0.0	1.0	0.000	.005	3.910	.947	47.250	52.112
27.	1.	2.	2.	3.	0.0	1.0	0.000	99.000	2.253	.360	80.125	82.738
28.	2.	2.	5.	1.	0.0	5.0	0.000	.175	3.660	.460	61.125	65.420
29.	2.	2.	5.	1.	0.0	2.0	.100	.045	4.253	1.767	118.500	124.570
30.	2.	2.	1.	1.	0.0	5.0	0.000	.035	.139	.170	43.375	43.719
31.	1.	2.	2.	1.	0.0	1.0	0.000	0.000	4.333	1.160	85.855	91.348
32.	2.	2.	2.	1.	0.0	5.0	.100	.035	3.553	1.240	96.125	100.950
33.	2.	2.	1.	1.	0.0	2.0	0.000	.020	1.310	.053	18.500	19.883
34.	2.	2.	5.	1.	0.0	5.0	0.000	.060	3.180	.980	101.090	105.310
35.	2.	2.	5.	1.	0.0	1.0	.050	.070	3.880	1.170	185.750	190.870
36.	1.	2.	5.	3.	0.0	1.0	.200	.050	3.993	1.540	112.630	118.210
37.	1.	2.	5.	3.	0.0	1.0	.200	.075	4.047	1.410	96.500	102.030
38.	1.	2.	4.	3.	0.0	1.0	0.000	.025	2.255	.340	38.000	40.620
39.	1.	2.	4.	3.	0.0	1.0	.100	.075	2.980	.853	54.750	58.658
42.	2.	2.	6.	3.	0.0	5.0	.290	.130	3.330	1.630	127.880	132.970
42.	2.	99.	99.	99.	40.0	45.0	.220	.135	3.620	2.120	129.750	135.630
42.	2.	99.	99.	99.	108.0	110.0	.150	.145	4.267	2.200	137.750	144.360
42.	2.	99.	99.	99.	168.0	170.0	0.000	.045	5.520	2.287	123.700	131.550
42.	2.	99.	99.	99.	308.0	310.0	0.000	.053	4.760	2.913	133.590	141.310
42.	2.	99.	99.	99.	361.0	370.0	.240	.165	7.440	1.430	79.200	88.235
42.	2.	99.	99.	99.	411.0	419.0	0.000	.040	6.993	.047	95.165	102.250
42.	2.	99.	99.	99.	556.0	563.0	.190	.030	4.070	1.200	85.000	90.300
43.	2.	2.	6.	3.	0.0	2.0	.100	.265	5.560	2.613	103.700	112.140

CHROMIUM (cont'd.)

A	B	C	D	E	F	G	H	I	J	K	L	M
46.	2.	2.	6.	3.	0.0	5.0	0.000	.085	3.960	2.180	135.500	141.730
46.	2.	99.	99.	99.	5.0	10.0	.250	.060	5.210	1.130	89.500	95.900
46.	2.	99.	99.	99.	10.0	15.0	.270	.065	4.510	1.580	95.000	101.160
46.	2.	99.	99.	99.	15.0	20.0	.150	.150	3.970	1.667	160.750	166.540
46.	2.	99.	99.	99.	20.0	25.0	.250	.105	3.910	1.640	123.750	129.410
46.	2.	99.	99.	99.	25.0	30.0	.050	.040	4.607	1.940	118.500	125.090
46.	2.	99.	99.	99.	30.0	35.0	.200	.055	3.300	1.940	121.500	126.800
46.	2.	99.	99.	99.	35.0	40.0	.150	.170	4.493	2.570	122.000	129.230
46.	2.	99.	99.	99.	40.0	45.0	.190	.100	4.440	1.847	121.630	128.010
46.	2.	99.	99.	99.	45.0	50.0	.240	.083	5.570	2.080	125.800	133.530
47.	1.	2.	6.	3.	0.0	1.0	.260	.100	4.847	1.467	120.380	126.790
50.	1.	1.	6.	3.	0.0	1.0	.260	.035	3.820	1.573	113.300	118.730
55.	1.	1.	6.	1.	0.0	1.0	.200	.130	4.440	1.580	138.130	144.280
56.	2.	2.	6.	1.	0.0	2.0	.100	.020	5.280	1.653	151.700	158.650
57.	2.	1.	6.	3.	0.0	2.0	0.000	.150	4.520	1.433	119.750	125.850
80.	2.	99.	99.	99.	0.0	2.0	.300	.080	.120	2.513	43.500	46.213
80.	2.	99.	99.	99.	2.0	4.4	.710	.263	.133	2.733	36.165	39.294
80.	2.	99.	99.	99.	4.4	7.5	.500	.280	.187	2.650	42.750	45.867
80.	2.	99.	99.	99.	7.5	11.1	.050	.255	.173	1.713	23.500	25.641
80.	2.	99.	99.	99.	11.1	15.0	.150	.180	.153	1.640	24.000	25.973
80.	2.	99.	99.	99.	15.0	23.0	.100	.160	.260	1.267	25.875	27.562
80.	2.	99.	99.	99.	23.0	31.0	.100	.100	.227	1.990	26.585	28.902
81.	2.	99.	99.	99.	99.0	99.0	2.970	.190	.665	6.653	63.750	71.258
82.	2.	99.	99.	99.	99.0	99.0	.940	.230	2.050	6.490	87.250	96.020
83.	2.	99.	99.	99.	99.0	99.0	.890	.190	2.220	6.700	81.100	90.210
84.	2.	99.	99.	99.	99.0	99.0	1.140	.240	3.840	6.790	126.500	137.370
85.	2.	99.	99.	99.	99.0	99.0	.660	.765	5.265	5.787	108.400	120.220

ALUMINUM

A	B	C	D	E	F	G	H	I	J	K	L	M
2.	2.	1.	5.	2.	0.0	2.0	.190	21.890	1517.500	3473.300	121190.000	126200.000
3.	1.	1.	5.	2.	0.0	1.0	0.000	31.680	608.020	1065.300	35997.000	36802.000
4.	2.	1.	1.	2.	0.0	5.0	0.000	20.460	916.580	580.890	8946.400	10464.000
5.	1.	1.	1.	2.	0.0	1.0	0.000	12.870	545.400	629.130	15567.000	16755.000
6.	1.	1.	1.	2.	0.0	1.0	0.000	33.880	1309.000	629.840	15617.000	17590.000
7.	1.	1.	1.	2.	0.0	1.0	0.000	33.440	852.440	395.970	14797.000	16078.000
9.	2.	1.	5.	2.	0.0	2.0	0.000	194.250	2478.500	2106.900	100560.000	105340.000
10.	2.	1.	6.	2.	0.0	2.0	0.000	96.495	1951.300	1953.300	110040.000	112290.000
10.	2.	1.	6.	99.	10.0	12.0	0.000	68.713	2101.600	2525.600	135460.000	140150.000
10.	2.	1.	4.	99.	45.0	47.0	0.000	92.290	2039.200	2277.300	104820.000	109230.000
10.	2.	1.	6.	99.	109.0	110.0	.100	33.935	1674.600	4643.100	75697.000	82048.000
10.	2.	1.	4.	99.	138.0	140.0	.100	10.560	2298.800	3455.200	106710.000	112470.000
10.	2.	1.	4.	99.	148.0	150.0	.250	33.220	1596.800	3706.400	80722.000	86058.000
10.	2.	1.	1.	99.	168.0	170.0	.100	11.852	1706.900	3676.300	107850.000	113240.000
10.	2.	1.	6.	99.	218.0	220.0	.150	38.220	1809.500	4116.500	105850.000	111810.000
10.	2.	1.	6.	99.	248.0	250.0	.220	38.335	1614.000	4006.600	132360.000	138020.000
10.	2.	1.	5.	99.	258.0	260.0	.190	35.134	1568.200	3983.800	134090.000	139680.000
10.	2.	1.	1.	99.	308.0	310.0	0.000	14.135	1560.800	2072.500	81782.000	85429.000
10.	2.	1.	4.	99.	328.0	330.0	.100	17.600	1569.500	2615.700	46460.000	50663.000
10.	2.	1.	4.	99.	358.0	360.0	0.000	22.825	1812.600	2594.900	86557.000	90987.000
10.	2.	1.	5.	99.	408.0	413.0	.100	25.025	1335.200	4116.500	120890.000	126360.000
10.	2.	1.	6.	99.	428.0	430.0	.100	41.965	1989.700	4627.000	126370.000	133030.000
10.	2.	1.	6.	99.	439.0	440.0	0.000	152.460	1666.500	3126.600	142850.000	147800.000
11.	1.	1.	5.	2.	0.0	1.0	.310	6.050	2006.500	2701.400	92862.000	97576.000
12.	1.	1.	5.	2.	0.0	1.0	.050	66.110	1757.400	3271.000	113560.000	118660.000
13.	1.	1.	5.	2.	0.0	1.0	.200	17.220	1648.300	2378.500	83274.000	87318.000
14.	2.	1.	5.	2.	0.0	2.0	.150	45.842	1366.500	3206.000	122740.000	127360.000
15.	1.	2.	5.	3.	0.0	1.0	.200	45.100	2617.900	2626.200	101830.000	107120.000
16.	1.	2.	5.	3.	0.0	1.0	.150	21.230	1662.500	2679.300	133330.000	137700.000
17.	1.	2.	5.	3.	0.0	1.0	.200	172.200	2027.600	2251.300	92500.000	96951.000
18.	1.	2.	6.	3.	0.0	1.0	.150	5.885	1920.400	2104.200	145570.000	149600.000
19.	1.	2.	6.	3.	0.0	1.0	.260	95.370	2217.000	2542.000	121970.000	126820.000
20.	2.	1.	6.	2.	0.0	2.0	0.000	47.880	1996.400	2434.100	136640.000	141120.000
25.	1.	1.	3.	3.	0.0	1.0	0.000	10.615	1362.800	2136.600	102800.000	106310.000
26.	1.	2.	1.	3.	0.0	1.0	0.000	23.650	1275.100	1455.200	79424.000	82178.000
27.	1.	2.	2.	3.	0.0	1.0	0.000	99.000	1109.500	316.130	48733.000	50158.000
28.	2.	2.	5.	1.	0.0	5.0	0.000	19.525	1489.800	1987.900	101570.000	105070.000
29.	2.	2.	5.	1.	0.0	2.0	.100	41.653	1604.500	2817.400	115520.000	119990.000
30.	2.	2.	1.	1.	0.0	5.0	0.000	43.120	1379.700	2042.200	64825.000	68290.000
31.	1.	2.	2.	1.	0.0	1.0	0.000	3.410	1548.700	1888.100	46337.000	49777.000
32.	2.	2.	2.	1.	0.0	5.0	.100	16.170	1327.100	1991.900	81757.000	85092.000
33.	2.	2.	1.	1.	0.0	2.0	0.000	17.325	1115.000	746.730	24101.000	25980.000
34.	2.	2.	5.	1.	0.0	5.0	0.000	40.845	1673.600	1732.600	72897.000	76344.000
35.	2.	2.	5.	1.	0.0	1.0	.050	60.148	1834.200	2743.000	117510.000	122150.000
36.	1.	2.	5.	3.	0.0	1.0	.200	26.345	1927.100	3020.300	101560.000	106530.000
37.	1.	2.	5.	3.	0.0	1.0	.200	73.122	2031.500	2104.200	112980.000	117190.000
38.	1.	2.	4.	3.	0.0	1.0	0.000	28.526	1234.200	1423.100	63667.000	66353.000
39.	1.	2.	4.	3.	0.0	1.0	.100	34.705	1456.400	1530.300	149370.000	152390.000
42.	2.	2.	6.	3.	0.0	5.0	.290	27.087	2124.000	2402.000	150770.000	155330.000
42.	2.	99.	99.	99.	40.0	45.0	.220	197.960	1608.900	2629.100	126590.000	130730.000
42.	2.	99.	99.	99.	108.0	110.0	.150	86.295	1823.600	2846.200	123080.000	127840.000
42.	2.	99.	99.	99.	168.0	170.0	0.000	40.443	1562.000	3113.500	150870.000	155580.000
42.	2.	99.	99.	99.	308.0	310.0	0.000	67.760	1780.600	3517.500	128410.000	133770.000
42.	2.	99.	99.	99.	361.0	370.0	.240	32.505	893.850	1973.800	70652.000	73587.000
42.	2.	99.	99.	99.	411.0	419.0	0.000	44.935	1873.200	1786.900	56085.000	59790.000
42.	2.	99.	99.	99.	556.0	563.0	.190	30.002	1461.800	2420.000	183490.000	187400.000
43.	2.	2.	6.	3.	0.0	2.0	.100	101.350	1999.300	2564.800	108480.000	113150.000

ALUMINUM (cont'd.)

A	B	C	D	E	F	G	H	I	J	K	L	M
46.	2.	2.	6.	3.	0.0	5.0	0.000	76.175	1496.800	2863.600	157630.000	162060.000
46.	2.	99.	99.	99.	5.0	10.0	.250	24.970	1469.600	2789.900	99631.000	103920.000
46.	2.	99.	99.	99.	10.0	15.0	.270	35.585	1770.500	2791.900	107540.000	112130.000
46.	2.	99.	99.	99.	15.0	20.0	.150	76.450	2423.300	2245.200	137970.000	142710.000
46.	2.	99.	99.	99.	20.0	25.0	.250	66.660	1972.500	2205.000	148130.000	152380.000
46.	2.	99.	99.	99.	25.0	30.0	.050	47.080	1649.300	2696.400	111430.000	115820.000
46.	2.	99.	99.	99.	30.0	35.0	.200	46.860	1959.400	2763.100	138820.000	143590.000
46.	2.	99.	99.	99.	35.0	40.0	.150	77.330	1881.600	3069.300	124440.000	129470.000
46.	2.	99.	99.	99.	40.0	45.0	.190	77.605	2232.100	3845.500	154900.000	161050.000
46.	2.	99.	99.	99.	45.0	50.0	.240	20.936	1550.000	3091.400	120610.000	125270.000
47.	1.	2.	6.	3.	0.0	1.0	.260	43.890	1545.300	2220.400	152660.000	156470.000
50.	1.	1.	6.	3.	0.0	1.0	.260	27.445	1646.300	2480.300	90664.000	94818.000
55.	1.	1.	6.	1.	0.0	1.0	.200	78.760	2011.400	2371.800	157680.000	162140.000
56.	2.	2.	6.	1.	0.0	2.0	.100	30.030	1847.800	3118.200	131500.000	136500.000
57.	2.	1.	6.	3.	0.0	2.0	0.000	51.535	1566.500	2769.800	122110.000	126500.000
80.	2.	99.	99.	99.	0.0	2.0	.300	159.600	1116.600	1388.200	16615.000	19279.000
80.	2.	99.	99.	99.	2.0	4.4	.710	895.870	1040.300	1524.100	25859.000	29319.000
80.	2.	99.	99.	99.	4.4	7.5	.500	646.150	943.340	1499.500	33128.000	36217.000
80.	2.	99.	99.	99.	7.5	11.1	.050	86.790	806.990	928.620	30216.000	32038.000
80.	2.	99.	99.	99.	11.1	15.0	.150	479.250	765.580	696.790	29205.000	31147.000
80.	2.	99.	99.	99.	15.0	23.0	.100	274.220	659.530	323.610	12878.000	14135.000
80.	2.	99.	99.	99.	23.0	31.0	.100	289.110	399.290	102.510	14325.000	15116.000
81.	2.	99.	99.	99.	99.0	99.0	2.970	1297.100	2742.200	3103.400	51737.000	58880.000
82.	2.	99.	99.	99.	99.0	99.0	.940	2280.300	2337.800	4103.100	99385.000	108110.000
83.	2.	99.	99.	99.	99.0	99.0	.890	2078.300	2425.400	3656.200	65856.000	74016.000
84.	2.	99.	99.	99.	99.0	99.0	1.140	1111.500	2702.100	3685.000	84320.000	91818.000
85.	2.	99.	99.	99.	99.0	99.0	.660	984.750	2838.800	3792.200	83800.000	91415.000

APPENDIX II
GRAPHITE CONTROL SETTINGS
FOR PERKIN ELMER 560
ATOMIC ADSORPTION SPECTROPHOTOMETER
WITH HGA:2200 GRAPHITE FURNACE

MATRIX: $MgCl_2$ (Exchangeable Fraction)

Signal = concentration (conc)
Mode = peak height (pk ht)
Recorder = TIC
Gas Flow = 7 normal:33 on Argon flow meter
Volume = 20 µl

Chromium:	atm	2700°C at 14 seconds
	char	1100°C at 30 seconds
	dry	100°C at 60 seconds
	mode	AA only
	time = 8.0 seconds reading	
Cobalt:	atm	2700°C at 8 seconds
	char	1000°C at 40 seconds
	dry	100°C at 60 seconds
	mode	AA-BG
	time = 6.0 seconds reading	
Nickel:	atm	2700°C at 10 seconds
	char	1000°C at 30 seconds
	dry	100°C at 60 seconds
	mode	AA-BG
	time = 6.0 seconds reading	
Aluminum:	atm	2700°C at 11 seconds
	char	1300°C at 20 seconds
	dry	100°C at 60 seconds
	mode	AA-BG
	time = 4.0 seconds reading	
Barium:	atm	2800°C at 13 seconds
	char	1500°C at 30 seconds
	dry	100°C at 60 seconds
	mode	AA only
	time = 4.0 seconds reading	
	Gas Flow increased for Ba	
Lead:	atm	2300°C at 10 seconds
	char	700°C at 10 seconds
	dry	100°C at 60 seconds
	mode	AA-BG
	time = 6.0 seconds reading	
	Gas Flow = 30	

MATRIX: .04 M $NH_2OH \cdot HCL$ in 25% (v/v) HOAc (Oxide Fraction)

Signal = concentration (conc)
Mode = peak height (pk ht)
Recorder = TIC
Gas Flow = 7 normal:33 on Argon flow meter
Volume = 20 µl

Chromium:	atm	2700°C at 12 seconds
	char	1100°C at 10 seconds
	dry	100°C at 20 seconds
	mode	AA only
	time = 6.0 seconds reading	
Cobalt:	atm	2700°C at 12 seconds
	char	1000°C at 20 seconds
	dry	100°C at 20 seconds
	mode	AA-BG
	time = 8.0 seconds reading	
Nickel:	atm	2700°C at 12 seconds
	char	1000°C at 20 seconds
	dry	100°C at 20 seconds
	mode	AA-BG
	time = 6.0 seconds reading	
Aluminum:	atm	2700°C at 12 seconds
	char	1400°C at 20 seconds
	dry	100°C at 20 seconds
	mode	AA-BG
	time = 6.0 seconds reading	
	Gas Flow increase for Al	
Barium:	atm	2800°C at 14 seconds
	char	1600°C at 20 seconds
	dry	100°C at 20 seconds
	mode	AA only
	time = 10.0 seconds reading	
	Gas Flow increase for Ba	
Lead:	atm	2300°C at 8 seconds
	char	600°C at 16 seconds
	dry	100°C at 20 seconds
	mode	AA-BG
	time = 6.0 seconds reading	
	Gas Flow = 7N:30	

MATRIX: 3.5 ratio .02HNO_3:3.2 NH_4OAc in 20% (v/v) HNO_3 (Organic Fraction)

Signal = concentration (conc)
Mode = peak height (pk ht)
Recorder = TIC
Gas Flow = 7 normal:33 on Argon flow meter
Volume = 20 µl

Chromium:
atm 2700°C at 12 seconds
char 1100°C at 20 seconds
dry 100°C at 20 seconds
mode AA only
time = 10.0 seconds reading

Cobalt:
atm 2700°C at 12 seconds
char 1000°C at 20 seconds
dry 100°C at 20 seconds
mode AA-BG
time = 6.0 seconds reading

Nickel:
atm 2700°C at 12 seconds
char 1000°C at 20 seconds
dry 100°C at 20 seconds
mode AA-BG
time = 6.0 seconds reading

Aluminum:
atm 2700°C at 12 seconds
char 1400°C at 30 seconds
dry 100°C at 20 seconds
mode AA-BG
time = 4.0 seconds reading

Barium:
atm 2800°C at 12 seconds
char 1500°C at 10 seconds
dry 100°C at 20 seconds
mode AA only
time = 6.0 seconds reading
Gas Flow increased for Ba

Lead:
atm 2300°C at 10 seconds
char 700°C at 20 seconds
dry 100°C at 20 seconds
mode AA-BG
time = 8.0 seconds reading
Gas Flow = 7N:30

MATRIX: $LiBO_3$ (Residual Fraction)

Signal = concentration (conc)
Mode = peak height (pk ht)
Recorder = TIC
Gas Flow = 7 normal:33 on Argon flow meter
Volume = 20 µl

Chromium:	atm	2700°C at 13 seconds
	char	1100°C at 30 seconds
	dry	100°C at 25 seconds
	mode	AA only
	time = 4.0 seconds reading	
Cobalt:	atm	2700°C at 12 seconds
	char	1000°C at 30 seconds
	dry	100°C at 25 seconds
	mode	AA-BG
	time = 6.0 seconds reading	
Nickel:	atm	2700°C at 12 seconds
	char	1000°C at 30 seconds
	dry	100°C at 25 seconds
	mode	AA-BG
	time = 8.0 seconds reading	
Aluminum:	atm	2600°C at 15 seconds
	char	1400°C at 30 seconds
	dry	100°C at 25 seconds
	mode	AA-BG
	time = 6.0 seconds reading	
Barium:	atm	2700°C at 14 seconds
	char	1600°C at 30 seconds
	dry	100°C at 25 seconds
	mode	AA only
	time = 6.0 seconds reading	
	Gas Flow increased for Ba	
Lead:	atm	2300°C at 12 seconds
	char	600°C at 10 seconds
	dry	100°C at 25 seconds
	mode	AA-BG
	time = 6.0 seconds reading	
	Gas Flow = 7N:30	

APPENDIX III
B-MATRIX OF WEIGHTS FROM Q-MODE AND R-MODE FACTOR ANALYSIS

Raw Q-Mode Factor Analysis

PA1*

Sample Location	Communality	Factor 1
2	.99870	.02474
3	.99849	.02474
4	.83878	.02267
5	.84175	.02271
6	.90706	.02358
7	.96277	.02429
9	.99887	.02474
10	.99396	.02468
11	.99982	.02475
12	.99919	.02474
13	.99914	.02474
14	.99875	.02474
15	.99977	.02475
16	.95771	.02423
17	.99978	.02475
18	.99985	.02475
19	.99924	.02475
20	.99616	.02471
25	.99972	.02475
26	.99865	.02474
27	.99119	.02465
28	.99713	.02472
29	.99874	.02474
30	.99845	.02474
31	.99819	.02473
32	.99997	.02475
33	.99856	.02474
34	.99911	.02474
35	.99972	.02475
36	.99821	.02473
37	.99986	.02475
38	.99830	.02473
39	.99967	.02475
42	.94691	.02409
43	.99826	.02473
46	.99945	.02475
47	.99562	.02470
50	.99634	.02470
55	.99945	.02475
56	.99642	.02471
57	.99929	.02475
	Variance	98.5
	Cum. Variance	98.5

*PA1 = Principal factoring without Iteration.

Transformed Q-Mode Factor Analysis

		Factor Score Coefficients	
Sample Location	Communality	Factor 1	Factor 2
2	.99904	-.03359	.07694
3	.97704	-.03402	.07687
4	.92040	.07805	-.05198
5	.84777	.05564	-.02497
6	.90567	.05313	-.02037
7	.90804	.06597	-.03645
9	.99404	.05992	-.02662
10	.99185	.06286	-.03036
11	.97462	.05409	-.01988
12	.99086	-.03125	.07446
13	.99054	-.03534	.07846
14	.99691	-.03669	.07991
15	.99727	-.03507	.07834
16	.97502	.05969	-.02680
17	.98611	.06046	-.02749
18	.99111	-.03392	.07726
19	.99415	.05386	-.01921
20	.98920	.05922	-.02574
25	.98732	.05845	-.02491
26	.97539	.04880	-.01313
27	.99882	.03942	-.00221
28	.99944	-.03371	.07705
29	.98462	-.03521	.07852
30	.97495	-.03222	.07527
31	.97432	.05991	-.02705
32	.99187	.03895	-.00169
33	.99489	-.03385	.07703
34	.98747	-.03696	.08012
35	.99507	.05740	-.02365
36	.99888	.05407	-.01936
37	.99515	-.03465	.07797
38	.99797	-.03597	.07917
39	.92482	-.03141	.07478
42	.99482	.05970	-.02806
43	.99562	-.03591	.07912
46	.99267	.06062	-.02753
47	.99454	.05369	-.01892
50	.98836	.06301	-.03063
55	.99431	.06457	-.03246
56	.99637	-.03471	.07797
57	.98825	.04442	-.00786
	Variance	85.1	12.9
	Cum. Variance	85.1	98.0

Transformed R-Mode Factor Analysis

		Factor Score Coefficients		
Variable	Communality	Factor 1	Factor 2	Factor 3
Ba hydromorphic	.97813	.43968	.42335	-.73635
Ba detrital	.82681	-.44567	.51495	-.29946
Cu hydromorphic	.47255	-.03200	-.07351	-.02796
Cu detrital	.69516	.08458	-.39477	.06976
Fe hydromorphic	.99442	-1.99033	3.68699	1.24704
Fe detrital	.29146	.04400	-.02217	.09278
Co hydromorphic	.43779	.08092	-.01364	-.14581
Co detrital	.77044	.33520	-.33985	-.07342
Mn hydromorphic	.83414	.45541	-.92104	-.49177
Mn detrital	.89422	1.05746	-.88667	-.13179
Zn hydromorphic	.88380	.23477	-1.20147	.15529
Zn detrital	.83561	.34932	-.37750	.23755
Ni hydromorphic	.64380	.14875	-.22425	-.11346
Ni detrital	.82108	-.27355	.03840	.52969
Pb hydromorphic	.53736	.09078	-.09969	-.03383
Pb detrital	.60302	.16213	-.00120	-.24376
Cr hydromorphic	.89696	.18542	.46088	-.02429
Cr detrital	.54842	-.10497	.14161	.18548
Al hydromorphic	.85187	.25574	-.48270	-.34914
Al detrital	.81213	.13346	-.13397	.16588
	Variance	72.3	10.5	7.3
	Cum. Variance	72.3	82.8	90.1

Raw R-Mode Factor Analysis

PA1*

Variable	Communality	Factor Score Coefficients Factor 1	Factor 2	Factor 3	Factor 4	Factor 5
Ba hydromorphic	.81095	.08720	.10476	-.03189	-.00251	-.13321
Ba detrital	.61631	-.03375	.41834	.18971	-.00334	-.07891
Cu hydromorphic	.69970	-.00150	-.05572	-.02903	.66590	.01868
Cu detrital	.58442	.02092	-.13135	.28220	-.00904	.21053
Fe hydromorphic	.94517	.05526	-.00047	.26001	.05483	.02307
Fe detrital	.64126	.11785	-.06084	-.11879	-.12587	.03125
Co hydromorphic	.74976	.04969	.21432	.05221	.27663	.41244
Co detrital	.64514	.06260	.24298	-.01958	-.23285	.01130
Mn hydromorphic	.82285	-.10605	.13254	.59668	-.04542	-.09965
Mn detrital	.78229	.08168	.11101	.05630	.04908	.11482
Zn hydromorphic	.91678	.08660	-.07337	.12930	.07550	.06580
Zn detrital	.79788	.10335	-.08994	-.02701	.03795	-.10587
Ni hydromorphic	.69948	.12661	-.08506	-.17530	-.06601	-.02897
Ni detrital	.64504	.09712	.02494	-.00823	-.29052	.11907
Pb hydromorphic	.55320	-.00218	-.33903	.13507	.12742	-.10807
Pb detrital	.80457	.00408	.00085	-.01145	.00463	.74933
Cr hydromorphic	.83955	.09248	-.01746	.05542	.03868	-.01126
Cr detrital	.60013	.09334	-.31387	-.05507	-.31201	.02555
Al hydromorphic	.76383	.11654	-.06544	-.14313	.04647	-.09746
Al detrital	.79544	.10258	-.01981	-.11538	.13008	-.14066
Variance		45.2	10.2	6.7	6.2	5.2
Cum. Variance		45.2	55.5	62.1	68.4	73.6

*PA1 = Principal factoring without Iteration

Raw R-Mode Factor Analysis

Variable	Communality	Factor Score Coefficients Factor 1	Factor 2	Factor 3	Factor 4	Factor 5
Total organic carbon	.76101	-.02520	.42397	-.03968	-.02519	.05073
Ba hydromorphic	.80949	.08581	.00635	.10451	-.02968	-.12831
Ba detrital	.60894	-.02358	.00181	.41687	.18904	-.06515
Cu hydromorphic	.71319	-.09710	.52394	.04369	-.00745	.01430
Cu detrital	.58316	.02377	-.02693	-.12903	.28443	.20548
Fe hydromorphic	.94390	.04876	.03083	.00648	.26128	.01629
Fe detrital	.65335	.14101	-.13975	-.07896	-.11863	.02095
Co hydromorphic	.68029	.04043	.12874	.24639	.05574	.38054
Co detrital	.64343	.10452	-.19412	.20525	-.02750	.01226
Mn hydromorphic	.81433	-.09960	-.02950	.12763	.59370	-.09018
Mn detrital	.78213	.08149	.02447	.11610	.05769	.10929
Zn hydromorphic	.91202	.07607	.04561	-.06312	.13205	.05603
Zn detrital	.80201	.08770	.05250	-.08072	-.02121	-.09940
Ni hydromorphic	.70685	.13882	-.08303	-.10005	-.17840	-.04748
Ni detrital	.61326	.13175	-.18999	-.01445	-.01393	.13243
Pb hydromorphic	.52819	-.02434	.06273	-.32343	.13624	-.13225
Pb detrital	.82147	.00775	.03574	.00936	-.00808	.76075
Cr hydromorphic	.83804	.08631	.02372	-.01246	.05765	-.01659
Cr detrital	.55398	.10928	-.15846	-.34531	-.05353	.05706
Al hydromorphic	.76387	.10760	.02896	-.06225	-.14210	-.10825
Al detrital	.80751	.07632	.12318	.00076	-.10814	-.13603
Variance		44.4	9.8	7.6	6.2	5.0
Cum. Variance		44.4	54.2	61.9	68.0	73.0